AWARD NUMBER: W81XWH-13-1-0078

TITLE: Can Exosomes Induced by Breast Involution Be Markers for the Poor Prognosis and Prevention of Postpartum Breast Cancer?

PRINCIPAL INVESTIGATOR: Dr. Virginia Borges

CONTRACTING ORGANIZATION: University of Colorado, Anschutz Medical Campus
                           Aurora, CO 80045

REPORT DATE: Septmeber 2016

TYPE OF REPORT: Final

PREPARED FOR: U.S. Army Medical Research and Materiel Command
               Fort Detrick, Maryland 21702-5012

REPORT DOCUMENTATION PAGE			*Form Approved* *OMB No. 0704-0188*

1. REPORT DATE September 2016	**2. REPORT TYPE** Final	**3. DATES COVERED** 1 Jul 2013-30 Jun 2016

4. TITLE AND SUBTITLE

Can exosomes induced by breast involution be markers for the poor prognosis and prevention of post-partum breast cancer?"

5a. CONTRACT NUMBER

5b. GRANT NUMBER
W81XWH-13-1-0078

5c. PROGRAM ELEMENT NUMBER

6. AUTHOR(S)
Virginia F. Borges, MD

5d. PROJECT NUMBER

5e. TASK NUMBER

5f. WORK UNIT NUMBER

E-Mail: Virginia.borges@ucdenver.edu

7. PERFORMING ORGANIZATION NAME(S) AND ADDRESS(ES)

University of Colorado Anschutz Medical Campus, Aurora, CO 80045

8. PERFORMING ORGANIZATION REPORT NUMBER

9. SPONSORING / MONITORING AGENCY NAME(S) AND ADDRESS(ES)
U.S. Army Medical Research and Materiel Command
Fort Detrick, Maryland 21702-5012

10. SPONSOR/MONITOR'S ACRONYM(S)

11. SPONSOR/MONITOR'S REPORT NUMBER(S)

12. DISTRIBUTION / AVAILABILITY STATEMENT
Approved for Public Release; Distribution Unlimited

13. SUPPLEMENTARY NOTES

14. ABSTRACT

Breast cancers diagnosed up to six years after a completed pregnancy have been referred to as pregnancy-associated breast cancer or PABC. Several studies show that PABC frequently metastasizes, resulting in poor prognosis for the patient. Post-partum mammary gland involution is a necessary physiologic process required to return the lactation-competent gland to a non-lactating state. Accumulating evidence indicates that tissue-remodeling programs similar to wound healing are utilized to remodel the lactating gland to its post-partum state and that these programs are characterized by immune modulation. To move this work forward into the clinic, further understanding of the complexity between the tumor microenvironment and circulating factors that both influence the metastatic potential of these tumors and compromise the host immune response to the tumor are of great importance. It would also be ideal to have a circulating marker that would both identify women at risk for a postpartum breast cancer (PPBC), as well as, to assess the potential clinical benefit from novel therapies aimed to reduce the metastatic potential of PPBC. We have therefore undertaken this project to show that extracellular vesicles[EVs] are released from the actively involuting gland and exist in the circulation during involution that carry pro-metastatic cargo These EVS can also influence tumor-microenvironment interactions, immune escape, and the metastatic niche. In this proposal, our objectives were to determine, for the first time, whether exosomes with unique properties can be identified during involution, are likewise present in women with PPBC, and whether anti-inflammatory agent treatment mitigates their numbers, content, and or function. In completing this work. We have identified important technologic requirements to be able to effectively study the EV proteome from plasma samples of animals and humans, adding significantly to the understanding of translational EV research in cancer. We have identified that the size, overall protein content and relative quantitation of EVs across species in either normal or cancer-bearing hosts does not vary. However, the functional capacity and proteomic content of these EVs varies significantly, with EVs from tumor bearing hosts having ability to increase invasion and migration of typically non-invasive breast cancer cells to the level of a highly aggressive TNBC breast cancer subtype. Moreoever, we have identified that EVs are selective phagocytosed by myeloid lineage cells and

15. SUBJECT TERMS
Young Women's Breast Cancer, Exosomes, postpartum breast cancer, immune suppression

16. SECURITY CLASSIFICATION OF:			**17. LIMITATION OF ABSTRACT**	**18. NUMBER OF PAGES**	**19a. NAME OF RESPONSIBLE PERSON** USAMRMC
a. REPORT U	**b. ABSTRACT** U	**c. THIS PAGE** U	UU	81	**19b. TELEPHONE NUMBER** *(include area code)*

Table of Contents

       Submitted manuscript version 3

       Approved Clinical Protocol

Introduction:

Breast cancers diagnosed up to six years after a completed pregnancy have been referred to as pregnancy-associated breast cancer or PABC. Several studies show that PABC frequently metastasizes, resulting in poor prognosis for the patient.[1-7] We have proposed the postpartum involution-hypothesis to account for the high metastatic occurrence of PABC.[7,8] Post-partum mammary gland involution is a necessary physiologic process required to return the lactation-competent gland to a non-lactating state. Accumulating evidence indicates that tissue-remodeling programs similar to wound healing are utilized to remodel the lactating gland to its post-partum state and that these programs are characterized by immune modulation. [9-15] Thus, we have proposed that the involuting microenvironment, with its similarities to wound healing microenvironments, supports dissemination of tumor cells through immune suppression. In rodent models, we have identified the period of postpartum involution as a critical time point that promotes breast cancers progression, invasion and metastasis in animal models, data consistent with involution driving tumor progression. We have also shown that the promotional effects of involution are blocked by anti-inflammatory drugs given during the involution time frame.[16-17] To move this work forward into the clinic, further understanding of the complexity between the tumor microenvironment and circulating factors that both influence the metastatic potential of these tumors and compromise the host immune response to the tumor are of great importance. It would also be ideal to have a circulating marker that would both identify women at risk for a postpartum breast cancer (PPBC), as well as, to assess the potential clinical benefit from novel therapies aimed to reduce the metastatic potential of PPBC. We hypothesize that exosomes with pro-metastatic cargo are released from the actively involuting gland, enter the circulation, and influence tumor-microenvironment interactions, immune escape, and the metastatic niche. In this proposal, our objectives are to determine, for the first time, whether exosomes with unique properties can be identified during involution, are likewise present in women with PPBC, and whether anti-inflammatory agent treatment mitigates their numbers, content, and or function.

Key words: Postpartum breast cancer, Young Women's Breast Cancer, Involution, Exosomes, Microvesicles, Immune Suppression

Accomplishments:

What were the major goals of the project?

Statement of Work: Task 1 – Identify samples to be used in Aims 1-3 of the research and finalize regulatory approvals through DOD and HRPO.

a. **Human Regulatory Issues** – The human specimens selected from the normal donor and cases of young women's breast cancer were successfully identified and the availability to adequate plasma confirmed for the initial testing of 20 normal and 20 YWBC cases, as well as the 10 control and 10 drug treated cases for aim 3. **Final report: Work on these samples is now complete. Data presented below. The IRB tissue re-use protocol created for the use of the samples is designated COMIRB #14-0662 and has remained under approved use through ongoing CRV process.**

b. **Animal Approval Issues –** The samples from our murine models of involution with and without tumor xenografts in the animals were all collected under previous projects. No new animals were used in the conduct of this research, only pre-existing samples. We were granted the approval to proceed with all animal work on 11/26/2013. **Final report: No changes since last report to animal approval.**

       Task 1 summary: completed

Task 2- Perform the exosome isolation from Aim 1 in the 4 animal cohorts: virgin and involution group and each with and without tumor xenografts and perform the characterization of the exosomes. **Months 3-12**

a. **Exosome Isolation** –With training and support from the Graner and Eisenmesser labs, we will start with the mouse samples to ensure we have optimal isolation techniques. If inadequate exosomes are obtained with currents methods, we will change to PEG precipitation or use of currently available Exosome kits to ensure best methodology with our specific samples.

b. **Exosome characterization–** Identification of the exosomes through western blot, Nanosight analysis, size distributions and quantification analysis as described will be performed. Bouyant density determination and acetylcholinesterase activity determination and transmission electron microscopy will be performed.

Task 2 Final Report:

This task resulted in a cross-species comparison of various available techniques pf exosomes, which I will now call extracellular vesicles or EVs, based on evolution of terminology in this field. This step was necessary as the available literature at the time of initiation of the project did not provide an optimal method of isolation for the planned patient and animal derived samples in comparison to the larger body of literature using solely cell line derived EVs. Also, the available isolation methods did not provide adequate purity of samples for subsequent proteomic analysis, due to the increase of blood contaminating proteins in primary patient or animal samples that does not confound cell line research. Five methods were systematically evaluated – two methods of ultracentrifugation with varying filtration techniques, commercially available kits using PEG/Exoquick methods, FPLC, and finally, modified size exclusion chromatography with a Sepharose column technique [SEC]. The SEC assay was the only method that provided pure enough enrichment of EVs that reliable documentation of the tetraspanins markers of EVs were present in rodents and human samples, as well as, was the

only method that provided for adequate elimination of contaminating blood proteins that were not EV specific to permit proteomic content analysis of the EVs across patient and rodent derived samples. While ultracentrifugation was adequate in our hands for excellent results with cell line derived EVs, the cross over to translational research with direct human samples would not be supportable using this methodology. We have a submitted paper under 3rd review at the Journal of Extracellular Vesicles and the current version of the manuscript is included in the appendix of this report. Figure 1 and 2 highlight the data that led to our determination that SEC would be the preferred method for our work:

Figure 1. Size-exclusion chromatography separates putative exosomes from contaminating plasma proteins. A. Murine and Human plasma samples were concentrated in ultrafiltration tubes (50kd molecular weight cut-off), layered over a Sepharose CL-2B size-exclusion column (GE Healthcare), and 1 ml fractions were collected by gravity filtration. The exosome content of each fraction was determined by Nanosight and the protein content was characterized by Bradford Assay. **B.** Exosome containing fractions from (A) were combined, concentrated, and analyzed by electron microscopy using a uranyl acetate negative stain. Two representative images are shown per species at two magnifications. **C.** Exosomes were diluted in 2x RIPA buffer and analyzed by western blot for the exosome markers Hsp70, CD63, and CD9. **D.** The particle yield and size of the combined and concentrated exosome fractions from (A) were analyzed by Nanosight and the protein yield was analyzed by the BCA Protein Assay (Pierce).
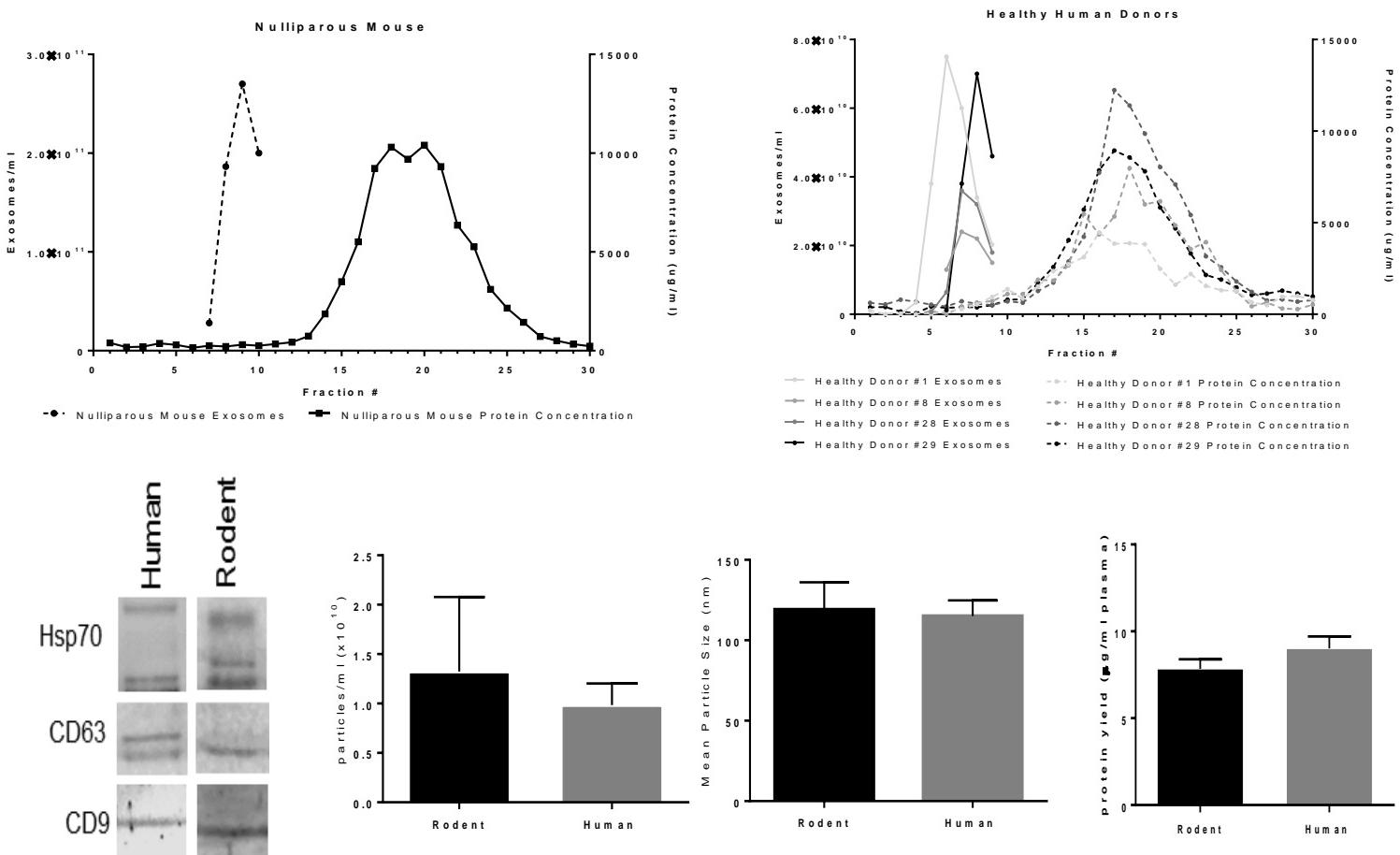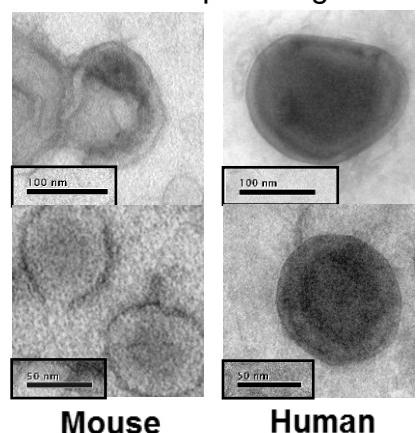
Task 2 Summary: Completed

Task 3 – Perform the characterization of the proteome content of the 4 animal cohorts of exosomes, virgin and involution group and each with and without tumor xenografts

Months 12-24

    a. In depth quantitative proteomic analysis on the exosomes identified from the virgin, involution, virgin with tumor and involution with tumor plasma samples will be performed according to our published protocols and methods as outlined in the methods paper manuscript in the appendix. This work has been be performed in the Hansen lab, with collaborative input from Eisenmesser and Graner as needed.

Task 3 Final Report: As previously reported, the initial proteomics analysis performed on rodent samples isolated by ultracentrifugation showed a high amount of the major serum proteins present in peripheral blood with no demonstrable enrichment for proteins associated with exosomes. After altering our techniques to use the size exclusion chromatography [SEC], we have moved forward again with proteomic analysis on rodent samples with clearly improved results. Methods of isolation and proteomics are incorporated into the manuscript under 3rd revision [see appendix and figure 2]. Briefly, we identify exosome proteins and show a positive enrichment with removal of major serum proteins. For ongoing completion of **Task 3**, the murine cohorts of virgin, involution,

Figure 2. Comparison of the protein content of rodent plasma EVs purified by ultracentrifugation and SEC by mass spectrometry. Heat map and analysis of peptide spectral matches from EVs isolated from pooled rodent plasma samples. Samples were analyzed on a Q Exactive Quadripole Orbitrap mass spectrometer. Spectra data was matched against the SwissProt database and filtered using Scaffold Proteome Software. Peptide and protein identifications were accepted if they could be established with greater than 95% probability and at least two identified unique peptides. A. Abundant plasma proteins (in beige) are the top 20 proteins in the Plasma Proteome Reference Set (46). SEC reduced the amount of contaminating plasma proteins in EV fractions. B. Abundant EV proteins are those that resulted in the highest ratio of spectral matches compared to plasma. Many EV-specific proteins were identified in the SEC EV sample, but not in the ultracentrifugation EV sample. C. Abundant ultracentrifugation pellet proteins are those with the highest ratio of spectral matches compared to ultracentrifugation supernatants. Although ultracentrifugation differentially separated some proteins from the supernatant, these were not EV-specific. *EV-specific proteins were only identified in the early SEC fractions containing EVs, likely due to the reduction in abundant plasma proteins with this method.*
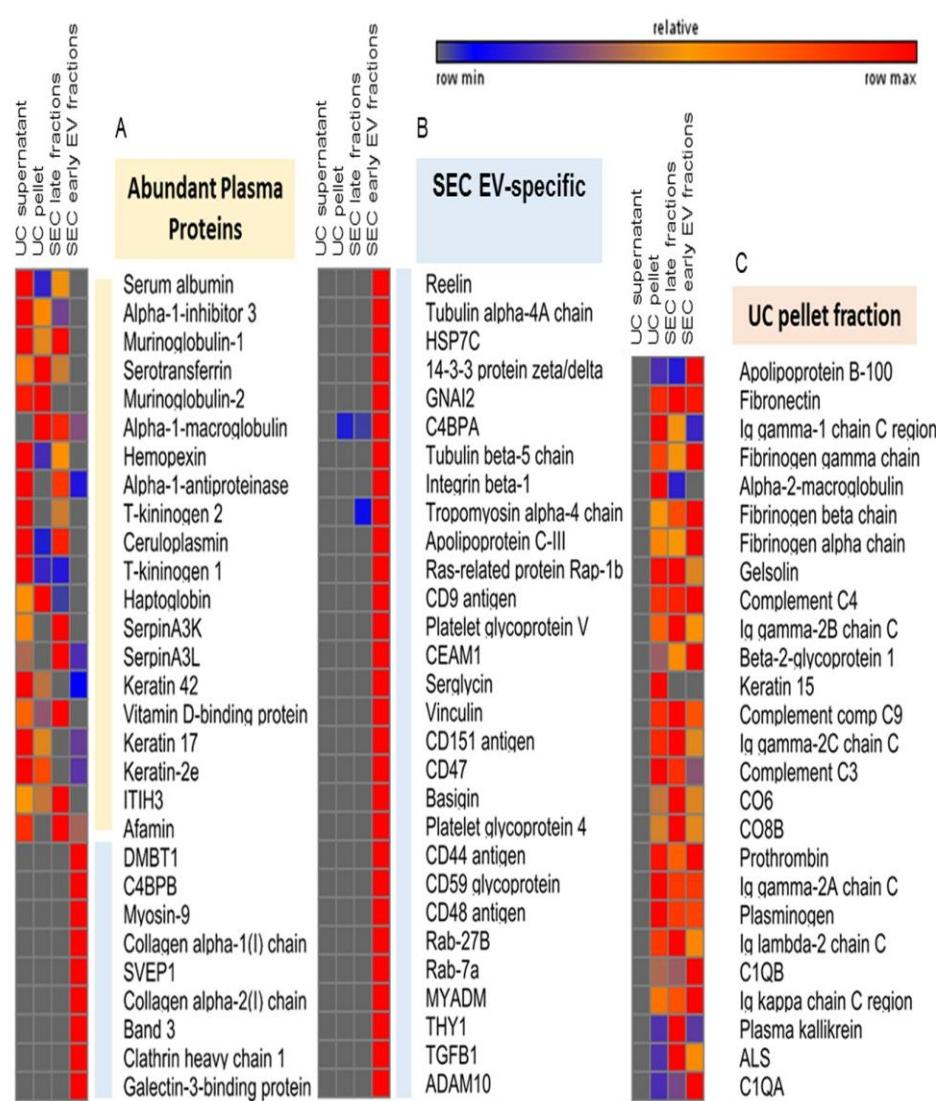
virgin with tumor and involution with tumor plasma samples have completed exosome isolation and proteomic analysis with the Hansen lab. The data are presented below in Figure 3 in combination with the results from Task 4. In summary, we did observe proteomic differences between the EVs isolated from virgin versus involution animals. In the context of tumor being present, there were additional tumor-specific changes seen that did not have a clear pattern of difference between the parity groups. Further detailed analysis of this data is required. Jessica Hall, UCCC Summer Research Student from 2016 in the Borges lab has now graduated college and will be working as a PRA in the Borges lab and will complete this data analysis, beginning in May funded though other resources.

Task 3 Summary: Nearing completion of complete data analysis.

Task 4 –Perform functional analysis of the exosomes from the animal cohorts on tumor cell behavior using the a target cell line for proliferation, migration and alteration of tumor morphology and apoptosis rates in 3D culture models.
Months 6-18

Task 4 final report: We developed optimal isolation methods for primary animal samples for isolation of EVs. We proceeded with the animal EV functional experiments and were challenged by the congenic animal breast cancer cell lines not performing as expected in wound closure migration and invasion assays. The tumor cells from the TNBC 66cl4 murine mammary cell line, which would be the best equivalent of the human TNBC MD-MBA-231 cell line, would either float off or fail to close the wound reliably in culture. We ran into similar challenges with the D2AR and D2OR cell lines. Therefore we developed a 3D Organoid model as a read out for functional changes induced by the EV onto the organoids, including increased branching, cell migration, abnormal structure formation and invasion. We then proceeded with the planned analysis and data is presented in Figure 4, along with the proteomic analysis from task 3.

Task 4 Summary: Complete. Data would benefit from additional numbers for replicates if additional animal samples become available in the future.
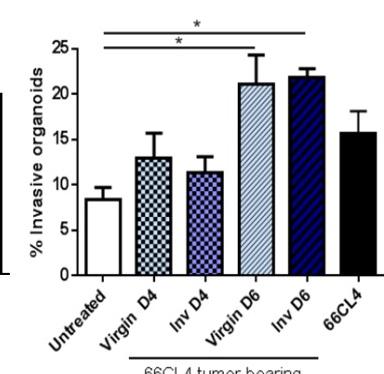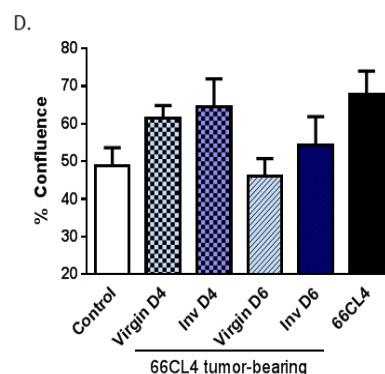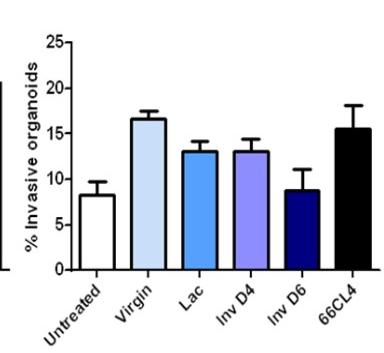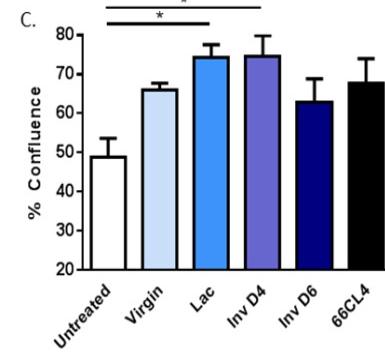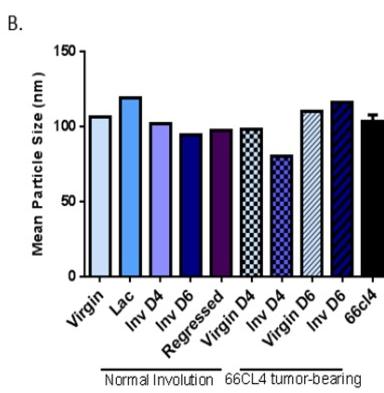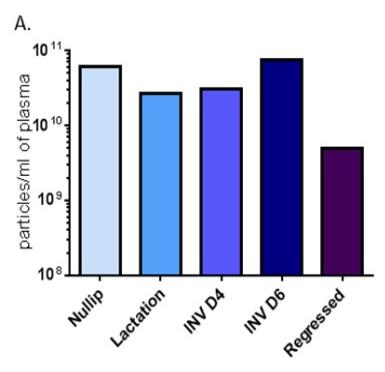
Figure 3. Mouse mammary involution affects the function and protein content of plasma EVs.

The particle yield (A) and mean size (B) of EVs purified from 1 ml of pooled mouse plasma (5 mice total) by SEC was determined using the Nanosight instrument. *There were no significant differences in particle size or yield across involution groups.* C. D2OR mouse mammary tumor cells were plated at 5,000 cells per well in the presence of purified EVs and imaged every 4 h using the Incucyte instrument (left). EV-treated D2OR cells were plated in 3D culture in a matrigel pad and grown for 8 d to establish organoids. Matrigel pads were fixed, harvested, imbedded in paraffin, H&E stained, and images were collected on the Vectra 3. Organoids from three sections were scored by three blinded readers for non-invasive (perfectly round, type 1), those with an invasive edge (type 2), and fully invasive (protruding cells or linear, type 3). The percentage of type 3 organoids was compared across groups using one-way ANOVA. *EVs from lactating and early involution mice (day 4) increase the proliferation of D2OR cells but not the invasive properties.* D. The effect of EVs purified from mice bearing 66CL4 mammary tumors throughout involution was determined as in (B). *EVs from mice bearing 6 day tumors increased the frequency of invasive organoids regardless of involution status.* E. The protein content of EVs throughout mouse mammary involution was determined in plasma pooled from 5 mice per group throughout involution. Samples were analyzed on a Q Exactive Quadripole Orbitrap mass spectrometer. Spectra data was matched against the SwissProt database and filtered using Scaffold Proteome Software. Peptide and protein identifications were accepted if they could be established with greater than 95% probability and at least two identified unique peptides. Spectral counts were normalized to the total number of spectral counts in each sample and fold change relative to virgin mice was calculated. Proteins with at least a 2 fold increase during involution are shown. Of the 862 proteins identified, 108 proteins were increased by day 4 of involution. *The proteomic content of EVs changes during involution, increasing proteins involved in cell growth, cell signaling, and enzymes involved in the regulation of energy metabolism. These proteins largely return to baseline in fully regressed animals (day 30).*

| | | Fold change in normalized spectral counts relative to virgin mice. | | | | | | | |
| | | Normal Involution | | | | 66CL4 tumor-bearing | | | |
	Gene Name	Lactation	Inv D4	Inv D6	Regressed	Virgin D4	Inv D4	Virgin D6	Inv D6
Cell Proliferation	Transforming growth factor beta-1	7	7	4	1	1	7	2	2
	Myc target protein 1	7	7	1	1	1	7	2	1
	Major vault protein	5	6	1	4	3	6	9	5
	Pyruvate kinase PKM	23	5	61	1	7	5	12	7
	Transforming protein RhoA	3	4	1	1	5	4	4	2
	14-3-3 protein eta	5	3	1	1	2	3	2	1
	14-3-3 protein epsilon	2	3	1	2	1	3	2	1
	14-3-3 protein zeta/delta	2	2	1	2	1	2	1	1
	ADAM10	2	3	1	1	2	3	7	5
Metabolism/Energy	Aspartyl aminopeptidase	1	19	24	1	1	19	20	1
	Deoxyribose-phosphate aldolase	5	7	1	1	1	7	11	10
	Fructose-bisphosphate aldolase A	17	5	20	1	10	5	9	6
	Flavin reductase (NADPH)	15	28	1	5	12	28	50	14
	Arginase-1	1	5	8	1	5	5	10	16
	ATP synthase alpha	1	7	1	1	9	7	29	24
	ATP synthase beta	2	5	1	1	6	5	12	9
	Na/K-transporting ATPase	2	3	1	1	3	3	3	2

Task 5- Perform functional analysis of the exosomes from the animal cohorts on their ability to induce immunosuppressive cells and drive the immune function of monocytes, Tregs, MDSC and effector T cells to a pro-tumor, immunosuppressive state.

Months 12-24

Task 5 Final Report: We began this task by working up the assays, as pre-existing methods were not available at the start of this grant of for understanding what EV do or have done to them in the context of co-culture with immune cells and the knowledge of what "dose" of EV would be needed to impart an immune effect was part of what needed to be optimized. We used EV from the MDMBA-231 TNBC human cell line, our positive control throughout this project, and have shown that EV are phagocytozed by immune cells of myeloid/monocytic lineage and not T cells, as would be expected. After uptake of EV, there is a fundamental shift in the myeloid lineage population with a dramatic decrease in lin negative/DR positive cell population. We have looked extensively to determine if a maturation or phenotypic shift occurs in the lin-DR+ population with no increase in other immune cell subsets seen, suggesting a phenotypic shift after EV exposure, if occurring, is not occurring torwards a typical myeloid or monocytic lineage cell. We did not see a clear increase in cell death either, but will need further work to clarify that result. After exposure of normal donor human PBMCs to EV, the ability of the myeloid/monocytic APC population to appropriately stimulate allogeneic T cells in mixed leukocyte reaction assays was significantly decreased, as measure by both proliferation and activation of CD25 of the effector T cell subset. These results are presented in Figure 4.

Figure 4: EV from human TNBC breast cancer are immunologically active and suppress effector T cell function. EV were rapidly phagocytozed by human PBMCs across most of the myeloid/monocytic lineage cells with a resulting decrease in the number of putative DCs [lin-DR+] antigen presenting cells in culture. When EV exposed PBMCs were co-cultured with allogenic CD8+ effector T cells from healthy donors in standard MLR assay, the ability of the CD8+ T cell to proliferate and upregulate CD25 expression as a marker of effective activation of T cell function were significantly reduced. These data show a significant immune suppressive effect on effective anti-cancer human immune function through direct interaction of EV with circulating immune cells as an additional means of cancer induced immune suppression that could have systemic implications as well as local paracrine effect in the tumor milieu.
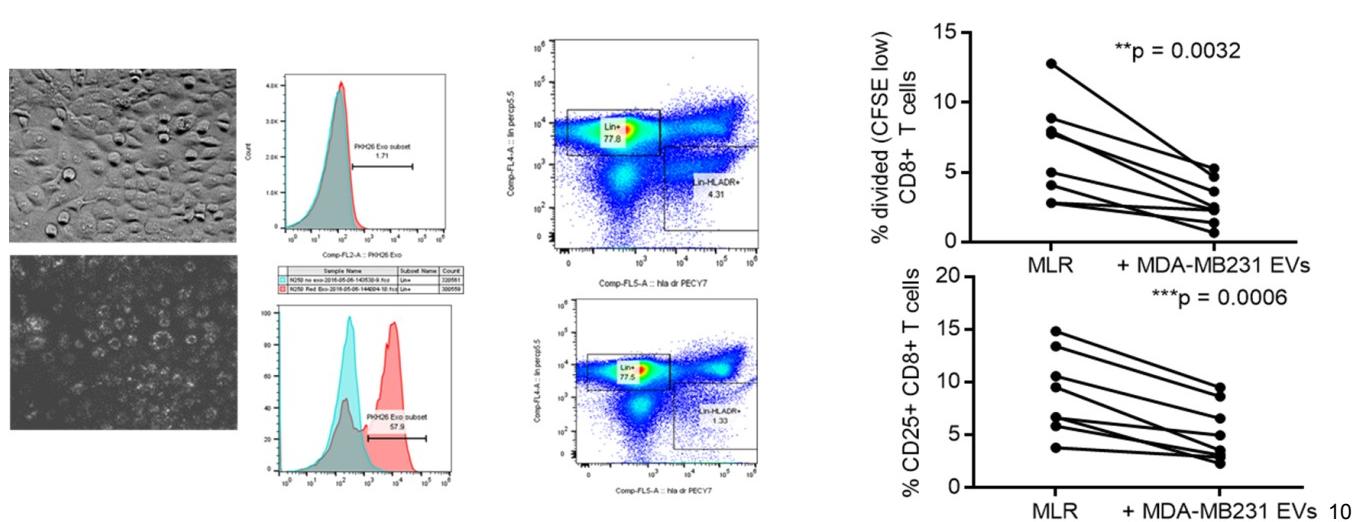
Two specific challenges have held up running the immune assays in the rodent samples of parity. The main rate limiting step was the amount of sample available and the number of EV which could be obtained from the animal plasma, which was insufficient to complete both the functional EV experiments from Task 4 and these experiments, as optimization of the assays would be needed before full results could be expected. Also, the challenge with the murine congenic cancer cell lines and their behavior in in vito culture for the proliferation, migration and invasion assays lead to a challenge of knowing which rodent EV cell line source would be the best positive control to know that the assays were working optimally. These problems continue to be worked on and we plan to obtain additional rodent samples from our collaborator to pursue the solutions and perform this task to completion under further funding.

**Task 5 summary: Started, not yet complete.**

Task 6- Exosome isolation and characterization from the human samples from normal young women and YWBC samples**Months 6-18**

Task 6 Final Report: Using our optimized isolation and characterization techniques from Task 1, we proceeded to isolate the planned cases of 20 unaffected young women and 20 cases of YWBC as outlined above. See table 1 for the cases used for this task:

Table 1: Clinical Characteristics of samples from the Colorado YWBC cohort

			Clinical characteristics				
PPBC Status	Pathologic Grade	Stage	Biologic Subtype	Histologic Subtype	Recurrance	KI67% (Tumor)	Ki67% (Stroma)
PPBC	Grade II	III	Luminal B	Ductal	None	64	2
PPBC	Grade III	II	Luminal B	Ductal	None	26	2
PPBC	Grade III	III	Luminal B	Inflammatory	Regional and Distant	57	13
PPBC	Grade III	II	Triple Negative	Ductal	None	34	12
PPBC	Grade II	II	Luminal A	Ductal	Distant	12	1
PPBC	Grade III	II	Luminal B	Ductal	None	n/a	n/a
PPBC	Grade III	II	Triple Negative	Ductal	None	66	11
PPBC	unknown	III	Luminal B	Other	Unknown	22	1
PPBC	Grade I	IV	Luminal B	Lobular	Never disease free	27	1
PPBC	Grade II	II	Luminal B	Ductal	None	40	1
Nulliparous	Grade II	II	Luminal B	Ductal	None	25	1
Nulliparous	Grade II	II	Luminal A	Ductal	Regional	7	3
Nulliparous	Grade II	IV	Luminal B	Inflammatory	None	61	3
Nulliparous	Grade III	II	Triple Negative	Ductal	None	60	11
Nulliparous	Grade II	II	Luminal B	Ductal	None	7	11
Nulliparous		I	Triple Neg	Ductal	Regional	n/a	n/a
Nulliparous	Grade III	II	Luminal B	Ductal	Local	n/a	n/a
Nulliparous	Grade III	II	Luminal B	Ductal	None	1	0

We have previously conducted an IRB approved, cohort study of women diagnosed with breast cancer at age ≤45, The Young Women's Breast Cancer [YWBC] Colorado Cohort Study. Cases from the Cohort were included in IRB approved and HRPO approved sample re-use protocol created specifically for this project/grant. Cases were chosen for this analysis if parity status/time between last childbirth and diagnosis was available from medical records. Parity status was defined as nulliparous or PPBC (up to 5 years postpartum). Clinicopathologic characteristics were obtained from pathology records. Outcomes data were obtained through the State Tumor Registrar. We isolated EVs using size-exclusion chromatography [SEC] from the plasma of 10 unaffected young women and 20 YWBC patients balanced for parity, age, subtype and stage as outlined above and in the methods paper in the appendix. Representative data of EV isolation results are above in Figure 1 with the rodent data and below in Figure 5. These EV were then used in the downstream assays outlined in the Tasks to follow.
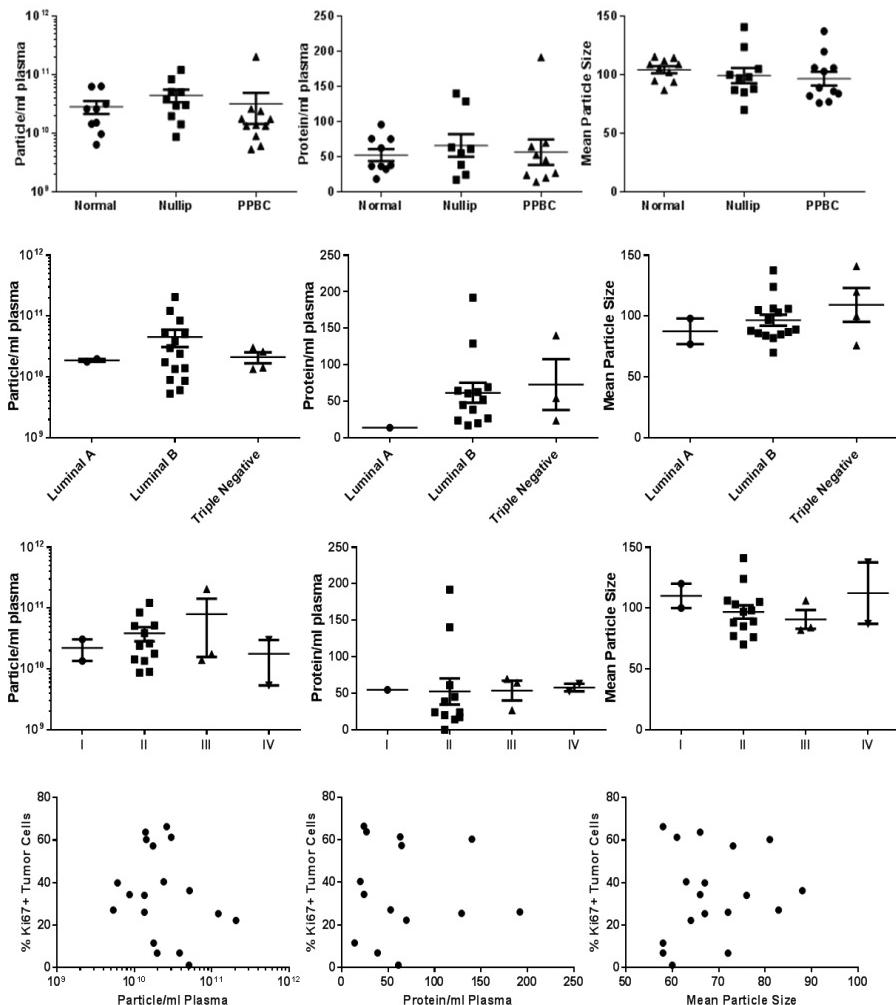
Figure 8. The size, yield, and protein content of human EVs do not correlate with known prognostic indicators in YWBC. The particle yield (left) and mean size (right) were measured for each human EV sample on a Nanosight instrument by nanoparticle tracking analysis. EV protein content was measured in lysed samples using a BCA assay measured against a standard curve of BSA. These measurements were compared with clinical information including parity status (A), tumor biologic sub-type (B), tumor stage (C), and % of Ki67+ measured by immunohistochemistry (D). No variables were found to associate with these clinical factors.

Task 6 summary: Complete

Task 7 –Proteomic analysis of the exosomes from normal and YWBC cases.
Months 12-30
- a. Work to be performed in the Hansen lab, similar to as outlined for the animal samples in Task 3
- b. Proteome content will be compared between the animal groups and the YWBC samples by parity status to correlate for similar content that may be unique to the effects of postpartum involution on PPBC. Unique proteins identified as matched between involution, involution with tumor and human PPBC will be explored in greater detail for functional characteristics and insight into possible mechanism of functioning.

Task 7 Final Report: We were able to rapidly proceed with the planned proteomics once the EV isolation methods determined that SEC would give us an enriched and pure enough sample with elimination of contaminating blood proteins to generate useable results. We proceed the samples as planned and the results are summarized in Figure 6 and 7 as well as Table 2 and 3. Initial approach was to evaluate cancer versus non-cancer bearing samples and then drill down on the differences between nulliparous YWBC and PPBC.
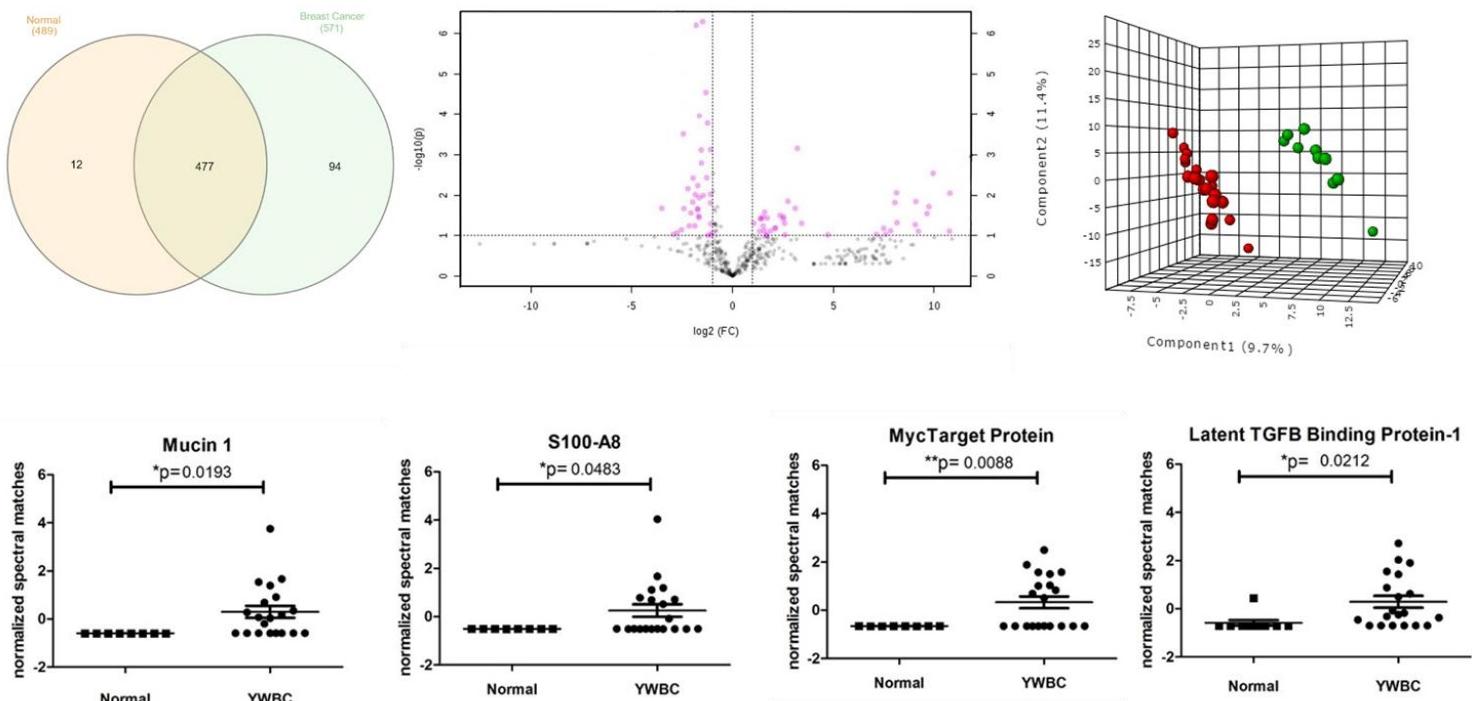
Figure 7. Comparison of the protein content of human EVs in healthy donors and YWBC patients. EVs were purified by SEC from the plasma of 10 healthy donors or 20 YWBC patients. Samples were analyzed on a Q Exactive Quadripole Orbitrap mass spectrometer. Spectra data was matched against the SwissProt database and filtered using Scaffold Proteome Software. Peptide and protein identifications were accepted if they could be established with greater than 95% probability and at least two identified unique peptides. A. Of the 583 proteins identified, 94 were unique to the YWBC dataset. B. Data were compared using MetaboAnalyst 3.0 software, with the lowest 25% of proteins filtered using the relative standard deviation method. Data were normalized by sum, transformed by calculating $\log_2$, and scaled using the autoscaling function. Univariate analysis was performed using a volcano plot to identify proteins that are significantly increased in YWBC patients (right half) or increased in healthy donors (left half) with thresholds of at least a two-fold change (x-axis) and a p value of at least 0.05 (y-axis), shown in pink. C. Multivariate analysis was performed using the partial least squares- discriminant analysis method. Variables were sorted into components according to their ability to discriminate between YWBC and healthy donors. The 3D plot of Component 1, 2, and 3 is shown, in which the number of spectral matches for proteins in these groups distinguish YWBC patients (green) from healthy donors (red). D. Spectral counts of proteins identified by volcano plot and as part of the component analysis were compared by t tests.

The results show typical cancer/breast cancer proteins, such as MUC1 [measured as serum CA27-29 in clinical practice], MYC and TGF-b. Interesting, S-100 is a melanoma marker that has been reported to be occasionally expressed in breast cancers. We plan to explore this particular marker further to determine if there is increased expression of S-100 in EV from YWBC in comparison to women older at diagnosis, as YWBC is known for a propensity towards increased risk of brain mets as is melanoma, and EVs are implicated in the ability to establish pre-metastatic niches.

13

**Table 2: Important proteins identified by volcano plot comparing EVs from healthy donors and YWBC patients.**

	Peaks(mz/rt)	FC	log2(FC)	p.value	-log10(p)
1	Chloride intracellular channel protein 1	0.35938	-1.4764	5.1379e-07	6.2892
2	L-lactate dehydrogenase A chain	0.28673	-1.8023	6.3518e-07	6.1971
3	Pyruvate kinase PKM	0.40268	-1.3123	2.9286e-05	4.5333
4	Tropomyosin alpha-3 chain	0.32108	-1.639	0.00011228	3.9497
5	Carbonic anhydrase 2	0.42568	-1.2321	0.00016421	3.7846
6	Ras GTPase-activating-like protein IQGAP2	0.18458	-2.4377	0.00030755	3.5121
7	Catalase	9.3408	3.2235	0.00069914	3.1554
8	Cell division control protein 42 homolog	0.47393	-1.0773	0.00075325	3.1231
9	Tropomyosin alpha-1 chain	0.34259	-1.5454	0.00076704	3.1152
10	GMP reductase 1	0.34512	-1.5348	0.001614	2.7921
11	Metalloproteinase inhibitor 1	994.74	9.9582	0.002893	2.5387
12	Coronin-1A	0.41347	-1.2742	0.0037129	2.4303
13	Ig kappa chain V-II region FR	0.25858	-1.9513	0.0038005	2.4202
14	6-phosphogluconate dehydrogenase, decarboxylating	0.30418	-1.717	0.0058448	2.2332
15	Cytosolic non-specific dipeptidase	0.21682	-2.2054	0.0069326	2.1591
16	Myc target protein 1	283.31	8.1462	0.0087325	2.0564
17	Target of Nesh-SH3	1769.6	10.789	0.0089352	2.0489
18	Complement C1q subcomponent subunit B	0.4726	-1.0813	0.0094976	2.0224
19	Thymidine phosphorylase	0.28019	-1.8355	0.0097511	2.0109
20	Guanine nucleotide-binding protein Gz subunit alpha	0.36684	-1.4468	0.010272	1.9883
21	Protein S100-A6	0.31982	-1.6447	0.011587	1.936
22	Calpain small subunit 1	6.7488	2.7546	0.014221	1.8471
23	Dynactin subunit 2	548.29	9.0988	0.014421	1.841
24	Tyrosine-protein phosphatase non-receptor type 6	0.25594	-1.9661	0.014906	1.8266
25	Ig kappa chain V-I region Lay	267.29	8.0623	0.015253	1.8166
26	Guanine nucleotide-binding protein GI/GS/GT subunit beta-1	0.472	-1.0831	0.015626	1.8061
27	Mucin-1	862.22	9.7519	0.0193	1.7144
28	Fatty acid synthase	0.088116	-3.5045	0.021167	1.6743
29	Latent-transforming growth factor beta-binding protein 1	8.6911	3.1195	0.021232	1.673
30	Glucose-6-phosphate isomerase	0.1888	-2.4051	0.021558	1.6664
31	Kinesin-like protein KIF2A	0.30112	-1.7316	0.02222	1.6533
32	Superoxide dismutase Cu-Zn	0.30435	-1.7162	0.022248	1.6527
33	Ig kappa chain V-I region Wes	3.0285	1.5986	0.026549	1.576
34	Rap1 GTPase-activating protein 2	0.2397	-2.0607	0.027737	1.5569
35	Major vault protein	806.86	9.6562	0.028637	1.5431
36	Junction plakoglobin	5.1189	2.3558	0.031799	1.4976
37	Serine/threonine-protein phosphatase PP1-alpha catalytic subunit	0.31304	-1.6756	0.033124	1.4799
38	Desmoplakin	5.7687	2.5282	0.034325	1.4644
39	Heat shock 70 kDa protein 1A	2.8601	1.516	0.035152	1.4541
40	Caldesmon	0.31793	-1.6532	0.035732	1.4469
41	Ig kappa chain V-I region Ka	3.3146	1.7288	0.036945	1.4324
42	Ig alpha-2 chain C region	2.6341	1.3973	0.038059	1.4195
43	Ficolin-1	5.762	2.5266	0.038423	1.4154
44	Thrombospondin-4	2.6685	1.416	0.038457	1.415
45	Protein S100-A8	287.2	8.1659	0.048277	1.3163
46	Angiopoietin-related protein 6	2.0887	1.0626	0.04981	1.3027
47	Proteasome subunit alpha type-6	6.0152	2.5886	0.049949	1.3015
48	Prolow-density lipoprotein receptor-related protein 1	10.821	3.4357	0.049964	1.3013

Table 2. EVs were purified from plasma of 10 healthy donors or 20 YWBC patients by SEC. Samples were analyzed on a Q Exactive Quadripole Orbitrap mass spectrometer. Spectra data was matched against the SwissProt database and filtered using Scaffold Proteome Software. Peptide and protein identifications were accepted if they could be established with greater than 95% probability and at least two identified unique peptides. Data were compared using MetaboAnalyst 3.0 software, with the lowest 25% of proteins filtered using the relative standard deviation method. Data were normalized by sum, transformed by calculating log_2, and scaled using the autoscaling function. Univariate analysis was performed using a volcano plot (shown in Figure 6B) to identify proteins that are significantly increased in YWBC patients (positive log_2 values) or increased in healthy donors (negative log_2 values) with thresholds of at least a two-fold change (x-axis) and a p value of at least 0.05 (y-axis)

We next proceeded to break our proteomic data out by parity subgroup to identify unique characteristiscs of EV from PPBC in comparison to nulliparous YWBC cases.
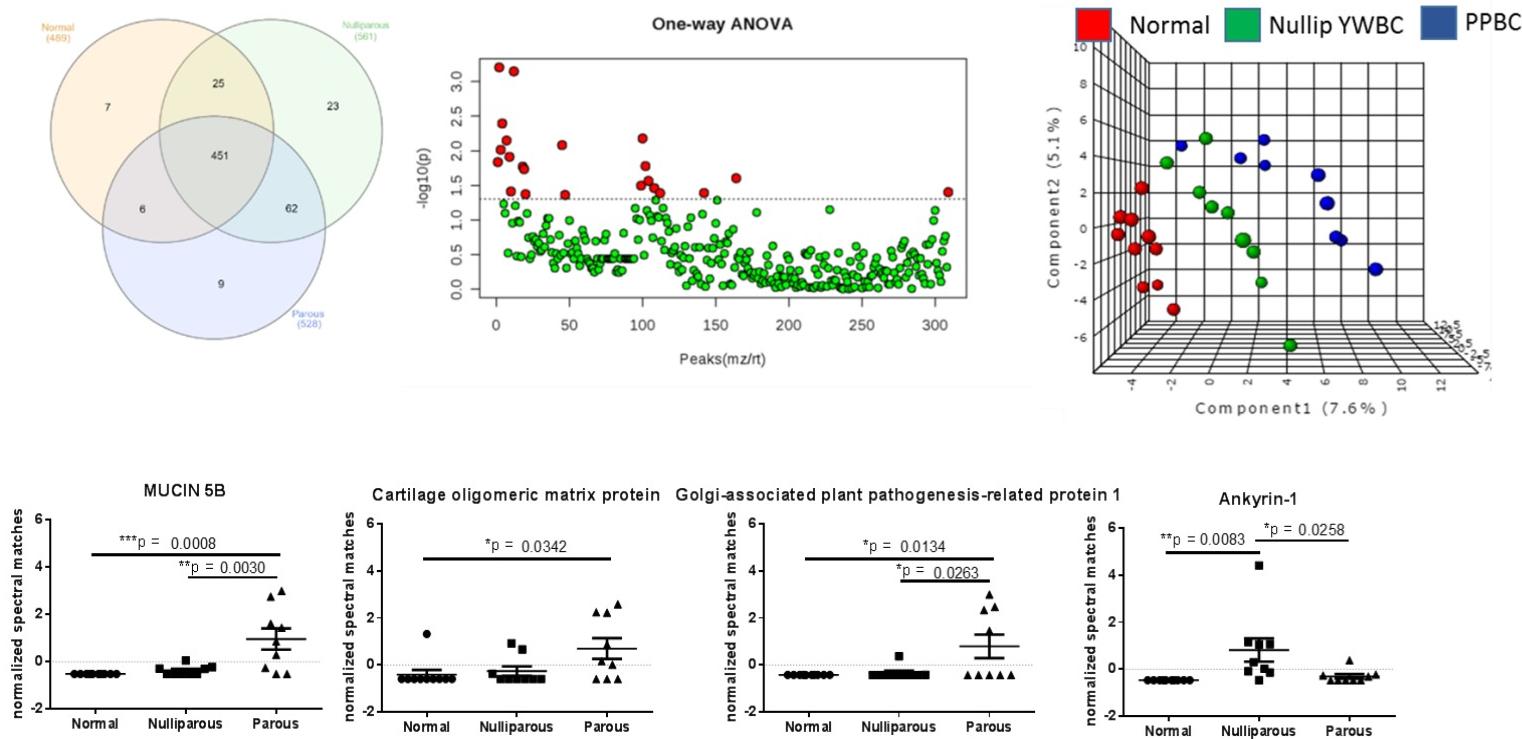
Figure 5. Extracellular vesicles YWBC and PPBC patients contain a unique set of proteins. EVs were purified by SEC from the plasma of 10 healthy donors or 20 YWBC patients. Samples were analyzed on a Q Exactive Quadripole Orbitrap mass spectrometer. Spectra data was matched against the SwissProt database and filtered using Scaffold Proteome Software. A. Of the 583 proteins identified, EVs from PPBC patients (bottom) contain 9 unique proteins compared to nulliparous YWBC patients (upper right), which contain 23 unique proteins. B. Data analysis was performed using univariate analysis was performed using one-way ANOVA with post-hoc analysis (Fisher's Least Significant Difference) and a p value threshold of 0.05 (y-axis). Multivariate analysis was performed using the partial least squares- discriminant analysis method. Variables were sorted into components according to their ability to discriminate between nulliparous YWBC patients, PPBC patients, and healthy donors. The 3D plot of Component 1, 2, and 3 is shown, in which the number of spectral matches for proteins in these groups distinguish nulliparous YWBC patients (green) from PPBC patients (blue) and healthy donors (red). D. Spectral matches for proteins identified with one-way ANOVA tests and as part of the principle component analysis were compared using one-way ANOVA.

These 4 proteins were highlighted due to their known roles in cancer, cancer invasion and metastasis. We are particularly interested in COMP as it has been specifically descried to have a role in invasion, which is a hallmark of PPBC we have identified in our prior research. We will be proceed to look at COMP expression in the tumors themselves and plan to proceed with mechanistic EV assays to see if blocking of COMP can eliminate the increased invasion and migration of EV [shown below] from PPBC.

Table 3: Important proteins identified by One-way ANOVA comparing healthy donors, nulliparous YWBC patients, and PPBC patients.

	Peaks (mz/rt)	f.value	p.value	-log10(p)	FDR	Fisher's LSD
1	Mucin-5B	10.05	0.00	3.20	0.11	Parous - Normal; Parous - Nulliparous
2	Monocyte differentiation antigen CD14	9.81	0.00	3.15	0.11	Parous - Normal; Parous - Nulliparous
3	Metalloproteinase inhibitor 1	6.93	0.00	2.39	0.42	Nulliparous - Normal; Parous - Normal
4	Catalase	6.17	0.01	2.18	0.43	Nulliparous - Normal; Parous - Normal
5	Mucin-1	6.07	0.01	2.15	0.43	Parous - Normal
6	Golgi-associated plant pathogenesis-related protein 1	5.84	0.01	2.08	0.43	Parous - Normal; Parous - Nulliparous
7	Target of Nesh-SH3	5.62	0.01	2.01	0.43	Nulliparous - Normal; Parous - Normal
8	Mucin-2	5.28	0.01	1.91	0.47	Parous - Normal; Parous - Nulliparous
9	Ankyrin-1	5.03	0.01	1.84	0.47	Nulliparous - Normal; Nulliparous - Parous
10	Cartilage oligomeric matrix protein	4.85	0.02	1.78	0.47	Parous - Normal; Parous - Nulliparous
11	Myc target protein 1	4.82	0.02	1.77	0.47	Nulliparous - Normal; Parous - Normal
12	Ig kappa chain V-region Lay	4.71	0.02	1.73	0.47	Nulliparous - Normal; Parous - Normal
13	Cholesteryl ester transfer protein	4.30	0.02	1.60	0.59	Parous - Normal; Parous - Nulliparous
14	Latent-transforming growth factor beta-binding protein 1	4.18	0.03	1.56	0.60	Nulliparous - Normal
15	Spectrin beta chain, erythrocytic	3.97	0.03	1.50	0.61	Nulliparous - Normal; Nulliparous - Parous
16	Ig kappa chain V-region Ka	3.86	0.03	1.46	0.61	Parous - Normal
17	Dynactin subunit 2	3.71	0.04	1.41	0.61	Nulliparous - Normal; Parous - Normal
18	Platelet glycoprotein V	3.68	0.04	1.40	0.61	Normal - Nulliparous
19	Thrombospondin-4	3.65	0.04	1.39	0.61	Parous - Normal
20	Nucleobindin-1	3.64	0.04	1.39	0.61	Parous - Normal; Parous - Nulliparous
21	Annexin A1	3.60	0.04	1.37	0.61	Parous - Normal; Parous - Nulliparous
22	Clathrin light chain A	3.57	0.04	1.36	0.61	Nulliparous - Normal

**Table 3. EVs were purified from plasma of 10 healthy donors or 20 YWBC patients by SEC.** Samples were analyzed on a Q Exactive Quadripole Orbitrap mass spectrometer. Spectra data was matched against the SwissProt database and filtered using Scaffold Proteome Software. Peptide and protein identifications were accepted if they could be established with greater than 95% probability and at least two identified unique peptides. Data were compared using MetaboAnalyst 3.0 software, with the lowest 25% of proteins filtered using the relative standard deviation method. Data were normalized by sum, transformed by calculating log$_2$, and scaled using the autoscaling function. Univariate analysis was performed using one-way ANOVA with post-hoc analysis (Fisher's Least Significant Difference) and a p value threshold of 0.05 (y-axis). Proteins that discriminate PPBC patients (Parous) from nulliparous patients, PPBC patients from healthy donors (normal), and Nulliparous patients from healthy donors are shown. The Fisher's LSD results indicate which groups are significantly different in the comparison.

Task 7 summary: Completed

Task 8 – Perform the functional analysis of the exosomes from unaffected young women and YWBC on tumor cell behavior using the target cell line of MCF10.DCIS human cell line for proliferation, migration and alteration of tumor morphology and apoptosis rates in 3D culture models. **Months 18-24**

Task 8 final report: As previously reported, we were able to develop assays and demonstrate that EV isolated by SEC from the human MD-MBA-231 cell line [TNBC] could transform the behavior of the non-invasive and minimally migratory human DCIS.com cell line *in vitro*. Of note, results were most pronounced when cells we co-cultured with the EV to allow for internalization and processing, suggesting that the EV effect is occurring through alteration of intracellular pathways in the cancer, not by merely cell contact or external autocrine/paracrine effects.
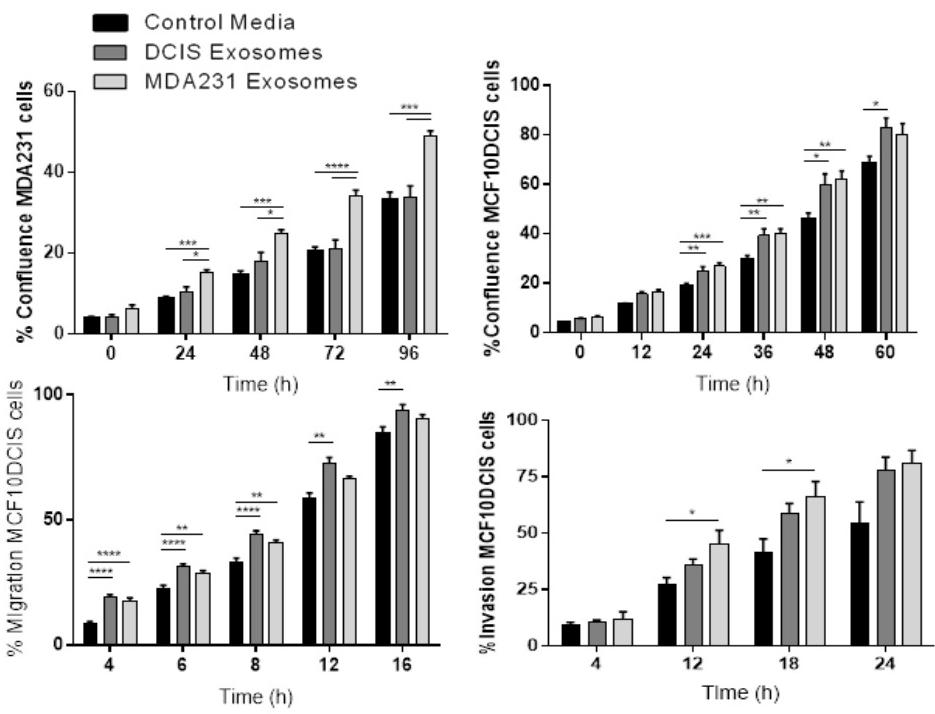
Figure 8. Exosomes isolated from the DCIS initially non-invasive human cell line and the triple negative breast cancer line MDA231 increase proliferation and migration of cells from both parent cell lines MDA231 and MCF7-DCIS.com respectively. To isolate exosomes from human breast cancer lines, MDA231 and MCF10-DCIS.com cells were grown to confluence and transferred into serum-free media. After 48 h media was harvested, concentrated in ultrafiltration tubes, and exosomes were isolated by size-exclusion chromatography. **A and B**. MDA231 or MCF10-DCIS.com cells were seeded at 4,000 cells per well in a 96-well plate +/- 5×10^8 exosomes and phase contrast images were taken over 96 or 60 h using an Incucyte instrument. **C**. MCF10-DCIS.com cells were plated and grown to confluence in a 96-well plate coated with 0.2 mg/ml matrigel. A scratch wound assay was performed +/- 5×10^8 exosomes and imaged over 16 h using an Incucyte instrument. **D**. For the invasion assays, cells were plated on matrigel-coated wells as in **(C)** and covered with a 2 mg/ml matrigel pad after wounding. Cell invasion was determined +/- 5×10^8 exosomes over 24 h using an Incucyte instrument.
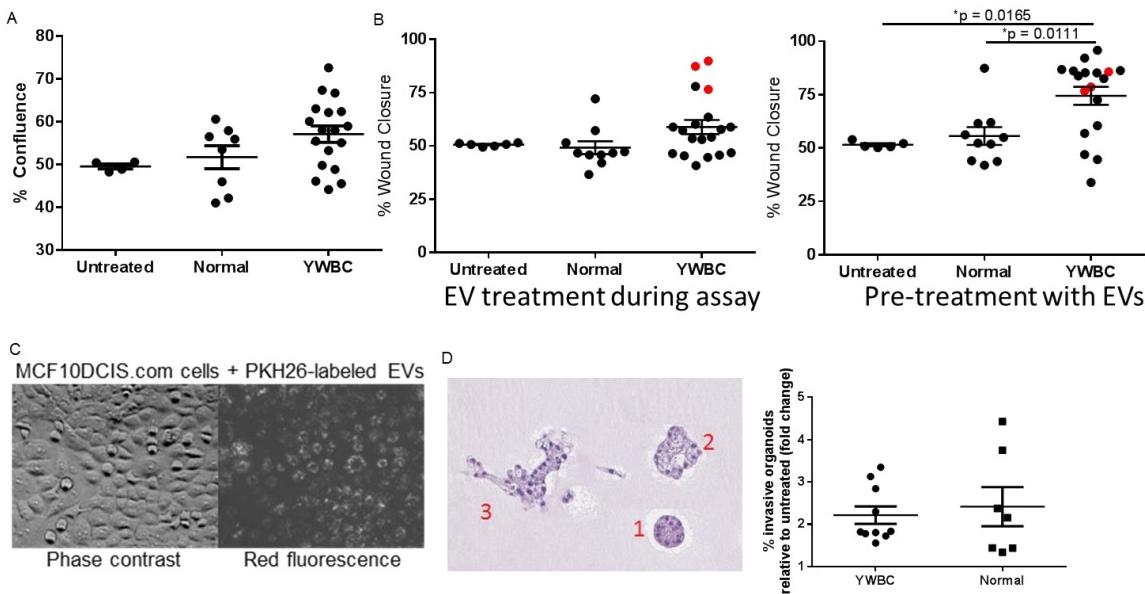
Figure 9. EVs from YWBC patients increase proliferation and invasive properties of breast cancer cells in vitro. A. EVs were purified from 10 PPBC patients, 9 nulliparous YWBC patients, and 10 healthy donors. Human MCF10 DCIS.com cells were plated at 5,000 cells per well in a 96 well plate and imaged with phase-contrast every 4 h on an Incucyte instrument. The percentage of surface area covered by cells was calculated using the IncuCyte Zoom software and compared accross groups using one-way ANOVA. *Although some EVs from some patients significantly*

17

increased proliferation of these tumor cells, the YWBC group as a whole did not have a significantly increased activity compared to untreated and EVs from healthy controls. B. DCIS cells were plated at 35,000 cells per well for 16 h on 0.2 mg/ml matrigel, wounded using a 96-well WoundMaker, washed and layered with a 2 mg/ml matrigel pad, and overlayed with low-serum (1%) media. EV treatment during the assay (left) was performed by adding $2.5x10^9$ particles/ml to both the matrigel pad and overlaying media. Pre-treatment with EVs (right) was performed by adding $2.5x10^9$ particles/ml to the media after cells were plated and washed out after wounding. Images were taken every 2 h for 48 h and relative wound density was calculated using IncucyteZoom software. Under these conditions, untreated cells closed the wounds within about 40 h and higher concentrations of matrigel prevented wound closure. Groups were compared using a one-way ANOVA. *EVs from YWBC patients significantly increased invasion of human MCF10DCIS.com cells into a matrigel pad in 2D culture conditions. Furthermore, this increase was highly significant after pre-treatment with EVs, suggesting that transcriptional changes may be required for an increased invasive phenotype.*
C. Human MCF10 DCIS.com cells internalize fluorescently-labeled EVs. The image shown is a black and white representation of punctate cytoplasmic PKH26-labeled EVs after 4 h of incubation, demonstrating that tumor cells that are pre-treated engulf EVs. D. EV-treated human MCF10.DCIS.com cells were plated in 3D culture in a 4 mg/ml matrigel pad and grown for 8 d to establish organoids. Matrigel pads were fixed, harvested, imbedded in paraffin, H&E stained, and images were collected on the Vectra 3. Organoids from three sections were scored by three blinded readers for non-invasive (perfectly round, type 1), those with an invasive edge (type 2), and fully invasive (protruding cells or linear, type 3), examples shown on the left. The percentage of type 3 organoids was compared across groups using a t test*. Human MCF10.DCIS.com cells form invasive organoids in 3D culture in the presence of EVs from both healthy donors and YWBC patients.

Table 4 recapitulates the clinical characteristics and demonstrates the EV activity in YWBC patients. Shown in grey are the patients included in subsequent proteomics analysis as patients with EVs that increase invasion and proliferation.

| | EV activity in *in vitro* assays | | | Clinical characteristics | | | | | | | |
Patient #	Pre-treatment invasion assay	During assay treatment invasion assay	Proliferation assay	PPBC Status	Pathologic Grade	Stage	Biologic Subtype	Histologic Subtype	Recurrence	KI67% (Tumor)	Ki67% (Stroma)
26	**	****	**	PPBC	Grade II	III	Luminal B	Ductal	None	64	2
23	**	****	*	PPBC	Grade III	II	Luminal B	Ductal	None	26	2
39	*	**	*	PPBC	Grade III	III	Luminal B	Inflammatory	Regional and Distant	57	13
67	**	none	**	PPBC	Grade III	II	Triple Negative	Ductal	None	34	12
98	**	none	**	PPBC	Grade II	II	Luminal A	Ductal	Distant	12	1
35	***	none	none	PPBC	Grade III	II	Luminal B	Ductal	None	n/a	n/a
108	*	none	none	PPBC	Grade III	II	Triple Negative	Ductal	None	66	11
43	none	*	none	PPBC	unknown	III	Luminal B	Other	Unknown	22	1
22	*	none	none	PPBC	Grade I	IV	Luminal B	Lobular	Never disease free	27	1
42	none	none	none	PPBC	Grade II	II	Luminal B	Ductal	None	40	1
24	n/a	****	**	Nulliparous	Grade II	II	Luminal B	Ductal	None	25	1
99	*	none	**	Nulliparous	Grade II	II	Luminal A	Ductal	Regional	7	3
36	**	none	none	Nulliparous	Grade II	IV	Luminal B	Inflammatory	None	61	3
34	***	none	none	Nulliparous	Grade III	II	Triple Negative	Ductal	None	60	11
16	***	none	none	Nulliparous	Grade II	II	Luminal B	Ductal	None	7	11
402	none	none	*	Nulliparous		I	Triple Neg	Ductal	Regional	n/a	n/a
53	none	none	none	Nulliparous	Grade III	II	Luminal B	Ductal	Local	n/a	n/a
110	none	none	none	Nulliparous	Grade III	II	Luminal B	Ductal	None	1	0

We plan to increase this sample size to be able to gain further insight to the effect of tumor EV on breast cancer outcomes, as there was a clear trend for cancers with more aggressive phenotypes o known recurrence to have functional EV, but more cases with and without recurrence by biologic subtype and parity status are required to increase the power for detection of these details.

Task 8 summary: Complete

Task 9- Perform functional analysis of the exosomes from the human cohorts on their ability to induce immunosuppressive cells and drive the immune function of monocytes, Tregs, MDSC and effector T cells to a pro-tumor, immunosuppressive state.
Months 18-24

Task will be completed months 24-30.

We ran out of time and were not able to start this task, as ongoing optimization of the assays involved is needed before using the somewhat limited resource of EV isolated from primary human sample.

Task 9 – not completed

Task 10 – Isolate exosomes from the samples collected pre and post drug intervention with either celecoxib or nil on our completed WOO human clinical trial.
Months 18-33
  a. Given the unique and precious nature of these samples and the effort it would take to recreate them, we will wait until we have completed significant work on the animal and human samples from the other studies and feel secure on our techniques and methods with isolation and functional read outs.

Task 10 Final results: The EVs from these patients were isolated as planned. There were no structural, protein content of size differences identified in EV characterization [data not shown]

Task 10 Summary: Completed

Task 11-Perform the proteomic analysis on exosomes from the WOO clinical trial samples.
Months 24-36
  a. We will continue with Task 11, using techniques optimized through Tasks 3 and 7.
  b. We will focus on those changes to the proteome content that correlates most with unique characteristics found in the involution, involution with tumor and PPBC samples.

Task 11 Final Report: using the same methods as outlined above, we performed this task. Results are shown below in Figure 10.

Task 11: completed

Task 12- Analyze the human exosome data (quantity, proteome content and functional data) from the YWBC samples and the WOO clinical trial and compare with known clinicopathologic parameters and study outcomes for clinical relevance
Months 24-33
  a. The results from the exosomes from the WOO trial samples pre and post on each of the 20 cases will be correlated with the pre and post Ki-67 index and its change across the study drug intervention time period and by cases status description of PPBC versus non-PPBC.
  b. Correlations with other known histologic parameters of breast cancer (stage, biologic subtype, age [young v very young] will be performed as well for all the YWBC cases
  c. Identification of any specific effects (Reversal) of the anti-inflammatory drug intervention assigned on the exosome quantity, proteome content or functioning with respect to the overall population and by the cohorts of interest (PPBC and non-PPBC). Correlations with biologic subtype of breast cancer will be explored in a hypothesis generating manner**.**

Task 12 Final Report: The clinicopathologic correlations from the YWBC cases is presented above in Table 4. The subset of the WOO study was too small to make any additional relevant findings. WE were fortunate to identify that we also had pre-existing rodent samples from the same experimental set up as used in the above tasks that included animals that had been treated with anti-inflammatories as part of a prior experimental design performed under other DOD funding to Schedin and Borges. We took advantage of this find and isolated EV from the parity groups and performed some analysis. Unfortunately sample size of the plasma from these animals limited how much work we could accomplish. Data presented below in Figure 11.

Task 12 Summary: Partially completed.
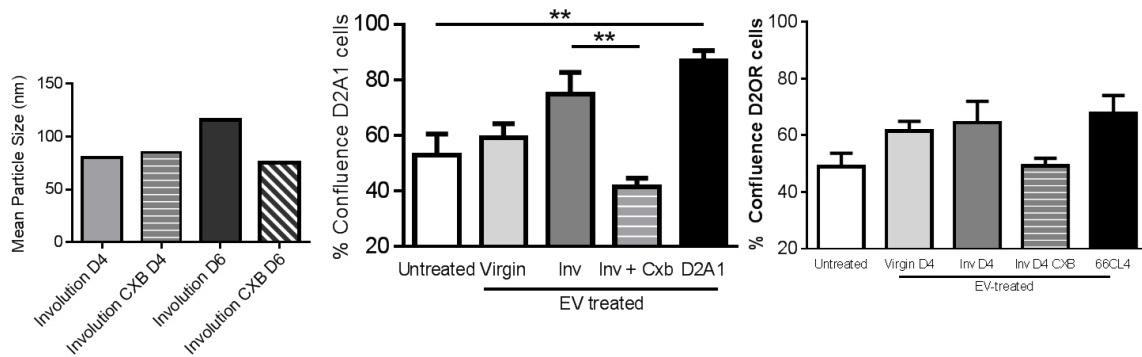
| | Normalized Spectral Counts | | | |
| | 66CL4 tumor-bearing | | | |
Gene Name	Inv D4	Inv D4 + CXB	Inv D6	Inv D6 + CXB
Transforming protein RhoA	13	8	6	5
14-3-3 protein eta	10	6	2	3
14-3-3 protein epsilon	15	5	6	3
14-3-3 protein zeta/delta	48	31	18	28
ADAM10	25	20	41	8
Aspartyl aminopeptidase	17	0	0	0
Deoxyribose-phosphate aldolase	6	2	22	9
Arginase-1	4	0	14	16
ATP synthase alpha	25	11	13	9
ATP synthase beta	25	7	46	13
Na/K-transporting ATPase	33	17	28	22
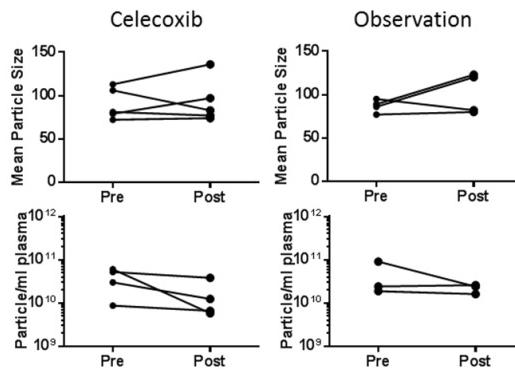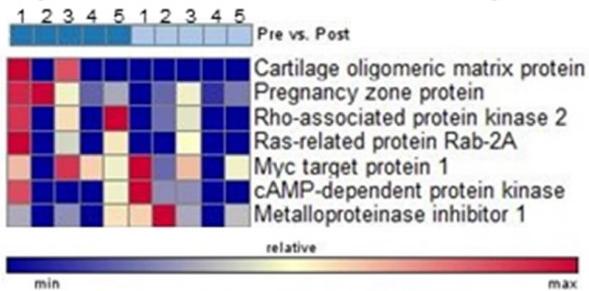
Figure 11. Celecoxib treatment may reduce EV activity in vitro and reduces proteins found to be increased in involuting mice with mammary tumor and YWBC patients. A. EVs were purified from plasma of 66CL4 tumor-bearing mice +/- celecoxib treatment and measured on the Nanosight instrument using nanoparticle tracking analysis. No changes in mean particle size were observed. B. D2A1 and D2OR cells were plated at 5,000 cells per well in a 96 well plate and imaged with phase-contrast every 4 h on an Incucyte instrument. The percentage of surface area covered by cells was calculated using the IncuCyte Zoom software and compared across groups using one-way ANOVA. *EVs from celexocib-treated mice had significantly reduced effects on D2A1 cells and a trend towards a reduced effect on D2OR cells.* C. The protein content of EVs throughout mouse mammary involution was determined in plasma pooled from 5 mice per group throughout involution. Samples were analyzed on a Q Exactive Quadripole Orbitrap mass

spectrometer. Spectra data was matched against the SwissProt database and filtered using Scaffold Proteome Software. Peptide and protein identifications were accepted if they could be established with greater than 95% probability and at least two identified unique peptides. Spectral counts were normalized to the total number of spectral counts in each sample and fold change relative to virgin mice was calculated. Proteins from Figure 3 with reduced spectral count after celecoxib treatment are shown. D. EVs were purified from plasma of YWBC patients either untreated (observation) treated with celecoxib during the window of time between diagnosis and definitive surgery. Particle size and yield was measured as in (A). *No significant changes were found following celecoxib treatment.* E. The protein content of EVs from PWBC patients before and after treatment with celecoxib was determined as in (C). *Many of the proteins that were found to be increased in YWBC patients were decreased after treatment with celecoxib. These changes were not found in the untreated patients*

Task 13 – Presentation of data accumulated to date at DOD Era of Hope Conference
Month 24 (approximately)

 Data will be presented at the next DOD Era of Hope Conference, when it is announced.

Task 14 - Preparation of manuscripts from the finalized data from the completion of Aims 1-3
Months 24-36

On target. We have submitted for 3rd review our methods paper [appendix]. The additional data is accepted fo presentation at the ISEV meeting in May. We have been invited to present at the ASEV meeting in the fall and a second manuscript is in preparation for submission in June.

Task 15 –Preparation and submission of ongoing grants based on outcomes from this work to continue to develop treatment and prevention strategies against the postpartum effect of involution on young women's breast cancer
Months 24-36

This is ongoing. In addition to the lead we plan to follow up outlined above, we have also identified in a separate body of work {Cancer Discovery, Goddard et al. 2016] that the liver undergoes involution with an increased frequency of live mets occurring that is recapitulated in our human epidemiologic data on sites of metastasis in YWBC/PPBC. We will explore the role of EV in this mechanism as well.

4. **Key Accomplishments:**

Summary of accomplishments under the three years of this award:

1. Complete detailed methodologic comparison of available exosome isolation techniques with optimization of techniques to our samples, representing a significant forthcoming contribution to the microvesicle field.

2. Identification of EV from YWBC and PPBC as having unique functional abilities and proteomic content with novel potential targets for prognostic, predictive of even potentially therapeutic approaches to be explored further.

3. Identification of tumor EV as having immune suppressive capacity in vitro.

Training opportunities:

4. A year of lab training for a post-doc, Dharanija Rao, who was recruited just after graduation to work on this project. Dr. Rao gained significant expertise in her year in my lab and on this project. However, she also decided that primary science was not her career goal and left with 2 weeks notice in August 2014. She is now a Medical Science Liason with Amgen and very happy.

5. New faculty position for Kimberly Jordan, PhD. Dr. Jordan is a young scientist whose career I have followed with interest since she was a graduate student in the lab of one of my collaborator Dr. Jill Slansky. Dr. Jordan did her post-doctoral fellowship with Dr. Martin McCarter in the Department of Surgery and worked on human tumor melanoma immune suppression. With this funded grant and the change of Dr. Rao's position, I was able to recruit Dr. Jordan to my lab and the Young Women's Breast Cancer Program. She began as part time in October of 2014 and became a full time Research Instructor in January 2015. She represents an outstanding addition to my lab and the team on this project. She has had two national poster presentations so far and is finalizing the methods paper for submission by end of August 2015. Dr. Jordan, based in part on her success in my lab, has been promoted to Assistant Professor and given an independent research position in the Department of Immunology.

6. A second research education opportunity for a summer student, Jenny Xiang, who has spent 6 weeks in the lab for a research experience as part of the University of Colorado Cancer Center Summer Student Research Program. Jenny will be returning to U of Maryland for second year of medical school and will present her poster both at out on campus symposium next week as well as at her school's student research symposium in September, 2015.

7. Training and research opportunity for a post-undergraduate student in my lab, Troy Schedin. Troy has done an outstanding job of helping with this project and as such is the lead author on our ISEV poster he will present in May 2017, which will be his first national scientific meeting, and he will be first author on the second manuscript from this work.

8. Publications, Abstracts, and Presentations

1. A methods paper outlining our work as is under 3rd review. A second paper is in preparation for the breast cancer EV data.

2. The following presentations have occurred:

    a. Exosome Expo, Denver, Colorado -May 2014, Poster presentation, Title: Characterizing Exosomes in Circulation in Rodent Models, Dr. Rao

    b. CANCER BIOLOGY PROGRAM, University of Colorado Cancer Center, Seminar Series, Oral presentation, May 2014, Title: Characterizing Exosomes in Circulation in Rodent Models, Dr. Rao

    c. SelectBio Exosomes and Single Cell Analysis Summit Sept 18th-19th 2014 in San Diego, Abstract #SCAS9, Dr. Jordan

d. ASEMV 2014 Oct 10-13th at Asilomar, Abstract #100, Dr. Jordan

    e. University of Colorado Cancer Center Summer Student Research Program Symposium, August 6th, 2015 Aurora, CO, Jenny Xiang

    f. UCCC Summer Student Research Program Symposium, Jessica Hall, August 5th 2016, Aurora Co.

    g. San Antonio Breast Cancer Symposium, Abstract P4-06-04, Virginia Borges, December 8th 2016

    h. Department of Medicine, Research in Progress Symposium, Virginia Borges, February 2017, Aurora CO

    i. Pending: ISEV May 2017, Troy Schedin

7. Inventions, Patents and Licenses: None

8. Reportable Outcomes: None

9. Other Achievements:

Dr. Borges, the project PI, was promoted to Director of the Breast Cancer Research Program at the University of Colorado Cancer Center. This promotion was made possible, in part, to the ongoing support of the DOD for the translational research of this grant as well as the other DOD grants received over the years which have provided the PI the opportunity to become a recognized leader in breast cancer translational research.

Dr. Borges was also awarded the Robert F and Patricia Young Connor Endowed Chair in Young Women's Breast Cancer Research. This chair was awarded in recognition of the PIs leadership in the field of young women's breast cancer research and the national recognition the Young Women's Breast Cancer Translational Program at UCCC has achieved. These achievements were supported, in part, by this grant and the prior DOD support to the PI that has led to many of the breakthroughs in young women's breast cancer achieved by this team.

In March 2016, Dr. Borges was promoted to Deputy Head of the Division of Medical Oncology in recognition of strong mentorship and leadership in translational reseach.

In February 2017, Dr. Borges was awarded the Pioneer Award from the University of Colorado Hospital, in recognition for the success of the Young Women's Breast Cancer Translational Program, which has been supported in part by this DOD award as well as other DOD awards to Borges and Schedin since 2006.

Lastly, word just came in that I will be promoted to Professor with Tenure in the Department of Medicine effective July 1, 2017. My gratitude to the DOD for both keeping my country a safe place to life and work and for the research support over the past decade cannot be put into words. I am the daughter of a WWII vet and if he were alive, he would be greatly moved by what you have done for me and my team.

10. References:

1.   Lambe M, Hsieh C, Trichopoulos D, Ekbom A, Pavia M, Adami HO: Transient increase in the risk of breast cancer after giving birth, The New England journal of medicine 1994, 331:5-9

2.   Robertson C, Primic-Zakelj M, Boyle P, Hsieh CC: Effect of parity and age at delivery on breast cancer risk in Slovenian women aged 25-54 years, International journal of cancer 1997, 73:1-9

3.   Albrektsen G, Heuch I, Hansen S, Kvale G: Breast cancer risk by age at birth, time since birth and time intervals between births: exploring interaction effects, British journal of cancer 2005, 92:167-175

4.   Albrektsen G, Heuch I, Kvale G: Further evidence of a dual effect of a completed pregnancy on breast cancer risk, Cancer Causes Control 1996, 7:487-488

5.   Albrektsen G, Heuch I, Tretli S, Kvale G: Breast cancer incidence before age 55 in relation to parity and age at first and last births: a prospective study of one million Norwegian women, Epidemiology 1994, 5:604-611

6.   Colditz GA, Frazier AL: Models of breast cancer show that risk is set by events of early life: prevention efforts must shift focus, Cancer Epidemiol Biomarkers Prev 1995, 4:567-571

7.   Lyons TR, Schedin PJ, Borges VF: Pregnancy and breast cancer: when they collide, Journal of mammary gland biology and neoplasia 2009, 14:87-98

8.   Schedin P: Pregnancy-associated breast cancer and metastasis, Nature reviews 2006, 6:281-291

9.   Schedin P, Strange R, Mitrenga T, Wolfe P, Kaeck M: Fibronectin fragments induce MMP activity in mouse mammary epithelial cells: evidence for a role in mammary tissue remodeling, J Cell Sci 2000, 113 (Pt 5):795-806

10.   Schedin P, Mitrenga T, McDaniel S, Kaeck M: Mammary ECM composition and function are altered by reproductive state, Molecular carcinogenesis 2004, 41:207-220

11.   Schedin P, O'Brien J, Rudolph M, Stein T, Borges V: Microenvironment of the involuting mammary gland mediates mammary cancer progression, Journal of mammary gland biology and neoplasia 2007, 12:71-82

12.   O'Brien J, Schedin P: Macrophages in breast cancer: do involution macrophages account for the poor prognosis of pregnancy-associated breast cancer?, Journal of mammary gland biology and neoplasia 2009, 14:145-157

13.   Bemis LT, Schedin P: Reproductive state of rat mammary gland stroma modulates human breast cancer cell migration and invasion, Cancer research 2000, 60:3414-3418

14.   Clarkson RW, Wayland MT, Lee J, Freeman T, Watson CJ: Gene expression profiling of mammary gland development reveals putative roles for death receptors and immune mediators in post-lactational regression, Breast Cancer Res 2004, 6:R92-109

15.   Stein T, Morris JS, Davies CR, Weber-Hall SJ, Duffy MA, Heath VJ, Bell AK, Ferrier RK, Sandilands GP, Gusterson BA: Involution of the mouse mammary gland is associated with an immune cascade and an acute-phase response, involving LBP, CD14 and STAT3, Breast Cancer Res 2004, 6:R75-91

16.   O'Brien J, Lyons T, Monks J, Lucia MS, Wilson RS, Hines L, Man YG, Borges V, Schedin P: Alternatively activated macrophages and collagen remodeling characterize the postpartum involuting mammary gland across species, The American journal of pathology 2010, 176:1241-1255

17.   Lyons TR, O'Brien J, Borges VF, Conklin MW, Keely PJ, Eliceiri KW, Marusyk A, Tan AC, Schedin P: Postpartum mammary gland involution drives progression of ductal carcinoma in situ through collagen and COX-2, Nat Med 2011, 17:1109-1115

11. Appendix:

.

Clinical protocol for sample use - current COMIRB approved version

Protocol Title: "Can exosomes induced by breast involution be markers for the poor prognosis and prevention of post-partum breast cancer?": Bio-sample re-purposing protocol for the ongoing study of immunosuppression in young onset breast cancers.

Coordinating Institution: University of Colorado Anschutz Medical Campus

Study nickname: Exosome re-use protocol

Principal Investigator:
Virginia F. Borges, MD, MMSc
Associate Professor
Director, Young Women's Breast Cancer Translational Program
Division of Medical Oncology
University of Colorado Anschutz Medical Campus
12801 E 17th Avenue, Room 8112
Aurora, CO 80045
virginia.borges@ucdenver.edu
Phone: 303-949-9964
Pager: 303-266-0178
Fax: 720-848-1620

Study Coordinator:
Emily Rozzo, BS
Translational Research Associate
Young Women's Breast Cancer Translational Program
Emily.rozzo@ucdenver.edu
Phone 303-724-0178
Pager: 303-266-4717

Study Synopsis:

Title: "Can exosomes induced by breast involution be markers for the poor prognosis and prevention of post-partum breast cancer?"

Clinical Development Phase: Translational study for the re-purposing of samples obtained under prior research protocols [COMIRB 08-1040, 09-0583 and 11-0357] for use under new funding source DOD/CDMRP Proposal Log Number BC121782, Award Number W81XWH-13-1-0078

Study Overview: We will utilize previously collected blood samples from three prospective, translational bioanalysis studies aimed at investigating immune suppressive parameters in the systemic circulation and tumor/stromal microenvironment at diagnosis and/or time of subsequent recurrence in women with breast cancer and normal control subjects. For this new protocol, we will specifically investigate a recently identified potential cause of immune suppression in cancer called exosomes. These are circulating microvesicles released into the extracellular environment that have been identified in the plasma of cancer patients and correlated with poorer prognosis and survival. At the time of initiation of all three clinical trials, enrolled subjects gave consent for use of their blood for the study of circulating factors that may be causative or related to tumor-induced immune suppression in young women's breast cancer. The knowledge and technology now exists for us to move forward with this planned aspect of the research through this in depth proposal to study circulating exosomes from women with young onset breast cancer, with young onset breast cancer who were exposed to immune modulating anti-inflammatory drugs and in women who have not been diagnosed with breast cancer as controls.

Objectives/Specific Aims:

Aim 1. Characterize the circulating exosomes present in YWBC. Determine the type of circulating exosomes, protein content and function between unaffected young women and age-matched newly diagnosed cases of YWBC and correlate these findings with parity status [post-partum breast cancer (PPBC) or non-post-partum breast cancer (non-PPBC) and known prognostic clinical tumor characteristics.

> **Innovation, Rationale and Impact:** The identification of increased or unique circulating exosomes in primary cases of YWBC as compared to unaffected young women may identify exosomes as potential targets for investigation into why YWBC, or subsets thereof like PPBC, are more prone to drug resistance, local recurrences and metastasis. The importance of the tumor microenvironment and immune system in breast cancer is increasingly identified as impacting prognosis and treatment benefit. Our data demonstrating altered stromal attributes of desmoplasia and immune suppressive milieu in preliminary human studies of PPBC supports an "exosome role" in mediating these events and if identified, also offer the potential for a biomarker to better identify the most "at risk" population among PPBC.

Aim 2: Determine if short-term drug intervention with anti-inflammatory agents in newly diagnosed young women with breast cancer alters the exosome presence, protein content or function, and correlate these exosome endpoints with parity status as in Aim 1. Whether these same exosome endpoints correlate with tumor Ki67, a relevant clinical marker, will also be evaluated.

> **2a.** Using plasma samples obtained from our completed window of opportunity clinical trial (COMIRB 08-1040) within the YWBC Translational Program, we will determine if short term anti-inflammatory intervention altered circulating exosomes quantity, protein content or function using proteomic methods and cell culture models.

> **2b.** Correlate the changes identified in the exosomes by patient status as being PPBC v non-PPBC and by whether there was a concomitant treatment induced reduction of breast cancer Ki67 expression, a validated marker of poorer prognosis in BC.

> **Innovation, Rationale, Impact:** Identification of an alteration in exosome quantity, protein content or function, either in promoting immune suppression and/or in tumor cell proliferation, migration, apoptosis

and invasive morphology in 3D culture, will identify potential mechanisms for exosome activity in YWBC. The ability to beneficially alter exosome function with clinical administration of COX-2 inhibiting drugs in humans is completely novel. Correlation of exosome changes with clinical outcomes and parity status may identify, for the first time that exosomes are present and may contribute to the poor prognosis of PPBC. Positive results would also support the ongoing investigation of exosomes as potential targets for therapy in PPBC patients whose prognosis remains poor despite current treatment advances, and/or identify a readily obtainable non-invasive marker of PPBC risk.

Eligibility: Cases from the three COMRIB protocols will be identified by review of our database (no PHI included) and selected based on their age, parity status, and the availability of collected sample to meet the experimental cohorts of interest for the two aims outlined above. There will be no subject contact or obtainment of new data or samples to complete the work as outlined in this protocol.

Patient Numbers: We have previously obtained blood and urine on 65 normal young female donors and 150 blood, tissue and urine samples from women ≤45 newly diagnosed with YWBC, untreated. From these samples, we have selected to start with twenty cases per cohort from which to isolate exosomes, balanced by PPBC to non-PPBC status, stage and clinical breast cancer subtype, as well as 20 normal age-matched controls.   We anticipate that samples may need to be replaced with additional cases based on technical issues as the assays and experiments to be performed are new for our lab. We also have 22 cases of pre and post samples from women with newly diagnosed young onset breast cancer who were enrolled on protocol 08-1040 and exposed to celecoxib or no drug that will be utilized for Aim 2.

Research studies: All samples will be subjected to exosome isolation and content analyzed via standardized protocols. The isolated exosomes will under proteomic analysis and studied in cell culture assays, such as determination of proliferation, migration and invasion capacity of tumor cells after co-culture with exosomes. The exosomes will be analyzed for their effect on cellular morphology and apoptosis in 3D culture assays and studied in immune assays to determine their immune suppressive effects on human peripheral blood mononuclear cells.

Table of contents

1.0 Background and significance: YWBC and the Poor Prognosis of PABC: Breast cancer is the leading cancer diagnosis in young, premenopausal women and it has a higher incidence than the combined incidence of next five most frequent cancers in this age. SEER database 2012 statistics show 12% of all breast cancers are expected to occur under age 45, resulting in 27,000 young women's breast cases annually in the US alone. This rate places young women's breast cancer (YWBC) in the same general rate of incidence (cancers in females of all ages) as ovarian cancer (22,000) and pancreatic (21,000), and in excess of Hodgkin's lymphoma (4,100), cervical (12,000), and myeloid leukemia (10,500). An identifiable risk for breast cancer in younger women is a recent completed pregnancy. Pregnancy has a dual effect on breast cancer risk, conferring an immediate increased risk of developing breast cancer to all women regardless of age at pregnancy, and only later providing long term protection for women who are younger at first birth [1-6]. Further, older first-time mothers are at an elevated risk for breast cancer than younger first-time mothers (Fig 1). While there is no consensus on the definition of pregnancy-associated breast cancer (PABC), it is often limited in definition to cases diagnosed during pregnancy or very shortly afterward (<6 months postpartum), which represents a small fraction of all YWBC [7-9]. The rationale for focusing on diagnoses during pregnancy is logical, given the dominant role estrogen stimulation plays in breast cancer promotion and the fact that circulating levels of estrogen are increased ~40 fold during pregnancy [10-14]. However, large-scale, multi-institutional studies

identify peak incidence of PABC at 5-7 years postpartum rather than during pregnancy (Fig 1) [3-5]. Furthermore, in our Colorado Cohort, relative risk for metastatic recurrence (HR 2.8) and death (HR 2.65) is significantly higher in young women diagnosed up to 5 years postpartum compared to nulliparous controls (Fig 2, VB, manuscript under revision). As shown in Fig 2, there is also a trend toward the increased risk of death persisting in the group diagnosed as late as 5-10 years postpartum. Our cohort is being expanded to better understand these later postpartum time points. Importantly, the effect size of the risk was not different when women were analyzed by each individual year post-partum up to year 5
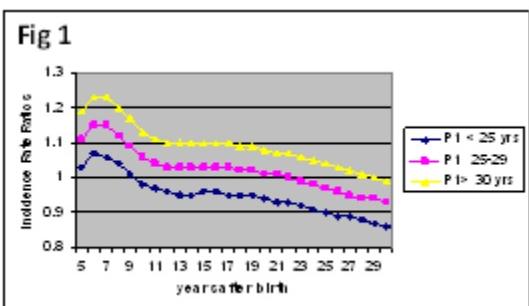
Figure 1: Evidence for a transient increase in breast cancer risk following pregnancy in uniparous women. Predicted incidence rate ratio of breast cancer for parous women by time since first birth, in subgroups by 'age at first birth'. For nulliparous women, the relative rate ratio is set to 1.0. In this cohort of 22,890 women with breast cancer, a transient increase in risk is seen up to 10 years post pregnancy for all age groups, but is highest in first time older mothers[38].

(data not shown), demonstrating that risk for poor prognosis persists beyond the classical 6 month to 1 year postpartum cut-off. Moreover, the postpartum window has been identified as an independent predictor of poor prognosis, whereas pregnancy has not [15-19]. We argue that these data provide strong rationale for expansion of the definition of PABC to include postpartum cases. **Significance of problem:** To account for the poor outcomes experienced by women diagnosed at least as late as 5 years postpartum, the definition of PABC needs to be outcomes based and expanded to include postpartum cases. We anticipate a number of significant clinical implications as a consequence of including postpartum cases in the definition of PABC. The first is identification of a completed pregnancy within the last 5 years (or longer) as a new breast cancer risk factor for young women. Second, the number of women who may benefit from a prevention strategy targeted to involution is increased many fold over current estimates. For example, in a Norwegian cohort of 3034 YWBC cases, only 1% of the cases were diagnosed during pregnancy, while 44% were diagnosed within 6 years of a completed pregnancy (**Fig 3a**). Similar trends are observed in our University of Colorado cohort (**Fig 3b**). If PABC is re-defined by incidence and prognostic outcomes then up to 50% of ALL YWBC may be PABC. If half of young women's BC cases are in the setting of recent pregnancy and thus negatively influenced by the effect of involution on metastasis, the resultant 14,000 **high risk** PABC would still be greater in number than many of the other cancers listed. Therefore, targeting this highly vulnerable population of young mother's for prevention of PABC is both highly innovative and of substantial potential impact to the field.

The Role of Postpartum Involution in Driving the Increased Risk for PABC:. Insight into why the postpartum window correlates strongly with poor prognosis has been obtained through rodent studies on postpartum mammary gland involution [20-22]. Work from our program and others demonstrate that postpartum involution utilizes wound healing and inflammatory programs to remodel the secretory-competent gland to a non-secretory state. Characteristics of provisional wound healing present in the involuting gland include accumulation of fibrillar collagen and the oncofetal extracellular matrix (ECM) protein tenascin-C, increases in matrix metalloproteinase (MMP) 2, 3, and 9, release of bioactive fragments of laminin and fibronectin with tumor activating properties, and an influx of alternatively activated macrophages with similarities to tumor-associated macrophages [21, 24-31] In tumor models, these same desmoplastic stromal attributes promote carcinogenesis and correlate with poor prognosis in breast cancer patients [21, 27, 31-37]. Based on this recent understanding of the cellular and molecular mechanisms of postpartum involution, we have proposed the 'involution-hypothesis' to account for the poor
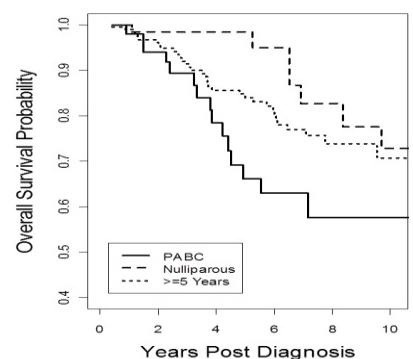
Figure 2: Evidence for decreased survival associated with PABC. Survival probability in PABC<5 (n=86), >=5 (n=172) and nulliparous (n=76) cases from the Colorado YWBC Cohort adjusted for tumor biologic subtype, clinical stage and year of diagnosis. PABC<5 have a markedly lower five-year survival of 65.8% in comparison with nulliparous cases, with a crude five-year survival of 98.0%. Cases >=5 had a crude five-year survival probability of 77.5%—intermediate to PABC<5 and nulliparous cases.

30

prognosis of PABC[7,28,38.] Specifically, we predict that wound healing attributes of the involuting gland drive promotion of pre-existing early stage lesions to overt, metastatic disease [27, 38]. To test this hypothesis, we developed rodent models for PABC where tumor cells are exposed to the mammary gland micro-environment in hosts with different reproductive states. Using a combination of fat pad and intraductal xenografts, and immune competent murine models, we consistently find that postpartum involution is tumor promotional[22.] Conversely, we find that pregnancy per se is not promotional in this model (unpublished data). These data reflect the human


Figure 8: A recent pregnancy as a poor prognostic factor is common in young women with breast Cancer. a) Norwegian YWBC cohort separated by parity status shows 45% of women have a completed pregnancy within 6 years of diagnosis. b) University of Colorado YWBC cohort separated by parity status demonstrates similar trends.

condition, where diagnosis in the postpartum window not pregnancy predicts outcomes for women with PABC[17, 18]. Recently, using our DCIS fat pad-xenograft model, a mechanism by which postpartum involution promotes tumor progression has been elucidated. In this model, fibrillar collagen, which is actively deposited during involution, induces cyclooxygenase-2 (COX-2) expression in tumor cells and drives COX-2 dependent tumor cell proliferation and invasion. At the same time as this tumorigenic microenvironment is developing, we identify the recruitment of "involution macrophages" with attributes of wound healing and tumor promotional M2 'alternatively' activated macrophages with expression of immunosuppressive cytokines, interleukin-1-(IL-10) ,macrophage chemoattractant protein-1(MCP-1) and IL-13 [21]. Additionally, we have identified, for the first time, that human involution also demonstrates an influx of CD45 leukocytes and specifically CD68 macrophages unique to the involution window, supporting the immune modulatory nature of human involution[21]. Based on these studies, we selected COX-2 as a target for intervention to modulate the tumor promotional and inflammatory involution microenvironment. Additional rationalization for targeting COX-2 comes from numerous epidemiologic studies [39-50]. In animal models, COX-2 overexpression induces mammary tumorigenesis [51] and in vitro inhibition of COX-2 reduces breast cancer cell proliferation, migration, and invasion [52]. Likewise, high COX-2 expression in breast tumor cells predicts infiltration of lung [47], bone [53], and brain [48]. In our preclinical postpartum BC model, we found that short-term NSAID treatment, with both non-specific ibuprophen and Cox-2 specific inhibitor celecoxib, limited to the 2 week window of mammary gland involution, sustainably reduces the ability of involution to promote tumor growth and metastasis [22]. We also found that both drugs reduced deposition of fibrillar collagen and ibuprophen reduced deposition of tenascin-C, to result in an ECM milieu with tumor-suppressive rather than activating properties (Fig4)[22, 54]. From this preclinical evidence, we moved forward into a translational Phase 0 Window of Opportunity human trial in newly diagnosed YWBC. The schema of this study is outlined in the research strategy and enrollment is completed. The primary aim of the parent study is to identify a decrease in Ki-67% index with the drug interventions, a known predictive marker for clinical benefit with short term intervention in breast cancer. Further, the biologic endpoints of identifying alterations in Cox-2 expression, M2- macrophage infiltration, collagen deposition, and other markers of desmoplasia and immune suppression at baseline and after drug intervention will provide supportive human data towards larger intervention clinical trials.

The role of exosomes in cancer as mediators of the tumor microenvironment and immune system: Exosomes are microvesicles formed by internalization of the plasma membrane and subsequently released into the extracellular environment. The inward budding of the endosome membrane results in exosomes that contain cellular RNA, protein and DNA which are spontaneously released from various cells upon fusion with the plasma membrane. Exosomes are found ubiquitously in human body fluids, including plasma, malignant effusions and breast milk, and contain a wide variety of proteins, such as annexins, heat shock proteins, major histocompatability markers, co-stimulatory proteins, integrins, adhesion molecules, or metabolic enzymes [55]. Exosomes have been identified in the plasma of cancer patients at significantly increased levels as compared to unaffected persons, with the increased number of exosomes correlating with poorer prognosis and shorter survival[56, 57]. Clinically, exosomes have also been implicated in drug resistance [58, 59]. The role of exosomes in the tumor microenvironment and malignant behavior is expanding[75, 76]. They have been identified from multiple cancers as releasing TGFβ and thus being capable of inducing fibroblasts to express smooth muscle actin (αSMA) and differentiate into myofibroblasts with expression of SDF-1, VEGF, CCL5 and TGFβ. These multiple protumorigenic characteristics of
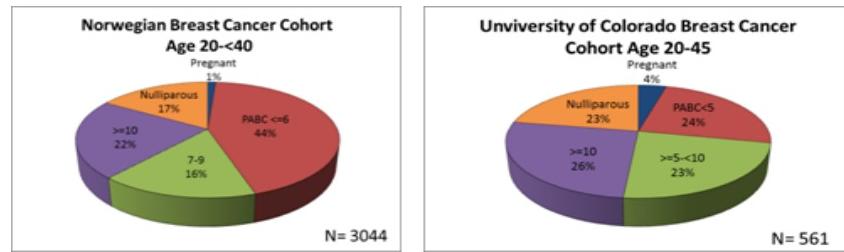
Fig 4.
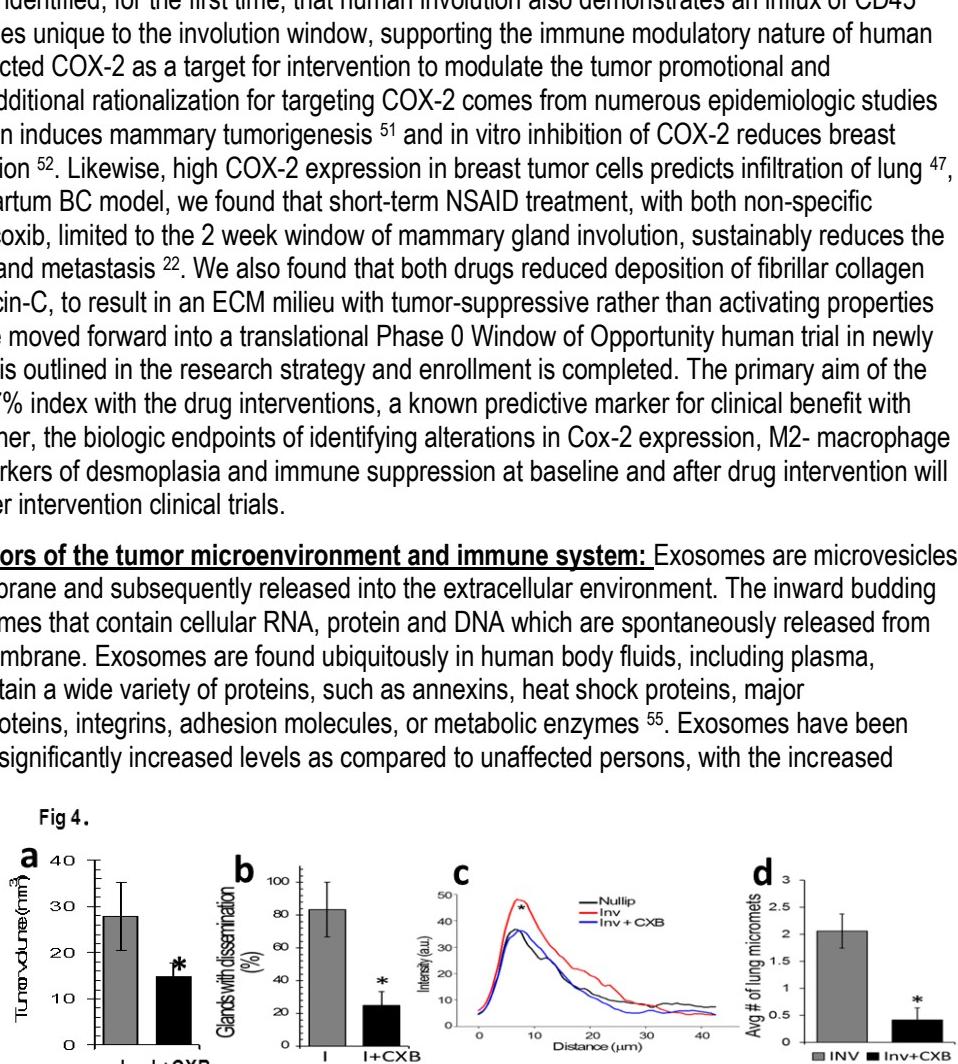
Fig 4. Celecoxib(CXB) abrogates the tumor promotional effects of involution and reverses mammary collagen to nulliparous levels. Mice were treated for 10 days with CXB during the window of postpartum involution. (a) Primary tumor volume reduced with CXB treatment at 3 weeks post-injection, *p=0.037, n=23 each cohort. (b) CXB reduces tumor cell dispersion that occurs during involution, p=0.0179, n=12 each cohort. (c) CXB reduces collagen deposition, as measured by SHG intensity versus distance from duct to levels observed in nulliparous animals (red) compared to drug treated nulliparous involuting mammary ducts (green) and nulliparous ducts (black), p<0.00001. (d) CXB reduced the average number of lung metastasis per animal compared with untreated involution, p=0.0002

exosomes support a role for exosomes in promoting stromal desmoplasia and driving cells toward a malignant phenotype[61, 60]. Likewise, tumor secreted exosomes home to local lymph nodes and other sites to prepare the metastatic niche for metastatic growth[62, 63]. In addition to the stromal effects of TGFβ releasing exosomes, they are also widely regarded as immunosuppressive[64].Exosomes excreted from various malignancies have immune suppressive effects, including inhibition of IL-2 induced T cell proliferation, inhibition of natural killer cell cytotoxicity[65], and induction of activated T lymphocyte apoptosis via FasL and TRAIL[66,67]. They also expand FoxP3+ regulatory T cells (Tregs) via TGFβ1 and IL-10 production[68], which in turn have increased FasL, IL-10, TGF-β1, granzyme B, perforin and increased suppressive capabilities. Furthermore, exosomes derived from malignant effusions can maintain Treg suppressive capacity and numbers[69]. Tumor secreted exosomes influence monocyte function and differentiation by inducing increased expression of IL10, TNFα, and IL-6 by monocytes[70] and driving their differentiation into putative myeloid derived suppressor cells (MDSC: CD14+HLA-DR−/low cells in humans, CD11b+Gr1+ in mice). The resulting MDSC haveTGFβ dependent T cell suppression ability, increased production of IL-6 and VEGF, and promote tumor growth that in one model, was reversed by prostaglandin E2 (PGE-2) and TGFβ blockade[71]. Moreover, tumor derived exosomes inhibit myeloid cell differentiation to dendritic cells (DC) in a Myd88 dependent fashion, with the resultant skew toward increased MDSC leading to increased lung metastasis in the 4T1 murine mammary tumor model[72]. Tumor produced exosomes clearly modulate tumor immunosuppression, and macrophages can also produce exosomes that shuttle microRNA back into breast cancer cells and alter them to a more invasive phenotype[73]. Given that we have identified abundant macrophages in the involuting mammary gland the potential for exosomes playing a role in involution induced metastasis is great.

The combination of exosome isolation with advanced proteomic technologies to interrogate the proteome of the exosomes is starting to offer deeper insight to commonalities and uniqueness that can be identified across cell types in protein content and offer putative mechanisms behind their functional abilities. Our collaborator, M. Graner has identified exosomes with unique protein content from medulloblastoma. These exosomes contain high levels of hepatocyte nuclear factor 4alpha with potential tumor suppressor function, several proteins important in migration and proliferation and, interestingly, induce dichotomous dose-dependent T cell responses. In this model, low dose exosome exposure inhibits T cell gamma Interferon release while high dose exosome exposure increased the T cell response, suggesting a plasticity to exosomes[74]. Additional collaborators to our research, E. Eisenmesser and K.Hansen, in collaboration with the Graner lab, used a comprehensive approach of biochemical, biological, and spectroscopic methods to elucidate the stimulatory roles and potential mechanism of secreted exosomes from multiple tumor cells lines. Their results indicate that purified exosomes preferentially stimulate secretion of several pro-oncogenic factors in monocytic cells but only harbor limited activity with regard to epithelial cells. In addition, by using fluorescence microscopy, they have successfully visualized internalization of exosomes into the recipient cells within minutes. Finally, they identified, for the first time, a functional role for CD147/ extracellular matrix metalloproteinase inducer (EMMPRIN), which is a tumor cell surface protein that induces MMP and pro-inflammatory cytokine secretion, and has been found in tumor secreted exosomes. Functionally, the EMMPRIN containing exosomes were potent stimulators of MMP-9, IL-6, TGFβ1 and induced the secretion of extracellular EMMPRIN itself, all pro-oncogenic factors that drive immune evasion, tumor cell invasion, as well as, inflammation in the tumor microenvironment. (EE, manuscript in preparation)

The potential for exosome influence in the microenvironment of involution and PPBC: We have characterized, for the first time, the immune environment of the murine mammary gland across virgin, pregnant, lactating, involution and fully regressed parous states in an immunocompetent model and identified unique peaks of immune cell influx during involution for DC, monocytes, Tregs and more modestly CD4 Tcells(Fig5). We also isolated macrophages isolated from actively involuting glands that expressed significantly higher amounts of mannose receptor a M2 macrophage marker and allograft-inflammatory factor-1 (Aif-1) a tumor promotional cytokine, and showed they were capable of suppressing T cell activation *ex vivo*. Isolated involution myeloid cells also suppressed T cell activation and INF-γ production in *ex vivo* co-culture assays (unpublished data not shown) all supporting the involuting mammary gland as having an immune suppressive milieu in addition to the already identified desmoplastic microenvironment[77]. Interestingly the putative MDSC (CD11b+) subset in circulation from involution was suppressive as well, though not numerically increased from the other parity states (data not shown). These data pair with our recent characterization of young women's immune function from unaffected and newly diagnosed breast cancer cases. As expected, there is an increase in Tregs in the cancer cases, but unexpectedly, we identify similar numbers of myeloid derived suppressor cells in both populations, yet with increased T cell suppressive activity in the cancer cohort (Fig 6). To date, human MDSC data has linked increased numbers with increased suppression, [78-80] and we attribute the difference in our results to be accounted for by the robust size of our cohorts, the use of age-matched, gender-matched controls, and/or reflective of a true biologic difference. Our data on immune modulation during involution, taken with the emerging role for exosomes in cancer promotion and immune suppression, lead us to hypothesize that
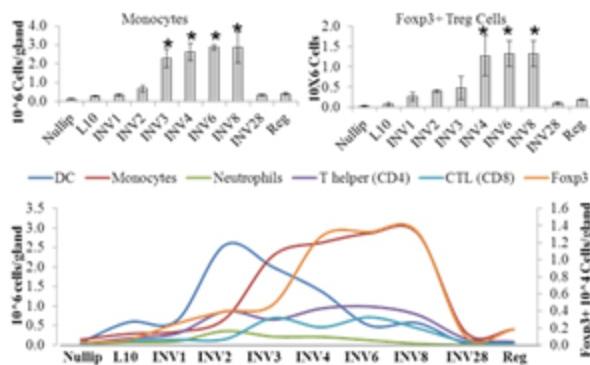
Fig 5. Involution demonstrates an increase in suppressive immune cells. Mammary gland digests from different time points of parity where subjected to FACs for phenotyping of infiltrating immune cells. A dominant pattern of monocyte and Tregs increase during mid involution without as dramatic an increase in other T cell subsets was identified, supportive of involution being an immunosuppressive milieu

32
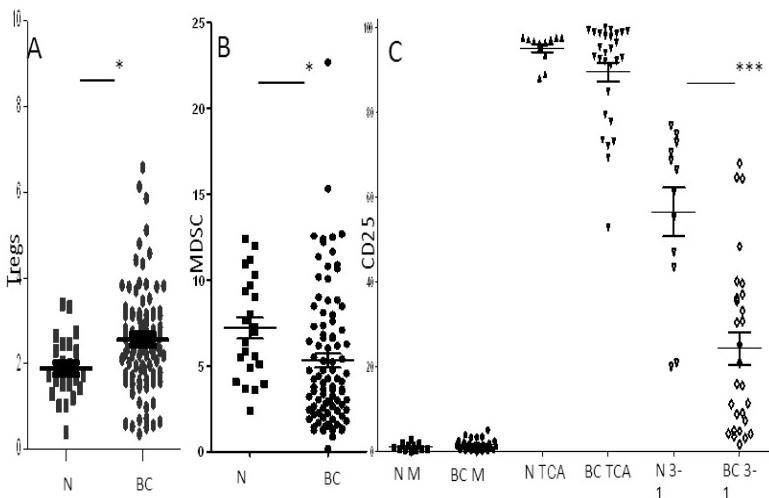
Figure 6 Characterization of an immune suppressive phenotype in YWBC. A. Significant increase in regulatory T cells as identified by FACS (CD4$^+$CD25^{hi}FOXP3$^+$) in YWBC (n=88) compared to normals (n=23). *p=.0131 **B.** MDSC (Lin$^{lo/-}$(CD3,CD14,CD19,CD20,CD56)HLA-DR$^-$CD33$^+$CD11b$^+$) are not different in normals (n=23) v. YWBC (n=101). *p=.0315 **C.** MDSCs from YWBC (n=27) are more suppressive (n=12). Suppression of T cell activation (TCA) by enriched CD11b+ MDSCs was assessed by FACS for CD25+ T cell levels. MDSCs were co-cultured at 3:1 with autologous T cells and CD3/CD28 stimulation beads for 96 hours. ***p=.0001

exosomes with pro-metastatic cargo are released from the actively involuting gland, enter the circulation, and influence tumor-microenvironment interactions, immune escape, and the metastatic niche. To begin to address this hypothesis, in this proposal, our objectives are to see whether exosomes with unique properties can be identified during involution, and are likewise present in women with PPBC. Specifically, we will characterize the protein content of involution exosomes, investigate their role in driving in vitro attributes of tumor cell invasiveness, and their ability to influence monocyte differentiation and promote Treg number and function. Importantly, we will determine whether exosomes can be blocked by PGE-2 inhibition in young women's breast cancer patients, supporting exosomes as a part of the tumor promotional attributes of involution that are modifiable by COX-2 inhibition. Complimentary murine studies will be performed as well. Our innovative hypothesis introduces the new paradigm that secreted exosomes unique to the life-window of postpartum breast involution contribute to the durable alteration of the involution microenvironment and its tumor promotional effects with potential to influence subsequent PPBC outcomes.

2.0 Hypothesis: We propose that postpartum breast involution results in the release of unique exosomes that enter circulation and have pro-tumorigenic interaction with tumor cells and the immune system. These unique exosomes will also be identifiable in post-partum breast cancer (PPBC) with altered protein composition and function and will correlate with known clinical markers of prognosis. Moreover, we predict that anti-inflammatory therapy targeting postpartum involution and/or the tumor microenvironment of PPBC will alter the circulating exosome composition and function, demonstrating a pro-tumorigenic, immunomodulatory role of exosomes in PPBC.

3.0 Specific Aims:

Aim 1. Characterize the circulating exosomes present in YWBC. Determine the type of circulating exosomes, protein content and function between unaffected young women and age-matched newly diagnosed cases of YWBC and correlate these findings with parity status (PPBC or non-PPBC) and known prognostic clinical tumor characteristics.

> **Innovation, Rationale and Impact:** The identification of increased or unique circulating exosomes in primary cases of YWBC as compared to unaffected young women may identify exosomes as potential targets for investigation into why YWBC, or subsets thereof like PPBC, are more prone to drug resistance, local recurrences and metastasis. The importance of the tumor microenvironment and immune system in breast cancer is increasingly identified as impacting prognosis and treatment benefit. Our data demonstrating altered stromal attributes of desmoplasia and immune suppressive milieu in preliminary human studies of PPBC supports an "exosome role" in mediating these events and if identified, also offer the potential for a biomarker to better identify the most "at risk" population among PPBC.

Aim 2: Determine if short-term drug intervention with anti-inflammatory agents in newly diagnosed young women with breast cancer alters the exosome presence, protein content or function, and correlate these exosome endpoints with parity status as in Aim 2. Whether these same exosome endpoints correlate with tumor Ki67, a relevant clinical marker, will also be evaluated.

> **2a**. Using plasma samples obtained from our completed window of opportunity clinical trial within the YWBC Translational Program, we will determine if short term anti-inflammatory intervention altered circulating exosomes quantity, protein content or function using proteomic methods and cell culture models.

2b. Correlate the changes identified in the exosomes by patient status as being PPBC v non-PPBC and by whether there was a concomitant treatment induced reduction of breast cancer Ki67 expression, a validated marker of poorer prognosis in BC.

Innovation, Rationale, Impact: Identification of an alteration in exosome quantity, protein content or function, either in promoting immune suppression and/or in tumor cell proliferation, migration, apoptosis and invasive morphology in 3D culture, will identify potential mechanisms for exosome activity in YWBC. The ability to beneficially alter exosome function with clinical administration of COX-2 inhibiting drugs in humans is completely novel. Correlation of exosome changes with clinical outcomes and parity status may identify, for the first time that exosomes are present and may contribute to the poor prognosis of PPBC. Positive results would also support the ongoing investigation of exosomes as potential targets for therapy in PPBC patients whose prognosis remains poor despite current treatment advances, and/or identify a readily obtainable non-invasive marker of PPBC risk

4.0 Eligibility

All cases previously enrolled to COMIRB protocols 08-1040, 09-0583 and 11-0357 will be considered as eligible for inclusion in this sample re-use protocol. Cases will be selected for inclusion in this work based on their age, parity status and available of needed plasma sample to meet the experimental cohorts as outlined. It is anticipated that only a subset of cases on 09-0583 and 11-0357 will be needed to meet the study endpoints and that all cases enrolled on 08-1040 who completed the study designated drug intervention or control prior to their surgery and on whom samples were obtained will be utilized. Full details of the inclusion and exclusion of the women enrolled in the parent protocols is available upon request to the PI.

5.0 Patient Numbers

We have previously obtained blood and urine on 65 normal young female donors and 150 blood, tissue and urine samples from women ≤45 newly diagnosed with YWBC, untreated. From these samples, we have selected to start with twenty cases from each experimental group which to isolate exosomes, balanced by PPBC to non-PPBC status, stage and clinical breast cancer subtype, as well as 20 normal age-matched controls.   We anticipate that samples may need to be replaced with additional cases based on technical issues as the assays and experiments to be performed are new for our lab. We also have 22 cases of pre and post samples from women with newly diagnosed young onset breast cancer who were enrolled on protocol 08-1040 and exposed to celecoxib or no drug that will be utilized for Aim 2.

6.0 Immunologic Studies and research approach

Aim 1. Identify if YWBC, including the subsets of PPBC and non-PPBC, is characterized by an increase in circulating exosomes and if those exosomes have unique proteome content, and/or tumor promoting and immune suppressive function.

We will utilize the experimental cohorts of normal versus PABC versus non-PABC human plasma with samples kept individual to provide ability to correlate results with clinical prognostic data. Exosomes will be isolated and aliquoted to proteomic analysis and to cell culture assays to determine their impact on the human MCF10-DCIS.com cell line that mimics *ductal carcinoma in situ*. The MCF10.DCIS cell line is chosen as the best representative xenograft model of early stage disease, and we have previously identified that involution promotes these cells to acquire increased proliferation, invasion, and metastatic ability in vivo and in vitro[22]. An aliquot will also go for immune assays where dilutions of exosomes will be co-cultured with bone marrow derived donor cells and assayed for Treg, and monocytic/ putative MDSC induction. CD3+ selection for splenic T cells will be performed, then cells exposed to the various exosomes in standard Tcell culture assays to determine whether Tcell function is modulated by differing exosome levels. Assay details are outlined below.

Sample Acquisition: We have obtained blood and urine on 65 normal young female donors and 150 blood, tissue and urine samples from women ≤45 newly diagnosed with YWBC, untreated. Dr. Borges is the PI of both of these IRB approved protocols and all samples were processed identically. From these samples, we will select approximately twenty cases from which to isolate exosomes, balanced by PABC to non-PABC status, stage and clinical breast cancer subtype.

Anticipated results: PPBC will be associated with more circulating exosomes that demonstrate pro-metastatic attributes and function, as well as, immune modulatory abilities at differing levels. YWBC will have similar results in comparison to normal, but the overall differences will be more modest, similar to the immune profiling results identified for MDSCs.

Potential problems and alternatives: We have already successfully isolated exosomes from human plasma, so that is not a concern at present. We also have urine to use if quantitations are too low. If PPBC does not prove to have exosomes with unique attributes, we still feel these experiments will add to the relatively small published literature on primary human breast cancer exosomes. Detailed proteome analysis on primary samples will be revealing and functional analysis will identify potential roles for targeting or biomarker development of exosomes, even if not PPBC specific. We have chosen one cell line as the read out for our cell culture assays; however, the Borges lab has multiple cell lines with genomic profiling to the major breast cancer biologic subtypes that can be added as the project progresses.

Aim 2 will determine if a short-term drug intervention with anti-inflammatory agents in newly diagnosed YWB C alters the exosome number, protein content or function and will correlate these exosome endpoints with parity status as in Aim 1, as well as tumor Ki67 index, a known, predictive marker for clinical benefit. The objective of Aim 2 is to demonstrate that anti-inflammatory intervention in human post-partum breast cancer can reduce the tumor-promotional attributes of these cancers, in part, through modulation of the exosome profile. Our program recently completed a "Window of Opportunity" (WOO), Phase 0, randomized, open label, drug intervention study in YWBC patients with the anti-inflammatory agent, celecoxib versus control study [COMIRB 08-1040].. Subjects were recruited pre-surgery and completed 7 days or more of drug. Tissue, blood and urine were collected pre and post intervention. We will utilize the plasma samples collected on this trial, but not usedpreviously, to demonstrate that the circulating exosomes can be altered by Cox-2 inhibition, with a decrease of their tumor promotional attributes. **Tissue acquisition:** Patient consented to our IRB approved WOO study included future analysis of plasma samples for tumor promoting and immune modulating properties. Borges is the study PI. All samples are immediately available. **Anticipate outcomes:** 10 control and 10 celecoxib samples will be used with individualized results for comparison both pre and post intra-patient and also drug naïve versus drug exposed cohorts. PPBC cases will demonstrate greater sensitivity to reversal of exosome pro-metastatic and immune suppressive function with celecoxib than non PPBC, suggesting a Cox-2 dependent effect on exosomes occurs with PPBC as predicted from our animal models.

Problem and alternatives: The effect of Cox-2 inhibition may not be identifiable on circulating exosomes. In this case, we can expand enrollment for additional subjects and take fresh tissue (permitted in the protocol) for isolation of breast cancer exosomes in patients drug naïve versus exposed. We may then lose the pre and post intra-patient comparison due to size limitations of core samples, but if the exosomes are relatively consistent amongst cancer patients, then group comparison will be adequate. If breast cancer subtype is a confounding factor to exosome function or reversibility with Cox-2 inhibition in PPBC v non-PPBC, we may see confusing results, requiring expansion of the Aim 2 cohort to better delineate.

Exosome isolation and identification: Using plasma frozen at -80°C, thawed samples will be mixed 1:1 with PBS, filtered through a 0.45 µm filter and spun at 200,000 x g for 2 hours at 4°C using a Beckman L7-55 Ultracentrifuge and the Ti-70.1 rotor. Supernatants are removed and exosome enriched pellets re-suspended in radio-Immunoprecipitation assay buffer for western blot analysis or phosphate buffered saline for analysis with the Nanosight and functional assays. Size distributions and quantification of exosomes from each experimental group will be determined by measuring the rate of Brownian motion using a NanoSight LM10 system equipped with a fast video capture and particle-tracking software. Density gradient centrifugation for buoyant density determination, acetylcholinesterase activity determination, and transmission electron microscopy will be performed by our previously published methods[74].**Proteomic analysis**: Proteomic analysis of exosomes will be performed by collaborator Dr. Kirk Hansen, who has extensive experience in this area.
Cell culture assays: All in vitro bioassays are generally run in quadruplicate and will be performed using exosomes from each experimental group Aim1-3. **Proliferation Assay**: Proliferation of the MCF10.DCIS cell line in response to co-culture with exosomes will be determined by standard KI-67% FACS staining of MCF10.DCIS cells after 48 hour exposure. **Migration Assay**: Human MCF10.DCIS cells will be set up at 100,000 cells per well in the upper well of a Boyden chamber (CytoSelect Cell Migration Assay, Cell BioLabs, Inc). Cells will be separated from the lower chamber, containing media that is either serum free, +10%FBS as positive control attractant, or with 50, 100 and 500ug/ml exosomes by an 8um pore size polycarbonate filter.

After 24-48 hours, the remaining non-motile cells will be removed from the upper chamber and the filter, with motile cells adhered, fixed with 10% NBF, stained with crystal violet, washed and number of migratory cells counted in 3 high power fields (40X), followed by an independent assessment using a dye extraction method. **Invasion Assay**: Invasion assays will be performed similarly with the exception that the filters are coated with high density reconstituted basement membrane (Matrigel) or collagen to assay for cellular invasion through ECM substratum. **3D culture assays:** Exosomes will be analyzed for their effect on cellular morphology, proliferation and apoptosis in 3D culture assays. Briefly, MCF10DCIS.com cells will be embedded in Matrigel + 10, 20, and 40% Collagen gels, previously shown to induce varying degrees of proliferation and invasive morphology. Cells will be incubated with exosomes for matrix embedding and analysis of 3D cultures for proliferation, apoptosis and morphology will be carried out as previously described[22]. **Immune assays:** Exosomes will be co-cultured with either BM derived progenitors or human donor PBMCs to determine induction rates for Treg or MDSCs, alterations of CD4:CD8 T cell ratios and alteration of macrophage Th1/Th2 polarization. Exosomes will be co-cultured with T cells and T cells + MDSCs in standard activation/suppression assays and then T cells analyzed by FACS for activation markers, CFSE-based proliferation assays, and γIFN release to determine suppression T cell function or enhancement of MDSC function. Supernatant will be collected for cytokine analysis using standard Luminex kits.

7.0 Concomitant medications
All enrolled subjects has recording of their concomitant medications at the time of sample collection, so that data is available for excluding any confounding drug effects from the research assays. No additional recording of data will occur

8.0 Study procedures
All data and tissue samples to be utilized in this research are on hand in the Young Women's Breast Cancer cohort, of which Borges is the PI. No PHI or identifiers will be used to conduct this research. No new data or subject contact will occur during this research. The data and samples to be used for this protocol do remain linked to the clinical information on the subjects through their medical record numbers and Borges holds this link. None of the lab personnel or collaborators have direct access to the clinical data, any PHI or to the link, nor will they ever be given access to them for any reason. The samples are kept linked for the purpose of eventually being able to correlate significant results in our longitudinal study of young women's breast cancer with patient outcomes of recurrence and survival in future research. In each of the three parent protocols from which the samples to be used in this protocol were obtained, enrolled subjects gave specific consent for their blood to be used for the study of exosomes and/or "circulating immune suppressive factors". Therefore, no new consenting of subjects is indicated for this work to proceed.

9.0 Adverse Event Reporting

Any adverse events related to the collection of the blood and urine samples would be reported under the specific protocol that the subject initially consented to. Any identified concern that the integrity of the security of our data system or risk that PHI may have been accessed by unauthorized persons will be immediately reported to COMIRB as per institutional guidelines.

10. Criteria for removal from study
Cases selected for inclusion in this protocol but deemed inadequate due to sample issues or failure of the research assays will be replaced by an additional matching case. Subjects enrolled to the parent protocols have the option of notifying us if the decide to withdraw consent. Any subject who withdraws consent and who has been slated for inclusion in this research protocol will be removed and replaced.

11.0 Statistical plan

Aim1: 20 samples from each of the normal, PPBC, and non-PPBC provide 80% power to detect a mean difference of 0.41 common within group standard deviation among the three groups using an F test with a 0.05 alpha level for each outcome described above. One-way ANOVA will be used to estimate and compare among (F test) and between groups (t-test).

Aim 2: 10 samples/experimental cohort provides 80% power to detect a mean of paired differences of 1.0 SD of differences with an alpha level of 0.05 using a two-sided paired t-test. 2x2 factorial design with 10 samples for each cohort provides 86% power to detect an effect size of 0.5 for drug or parity or interaction between the two using F test with a 0.05 alpha level . ANOVA will be used to estimate these effects and t-test for testing difference between effects. Spearman correlation coefficients and p-values will be calculated to correlate function and prognostic factors.

12. Data Quality Assurance and Monitoring of Study

All data to be used in this research protocol have been under ongoing review and audit by the University of Colorado Cancer Center Data Safety Monitoring Committee through the approved parent protocols from which the samples are derived. These three protocols have passed all audits with no outstanding concerns or queries. Regulatory approval for the three parent protocols remains in place and will continue to be maintained. Any concerns or actions against the parent protocols will also be reported to COMIRB, the DOD and HRPO in connection with any samples included in this research.

13. Ethical Aspects

The PI, Borges, attests that the three parent protocols under which the samples to be use in this research protocol were and continue to be conducted in full conformance with the principles of the "Declaration of Helsinki" and with laws and regulations of the United States of America. The studies have fully adhered to the principles outlined in the "Guidance for Good Clinical Practice" ICH Tripartite Guideline (January 1997) and the PI ensures that the basic principles of "Good Clinical Practice" as outlined in the current version of 21 CFR, subchapter D, part 312, "Responsibilities of Sponsors and Investigators", part 50, "Protection of Human Subjects", and part 56, "Institutional Review Boards" have been and will be adhered to.
The PI also attests that appropriate protocol was followed to obtain written informed consent from each subject participating in the three parent protocols, including adequate explanation of the aims, methods, anticipated benefits, and potential hazards of the studies. The investigator or designee also explained that the subjects were/are completely free to refuse to enter the study or to withdraw from it at any time for any reason. It is also the responsibility of the PI to assure that all Protected Health Information has been and will continue to be appropriately guarded to ensure subject confidentiality and that all potential subjects completed a "HIPPA B" form to allow the release of their identity to appropriately qualified protocol staff. Since the investigator on the study have a treatment relationship with the potential recruits, "HIPPA A" forms were required. All ICFs and Hippa forms are on file and will be provided to authorized parties upon request if needed.

14. Conditions for terminating the study

The study will be subject to termination if funding is withdrawn or at the discretion of the investigator.

15. Study documentation, CRFs and Record Keeping

There are no new patient data being collected. The clinical data to be utilized in this research already exists in the PIs password protected and secure RedCap database without PHI or identifiers available to the laboratory personnel. No PHI will be accessed as part of this research. The source documents and CRFs for the original data collections are maintained through the oversight of the individual protocols under which the samples to be used in this research protocol were obtained.

16. Publication of data

The results of this study may be published or presented at scientific meetings. The investigators will publish the data without the use of any information that would allow for individual subjects to be identified.

17. References

1.	Lambe M, Hsieh C, Trichopoulos D, Ekbom A, Pavia M, Adami HO: Transient increase in the risk of breast cancer after giving birth, The New England journal of medicine 1994, 331:5-9
2.	Robertson C, Primic-Zakelj M, Boyle P, Hsieh CC: Effect of parity and age at delivery on breast cancer risk in Slovenian women aged 25-54 years, International journal of cancer 1997, 73:1-9
3.	Albrektsen G, Heuch I, Hansen S, Kvale G: Breast cancer risk by age at birth, time since birth and time intervals between births: exploring interaction effects, British journal of cancer 2005, 92:167-175
4.	Albrektsen G, Heuch I, Kvale G: Further evidence of a dual effect of a completed pregnancy on breast cancer risk, Cancer Causes Control 1996, 7:487-488
5.	Albrektsen G, Heuch I, Tretli S, Kvale G: Breast cancer incidence before age 55 in relation to parity and age at first and last births: a prospective study of one million Norwegian women, Epidemiology 1994, 5:604-611
6.	Colditz GA, Frazier AL: Models of breast cancer show that risk is set by events of early life: prevention efforts must shift focus, Cancer Epidemiol Biomarkers Prev 1995, 4:567-571
7.	Lyons TR, Schedin PJ, Borges VF: Pregnancy and breast cancer: when they collide, Journal of mammary gland biology and neoplasia 2009, 14:87-98
8.	Vinatier E, Merlot B, Poncelet E, Collinet P, Vinatier D: [Breast cancer and pregnancy], Gynecol Obstet Fertil 2009, 37:495-503
9.	Petrek JA: Pregnancy safety after breast cancer, Cancer 1994, 74:528-531
10.	Vinatier E, Merlot B, Poncelet E, Collinet P, Vinatier D: Breast cancer during pregnancy, Eur J Obstet Gynecol Reprod Biol 2009, 147:9-14
11.	Henderson BE, Pike MC, Casagrande JT: Breast cancer and the oestrogen window hypothesis, Lancet 1981, 2:363-364
12.	Pike MC, Krailo MD, Henderson BE, Casagrande JT, Hoel DG: 'Hormonal' risk factors, 'breast tissue age' and the age-incidence of breast cancer, Nature 1983, 303:767-770
13.	Pike MC, Spicer DV, Dahmoush L, Press MF: Estrogens, progestogens, normal breast cell proliferation, and breast cancer risk, Epidemiol Rev 1993, 15:17-35
14.	Tulchinsky D, Hobel CJ, Yeager E, Marshall JR: Plasma estrone, estradiol, estriol, progesterone, and 17-hydroxyprogesterone in human pregnancy. I. Normal pregnancy, American journal of obstetrics and gynecology 1972, 112:1095-1100
15.	Bladstrom A, Anderson H, Olsson H: Worse survival in breast cancer among women with recent childbirth: results from a Swedish population-based register study, Clinical breast cancer 2003, 4:280-285
16.	Whiteman MK, Hillis SD, Curtis KM, McDonald JA, Wingo PA, Marchbanks PA: Reproductive history and mortality after breast cancer diagnosis, Obstet Gynecol 2004, 104:146-154
17.	Stensheim H, Moller B, van Dijk T, Fossa SD: Cause-specific survival for women diagnosed with cancer during pregnancy or lactation: a registry-based cohort study, J Clin Oncol 2009, 27:45-51
18.	Johansson AL, Andersson TM, Hsieh CC, Cnattingius S, Lambe M: Increased Mortality in Women with Breast Cancer Detected during Pregnancy and Different Periods Postpartum, Cancer Epidemiol Biomarkers Prev 2011, 20:1865-1872
19.	Beadle BM, Woodward WA, Middleton LP, Tereffe W, Strom EA, Litton JK, Meric-Bernstam F, Theriault RL, Buchholz TA, Perkins GH: The impact of pregnancy on breast cancer outcomes in women<or=35 years, Cancer 2009, 115:1174-1184
20.	McDaniel SM, Rumer KK, Biroc SL, Metz RP, Singh M, Porter W, Schedin P: Remodeling of the mammary microenvironment after lactation promotes breast tumor cell metastasis, The American journal of pathology 2006, 168:608-620
21.	O'Brien J, Lyons T, Monks J, Lucia MS, Wilson RS, Hines L, Man YG, Borges V, Schedin P: Alternatively activated macrophages and collagen remodeling characterize the postpartum involuting mammary gland across species, The American journal of pathology 2010, 176:1241-1255
22.	Lyons TR, O'Brien J, Borges VF, Conklin MW, Keely PJ, Eliceiri KW, Marusyk A, Tan AC, Schedin P: Postpartum mammary gland involution drives progression of ductal carcinoma in situ through collagen and COX-2, Nat Med 2011, 17:1109-1115
24.	Schedin P, Strange R, Mitrenga T, Wolfe P, Kaeck M: Fibronectin fragments induce MMP activity in mouse mammary epithelial cells: evidence for a role in mammary tissue remodeling, J Cell Sci 2000, 113 (Pt 5):795-806
25.	Schedin P, Mitrenga T, McDaniel S, Kaeck M: Mammary ECM composition and function are altered by reproductive state, Molecular carcinogenesis 2004, 41:207-220
26.	Schedin P, O'Brien J, Rudolph M, Stein T, Borges V: Microenvironment of the involuting mammary gland mediates mammary cancer progression, Journal of mammary gland biology and neoplasia 2007, 12:71-82
27.	O'Brien J, Schedin P: Macrophages in breast cancer: do involution macrophages account for the poor prognosis of pregnancy-associated breast cancer?, Journal of mammary gland biology and neoplasia 2009, 14:145-157
28.	Bemis LT, Schedin P: Reproductive state of rat mammary gland stroma modulates human breast cancer cell migration and invasion, Cancer research 2000, 60:3414-3418
29.	Clarkson RW, Wayland MT, Lee J, Freeman T, Watson CJ: Gene expression profiling of mammary gland development reveals putative roles for death receptors and immune mediators in post-lactational regression, Breast Cancer Res 2004, 6:R92-109

30.   Stein T, Morris JS, Davies CR, Weber-Hall SJ, Duffy MA, Heath VJ, Bell AK, Ferrier RK, Sandilands GP, Gusterson BA: Involution of the mouse mammary gland is associated with an immune cascade and an acute-phase response, involving LBP, CD14 and STAT3, Breast Cancer Res 2004, 6:R75-91

31.   Stein T, Salomonis N, Nuyten DS, van de Vijver MJ, Gusterson BA: A mouse mammary gland involution mRNA signature identifies biological pathways potentially associated with breast cancer metastasis, Journal of mammary gland biology and neoplasia 2009, 14:99-116

32.   Hancox RA, Allen MD, Holliday DL, Edwards DR, Pennington CJ, Guttery DS, Shaw JA, Walker RA, Pringle JH, Jones JL: Tumour-associated tenascin-C isoforms promote breast cancer cell invasion and growth by matrix metalloproteinase-dependent and independent mechanisms, Breast Cancer Res 2009, 11:R24

33.   Ioachim E, Charchanti A, Briasoulis E, Karavasilis V, Tsanou H, Arvanitis DL, Agnantis NJ, Pavlidis N: Immunohistochemical expression of extracellular matrix components tenascin, fibronectin, collagen type IV and laminin in breast cancer: their prognostic value and role in tumour invasion and progression, Eur J Cancer 2002, 38:2362-2370

34.   Levy P, Ripoche H, Laurendeau I, Lazar V, Ortonne N, Parfait B, Leroy K, Wechsler J, Salmon I, Wolkenstein P, Dessen P, Vidaud M, Vidaud D, Bieche I: Microarray-based identification of tenascin C and tenascin XB, genes possibly involved in tumorigenesis associated with neurofibromatosis type 1, Clin Cancer Res 2007, 13:398-407

35.   Taraseviciute A, Vincent BT, Schedin P, Jones PL: Quantitative analysis of three-dimensional human mammary epithelial tissue architecture reveals a role for tenascin-C in regulating c-met function, The American journal of pathology 2010, 176:827-838

36.   Conklin MW, Eickhoff JC, Riching KM, Pehlke CA, Eliceiri KW, Provenzano PP, Friedl A, Keely PJ: Aligned collagen is a prognostic signature for survival in human breast carcinoma, The American journal of pathology 2011, 178:1221-1232

37.   Schedin P, Keely PJ: Mammary gland ECM remodeling, stiffness, and mechanosignaling in normal development and tumor progression, Cold Spring Harb Perspect Biol 2011, 3:a003228

38.   Schedin P: Pregnancy-associated breast cancer and metastasis, Nature reviews 2006, 6:281-291

39.   Singh-Ranger G, Salhab M, Mokbel K: The role of cyclooxygenase-2 in breast cancer: review, Breast Cancer Res Treat 2008, 109:189-198

40.   Mazhar D, Ang R, Waxman J: COX inhibitors and breast cancer, British journal of cancer 2006, 94:346-350

41.   Kwan ML, Habel LA, Slattery ML, Caan B: NSAIDs and breast cancer recurrence in a prospective cohort study, Cancer Causes Control 2007, 18:613-620

42.   Holmes MD, Chen WY, Li L, Hertzmark E, Spiegelman D, Hankinson SE: Aspirin intake and survival after breast cancer, J Clin Oncol 2010, 28:1467-1472

43.   Ristimaki A, Sivula A, Lundin J, Lundin M, Salminen T, Haglund C, Joensuu H, Isola J: Prognostic significance of elevated cyclooxygenase-2 expression in breast cancer, Cancer research 2002, 62:632-635

44.   Denkert C, Winzer KJ, Muller BM, Weichert W, Pest S, Kobel M, Kristiansen G, Reles A, Siegert A, Guski H, Hauptmann S: Elevated expression of cyclooxygenase-2 is a negative prognostic factor for disease free survival and overall survival in patients with breast carcinoma, Cancer 2003, 97:2978-2987

45.   Spizzo G, Gastl G, Wolf D, Gunsilius E, Steurer M, Fong D, Amberger A, Margreiter R, Obrist P: Correlation of COX-2 and Ep-CAM overexpression in human invasive breast cancer and its impact on survival, British journal of cancer 2003, 88:574-578

46.   Howe LR: Inflammation and breast cancer. Cyclooxygenase/prostaglandin signaling and breast cancer, Breast Cancer Res 2007, 9:210

47.   Minn AJ, Gupta GP, Siegel PM, Bos PD, Shu W, Giri DD, Viale A, Olshen AB, Gerald WL, Massague J: Genes that mediate breast cancer metastasis to lung, Nature 2005, 436:518-524

48.   Bos PD, Zhang XH, Nadal C, Shu W, Gomis RR, Nguyen DX, Minn AJ, van de Vijver MJ, Gerald WL, Foekens JA, Massague J: Genes that mediate breast cancer metastasis to the brain, Nature 2009, 459:1005-1009

49.   Gauthier ML, Berman HK, Miller C, Kozakeiwicz K, Chew K, Moore D, Rabban J, Chen YY, Kerlikowske K, Tlsty TD: Abrogated response to cellular stress identifies DCIS associated with subsequent tumor events and defines basal-like breast tumors, Cancer cell 2007, 12:479-491

50.   Visscher DW, Pankratz VS, Santisteban M, Reynolds C, Ristimaki A, Vierkant RA, Lingle WL, Frost MH, Hartmann LC: Association between cyclooxygenase-2 expression in atypical hyperplasia and risk of breast cancer, Journal of the National Cancer Institute 2008, 100:421-427

51.   Liu CH, Chang SH, Narko K, Trifan OC, Wu MT, Smith E, Haudenschild C, Lane TF, Hla T: Overexpression of cyclooxygenase-2 is sufficient to induce tumorigenesis in transgenic mice, The Journal of biological chemistry 2001, 276:18563-18569

52.   Larkins TL, Nowell M, Singh S, Sanford GL: Inhibition of cyclooxygenase-2 decreases breast cancer cell motility, invasion and matrix metalloproteinase expression, BMC cancer 2006, 6:181

53.   Singh B, Berry JA, Shoher A, Ayers GD, Wei C, Lucci A: COX-2 involvement in breast cancer metastasis to bone, Oncogene 2007, 26:3789-3796

54.   O'Brien J, Hansen K, Barkan D, Green J, Schedin P: Non-steroidal anti-inflammatory drugs target the pro-tumorigenic extracellular matrix of the postpartum mammary gland, Int J Dev Biol 2011, 55:745-755

55.   Ge R, Tan E, Sharghi-Namini S, Asada HH: Exosomes in Cancer Microenvironment and Beyond: have we Overlooked these Extracellular Messengers?, Cancer Microenviron 2012,

56.   Silva J, Garcia V, Rodriguez M, Compte M, Cisneros E, Veguillas P, Garcia JM, Dominguez G, Campos-Martin Y, Cuevas J, Pena C, Herrera M, Diaz R, Mohammed N, Bonilla F: Analysis of exosome release and its prognostic value in human colorectal cancer, Genes Chromosomes Cancer 2012, 51:409-418

57.   Bergmann C, Strauss L, Wieckowski E, Czystowska M, Albers A, Wang Y, Zeidler R, Lang S, Whiteside TL: Tumor-derived microvesicles in sera of patients with head and neck cancer and their role in tumor progression, Head Neck 2009, 31:371-380

58.   Safaei R, Larson BJ, Cheng TC, Gibson MA, Otani S, Naerdemann W, Howell SB: Abnormal lysosomal trafficking and enhanced exosomal export of cisplatin in drug-resistant human ovarian carcinoma cells, Mol Cancer Ther 2005, 4:1595-1604

59. Hercpetin

60.   Webber J, Steadman R, Mason MD, Tabi Z, Clayton A: Cancer exosomes trigger fibroblast to myofibroblast differentiation, Cancer Res 2010, 70:9621-9630

61.   Cho JA, Park H, Lim EH, Lee KW: Exosomes from breast cancer cells can convert adipose tissue-derived mesenchymal stem cells into myofibroblast-like cells, Int J Oncol 2012, 40:130-138

62.   Hood JL, San RS, Wickline SA: Exosomes released by melanoma cells prepare sentinel lymph nodes for tumor metastasis, Cancer Res 2011, 71:3792-3801

63.   Jung T, Castellana D, Klingbeil P, Cuesta Hernandez I, Vitacolonna M, Orlicky DJ, Roffler SR, Brodt P, Zoller M: CD44v6 dependence of premetastatic niche preparation by exosomes, Neoplasia 2009, 11:1093-1105

64.   Huber V, Filipazzi P, Iero M, Fais S, Rivoltini I. (2008) More insights into the immunosupresive potential of tumor exosomes, J Transl Med 6:63

65.   Clayton A, Mitchell JP, Court J, Mason MD, Tabi Z: Human tumor-derived exosomes selectively impair lymphocyte responses to interleukin-2, Cancer Res 2007, 67:7458-7466

66.   Andreola G, Rivoltini L, Castelli C, Huber V, Perego P, Deho P, Squarcina P, Accornero P, Lozupone F, Lugini L, Stringaro A, Molinari A, Arancia G, Gentile M, Parmiani G, Fais S: Induction of lymphocyte apoptosis by tumor cell secretion of FasL-bearing microvesicles, J Exp Med 2002, 195:1303-1316

67.   Huber V, Fais S, Iero M, Lugini L, Canese P, Squarcina P, Zaccheddu A, Colone M, Arancia G, Gentile M, Seregni E, Valenti R, Ballabio G, Belli F, Leo E, Parmiani G, Rivoltini L: Human colorectal cancer cells induce T-cell death through release of proapoptotic microvesicles: role in immune escape, Gastroenterology 2005, 128:1796-1804

68.   Szajnik M, Czystowska M, Szczepanski MJ, Mandapathil M, Whiteside TL: Tumor-derived microvesicles induce, expand and up-regulate biological activities of human regulatory T cells (Treg), PLoS One 2010, 5:e11469

69.   Wada J, Onishi H, Suzuki H, Yamasaki A, Nagai S, Morisaki T, Katano M: Surface-bound TGF-beta1 on effusion-derived exosomes participates in maintenance of number and suppressive function of regulatory T-cells in malignant effusions, Anticancer Res 2010, 30:3747-3757

70.   Valenti R, Huber V, Filipazzi P, Pilla L, Sovena G, Villa A, Corbelli A, Fais S, Parmiani G, Rivoltini L: Human tumor-released microvesicles promote the differentiation of myeloid cells with transforming growth factor-beta-mediated suppressive activity on T lymphocytes, Cancer Res 2006, 66:9290-9298

71.   Xiang X, Poliakov A, Liu C, Liu Y, Deng ZB, Wang J, Cheng Z, Shah SV, Wang GJ, Zhang L, Grizzle WE, Mobley J, Zhang HG: Induction of myeloid-derived suppressor cells by tumor exosomes, Int J Cancer 2009, 124:2621-2633

72.   Liu Y, Xiang X, Zhuang X, Zhang S, Liu C, Cheng Z, Michalek S, Grizzle W, Zhang HG: Contribution of MyD88 to the tumor exosome-mediated induction of myeloid derived suppressor cells, Am J Pathol 2010, 176:2490-2499

73.   Yang M, Chen J, Su F, Yu B, Lin L, Liu Y, Huang JD, Song E: Microvesicles secreted by macrophages shuttle invasion-potentiating microRNAs into breast cancer cells, Mol Cancer 2011, 10:117

74.   Eppel

75.   Filipazzi P, Burdek M, Villa A, Rivoltini L, Huber V: Recent advances on the role of tumor exosomes in immunosuppression and disease progression, Semin Cancer Biol 2012, 22:342-349

76.   Iero M, Valenti R, Huber V, Filipazzi P, Parmiani G, Fais S, Rivoltini L: Tumour-released exosomes and their implications in cancer immunity, Cell Death Differ 2008, 15:80-88

Size-exclusion chromatography reliably purifies extracellular vesicles from plasma for translational studies of EV functionality and proteomics in breast cancer.

Kimberly R. Jordan[1,2], Dharanija Rao[1,2], Jenny J. Xiang[3,4], Monika Dzieciatkowska[5], Elan Z. Eisenmesser[5], Pepper Schedin[1,6], Kirk C. Hansen[5], Virginia F. Borges[1,2,3]

1. Young Women's Breast Cancer Translational Program, University of Colorado Anschutz Medical Campus, Aurora, CO, USA.
2. Division of Medical Oncology, Department of Medicine, University of Colorado Anschutz Medical Campus, Aurora, CO, USA
3. University of Colorado Cancer Center, Anschutz Medical Campus, Aurora, CO, USA
4. School of Medicine, University of Maryland, Baltimore, MD, USA
5. Department of Biochemistry and Molecular Genetics, School of Medicine, University of Colorado Anschutz Medical Campus, Aurora, CO
6. Knight Cancer Institute and Department of Cell, Developmental & Cancer Biology, Oregon Health Science University, Portland, OR, USA

Correspondence: Virginia F. Borges, Virginia.borges@ucdenver.edu, Division of Medical Oncology, University of Colorado Anschutz Medical Campus, Mailstop 8117, 12801 E 17th Ave, Aurora, CO 80045

Abstract: Extracellular vesicles (EVs) have been found in an increasing number of body fluids including blood, urine, saliva, breast milk and cerebrospinal fluid. One of the reasons for increased and continued interest in studying EVs is their potential to serve as biomarkers in various disease states. In addition, understanding their role in establishing communication with nearby and distant cells and tissues through the transport of biologically significant proteins and nucleic acids can give important insights into their use as therapeutic targets. It is therefore critical to establish methods that consistently and successfully isolate these vesicles from their surrounding fluid, enabling the characterization of their molecular makeup and helping to define their biologic function in multiple species. In our current translational studies, we characterized EVs isolated from human and rodent plasma samples using size-exclusion chromatography (SEC). We found that SEC consistently separates EV-associated proteins from abundant plasma proteins in both human and rodent samples, allowing for the identification of EV proteins by mass spectrometry. Furthermore, we demonstrate the functionality of SEC-purified EVs in tumor cell motility assays for the first time, wherein EVs separated from the conditioned media of invasive breast cancer cells by SEC increase the proliferation, migration, and invasion of non-invasive breast cancer cells. Finally, we compared the protein content of EVs from invasive and non-invasive breast cancer cells and report the first proteomic analyses of EVs from the tumorigenic but non-invasive MCF10DCIS.com cells. The proteome of EVs from these breast cancer cells reflects their functionality in tumor motility assays and may help elucidate the role of EVs in breast cancer progression.

Key Words: exosomes; mass spectrometry; tumor; invasion; migration; proliferation; liquid biopsy

2

Introduction

Extracellular vesicles (EVs) are cell-derived nanoparticles with a characteristic double membrane that contain nucleic acids and proteins, including microRNA, DNA, mRNA, transcription factors, integrins, signaling molecules, and growth factors (1, 2). Although EVs were discovered in the late 1970's, their importance in disease states such as cancer and inflammation have only recently been appreciated by the wider scientific community (3). EVs enable local communication between neighboring cells and cells in distant locations by travelling through various biologic fluids such as blood, urine, and saliva (4-6). In cancer, EVs have been shown to increase tumor growth, to enhance tumor cell invasion, and to potentially establish permissive microenvironments that enable tumor cell metastasis (7-10). Important for cancer patient diagnosis and prognosis, EVs hold promise as a diagnostic and/or monitoring tool of a patient's disease state with the potential of providing biomarkers for patient outcomes and/or responses to cancer treatments (11-15). Furthermore, EVs are emerging as an important tool in drug delivery and vaccine design, and may be targets of future cancer therapies (16-20).

Despite recent advances in targeted therapy for specific breast cancer subtypes, breast cancer continues to cause 40,000 deaths in the United States annually and new therapeutic strategies are needed (21). EVs may provide avenues for novel therapeutics, as several studies have demonstrated that breast cancer cells secrete EVs containing functional molecules with the potential to change the behavior of other cells in their microenvironment (22-24). For example, EVs isolated from breast cancer cell lines contain metalloproteases with catalytic activity that increase the migration of less aggressive breast cancer lines (25, 26). Furthermore, breast cancer EVs can contain EGF ligand and microRNA that contribute to increased tumor cell invasion (27, 28). The composition and role of EVs circulating in human breast cancer patients remains

3

largely unknown and more research is needed to understand the importance of breast cancer-derived EVs in human disease and their potential as diagnostics or therapeutic targets.

Both technologic and biologic barriers have prevented comparisons of the protein content of EVs produced by breast cancer cell lines to those found in breast cancer patient blood samples. Ultracentrifugation and commercially-available precipitation reagents, the most common techniques used to isolate EVs from conditioned media, can be problematic when isolating EVs from patient plasma. Plasma has a higher viscosity than cell culture media and a higher concentration of plasma proteins such as clotting factors, immunoglobulins, and albumin (3, 29). These plasma proteins often aggregate and are purified along with EV pellets during ultracentrifugation and precipitation, making it difficult to detect lower abundance EV-specific proteins by mass spectrometry (30-32). Multi-step purification methods that include ultrafiltration, ultracentrifugation over density gradients, and/or size-exclusion chromatography effectively reduce contaminating soluble proteins and yield a cleaner preparation of plasma EVs (30, 32-35). EVs isolated by size-exclusion chromatography (SEC) from cell culture media and plasma of healthy donors have been validated by electron microscopy, nanoparticle tracking analysis (NTA), and expression of putative EV proteins (33, 35, 36). Furthermore, EVs from the plasma of healthy donors have been successfully characterized using proteomics approaches after purification by size-exclusion chromatography (34). However, purification of plasma EVs using SEC has not yet been validated across species, a requisite for translational research comparing the roles of EVs in rodent models of breast cancer and human breast cancer patients. Here, we confirm that EVs isolated from murine, rat, and human plasma by SEC have a consistent size, morphology, and contain typical EV markers despite differences in concentrations of blood coagulation factors, plasma proteins, and white blood cell counts (37,

4

38). Furthermore, we demonstrate that purification of plasma EVs by SEC reduces

contaminating plasma proteins to a level that allows for the identification of EV-specific proteins

in both rodent and human samples using a basic proteomics approach.

The choice of purification method has been shown to affect the function of EVs in

downstream assays (3, 36, 39). Although EVs isolated by ultracentrifugation from breast cancer

conditioned media have been shown to increase migration and invasion of less invasive cell lines

(25, 26), the functional capacity of EVs isolated by SEC has yet to be confirmed. We show here

that EVs purified by SEC from the conditioned media of breast cancer cells are functionally

active in tumor cell proliferation and motility assays. Furthermore, we show that the protein

content of EVs isolated by SEC from either invasive or non-invasive breast cancer cells may

reflect differences in their functionality in downstream tumor cells assays. Overall, these results

demonstrate that low cost benchtop size-exclusion chromatography successfully purifies plasma

EVs from multiple species and from the conditioned media of breast cancer cells, resulting in

intact and functional particles that can readily be analyzed using a proteomics approach without

the need for serum protein depletion.

Methods

Plasma collection method: Whole blood was collected from mice (cardiac puncture) in heparin

coated tubes or from rats (cardiac puncture) and humans (antecubital fossa venipuncture) in

sodium citrate tubes and plasma was separated by centrifugation at $2000 \times g$ for 15 min at room

temperature. The supernatant was collected and centrifuged at 2000 x g for 10 min at room

temperature and stored at - 80°C. All mouse and rat procedures were approved by the University

5

of Colorado IACUC and human sample collection was performed using a protocol approved by the Colorado Multi-Institutional Review Board. Human samples were collected from 3 healthy women aged 30, 34, and 40 years old. Study data were collected and managed using REDCap electronic data capture tools hosted at the University of Colorado Anschutz Medical Campus (40).

EV Isolation from plasma: Plasma samples were thawed on ice and spun at 15,000 x g for 10 min at room temperature. For isolation of EVs by ultracentrifugation, 250 µl plasma was diluted with 5 mL PBS and filtered through a 0.22µm syringe filter. The diluted plasma was then ultracentrifuged at 100,000 $\times$ g overnight at 4°C. The supernatant was removed and mixed with lysis buffer for comparison by western blot and the pellets were resuspended in PBS for nanosight measurements or lysis buffer for western blot analysis. For size-exclusion chromatography, plasma samples were filtered through a 0.22 µm syringe filter, and concentrated from 1 ml to about 125 µl for rodent plasma and from 4 ml to about 500 µl for human plasma in 100 kDa molecular weight cutoff ultrafiltration tubes (Sartorius). The concentrated plasma samples were layered over a Sepharose CL-2B size exclusion column (GE Healthcare, UK), 0.7 x 10 cm high (Kimble-Chase) for rodent plasma and 1.5 x 10 cm high for human plasma. Thirty serial fractions (250 µl each for the 0.7 x 10 cm columns with rodent plasma, or 1 ml each for the 1.5 x 10 cm columns with human plasma) were eluted by gravity filtration with 0.32% sodium citrate in PBS as previously described (35). Fractions were analyzed for the presence of EVs by NTA and fractions 5 through 10 were combined and concentrated in 100 kDa molecular weight cutoff ultrafiltration tubes (Sartorius). Purified EVs used in protein analysis were stored at -80°C, EVs for electron microscopy and functional assays

6

were stored at 4°C for less than one week prior to use.

EV Isolation from culture media: The human breast cancer cell line MDA-MB231 (41) was cultured in RPMI (Corning) containing 10% Human AB serum (Corning), 2 mM L-Glutamine (Corning), 100 IU penicillin, and 100 ug/ml streptromycin (Corning) in a 37°C incubator with 5% CO_2. The MCF10DCIS.com cell line was cultured as previously described (42, 43). The cells were tested every three months to confirm mycoplasma negativity (MycoAlert[TM] Mycoplasma Detection Kit, Lonza), and validated for authenticity by fingerprinting performed by Dr. Christopher Korch (University of Colorado Cancer Center Sequencing Facility). To make conditioned media, cells were rinsed with Hanks Buffered Saline Solution, incubated at 37°C in serum-free media for 4 h, then transferred to fresh serum-free media and incubated for 48 h at 37°C. Cell debris was removed by centrifugation at 500 x *g* for 5 min and 2,000 x g for 10 min, and filtration through a sterile 0.22 µm syringe filter and stored at 4°C. Approximately 180 ml of conditioned media was concentrated with a 50 kDa molecular weight cutoff ultrafiltration tube (Sartorius) and EVs were isolated over a size-exclusion column as described above.

Nanoparticle Tracking Analysis: EV concentration and size was analyzed using a Nanosight NS300 instrument using a 532 nm laser (Malvern). Images were captured using an sCMOS camera, a gain of 1.0, and camera level of 13. Samples were diluted 200-fold in phosphate buffered saline (PBS) and injected using a Nanosight autopump (Malvern) in script mode commanding a set temperature of 22°C, an infusion rate of 25 µl/min, and video capture of five consecutive 30 sec videos with a 5 sec delay. Data were captured and analyzed using NTA Analytical Software suite version 3.1 (Malvern) using a detection threshold of 5.0. The

7

instrument was calibrated using 100 nm silicone beads. Samples that were below 20 particles

per frame or above 100 particles per frame were re-diluted to a concentration within this range.

Protein Concentration: Protein content was characterized by Bradford Protein Assay (Bio-Rad,

Hercules, CA) and Pierce^{TM} BCA Protein Assay (Thermo-Scientific) according to the

manufacturer's instructions and compared to a standardized curve of bovine serum albumin

(BSA).

Electron Microscopy: EVs purified by size exclusion chromatography were incubated on

formar-coated grids and negatively stained using 5% uranyl acetate. The grids were rinsed and

the size and morphology of EVs was analyzed using a Technai 10 Transmission Electron

Microscope (Field Emissions Inc) and images were captured at 25,000x using a First Light

digital camera (Gatan) located at the CU AMC Electron Microscopy Center (Aurora, CO).

Western Blots: Western blots were performed by separating 20 μg of protein in 1 x RIPA

buffer by 10% SDS-PAGE. Protein bands were transferred to PVDF membranes by wet transfer

at 100V for 1 hour. The membranes were blocked with 5% non-fat dry milk in TBST and 10%

goat serum and incubated with primary antibodies (Hsp70, CD81, CD63, CD9, System

Biosciences) at 4°C overnight. The membranes were washed in TBST and incubated in goat-anti

rabbit IgG-HRP secondary antibody (Systems Biosciences) at room temperature for 1 hour. The

protein bands were visualized using the ECL Plus Substrate solution (Pierce) or SuperSignal

West Pico Substrate (Pierce). For total protein visualization, UC and SEC EVs were lysed in 1 x

RIPA buffer containing a protease inhibitor mix and equal amounts of protein were separated by

8

SDS-PAGE on a 10% Tris-HCl gel. The gel was then stained with Coomassie Blue and imaged using an Odyssey instrument (Licor Biotechnology).

Sample Preparation for Proteomics: Human and rodent EVs samples were analyzed via mass spectrometry (CU AMC Mass Spectrometry and Proteomics Shared Resource, Aurora, CO). The samples were digested according to the FASP protocol using a 30 kDa molecular weight cutoff filter (44). In brief, samples were mixed in the filter unit with 8 M urea in 0.1 M ammonium bicarbonate (ABC), pH 8.5 and centrifuged at 14,000 x g for 15 min. The proteins were reduced by addition of 100 µl of 10 mM DTT in 8 M urea and 0.1 M ABC, pH 8.5, incubated for 30 min at room temperature, and centrifuged. Subsequently, 100 µl of 55 mM iodoacetamide in 8M urea and 0.1 M ABC, pH 8.5 were added to the samples, incubated for 30 min at room temperature in the dark, and centrifuged. The samples were washed three times with 100 µl 8M urea in 0.1 M ABC, pH 8.5, then three times in 100 µl of 0.1 M ABC buffer. The proteins were digested overnight at 37°C with 0.02% Protease Max (Promega). Peptides were recovered by transferring the filter unit to a new collection tube and spinning at 14,000 x g for 10 min. To complete peptide recovery, the filters were rinsed twice with 50 µl 0.2% FA and 10 mM ABC and collected by centrifugation. The peptide mixture was desalted and concentrated on a C18 Tip (Thermo Scientific Pierce).

Mass Spectrometry: Samples were analyzed on a Q Exactive quadrupole orbitrap mass spectrometer (Thermo Fisher Scientific) coupled to an Easy-nLC 1000 UHPLC (Thermo Fisher Scientific) through a nanoelectrospray ion source. Peptides were separated on a self-made 15 cm C18 analytical column (100 µm x 10 cm) packed with 2.7 µm Phenomenex Cortecs C18 resin.

9

After equilibrations with 3 µl 5% acetonitrile and 0.1% formic acid, the peptides were separated by a 180 min linear gradient from 2% to 32% acetonitrile with 0.1% formic acid at 350 nL/min. LC mobile phase solvents and samples dilutions used 0.1% formic acid in water (Buffer A) and 0.1% formic acid in acetonitrile (Buffer B) (Optima^{TM} LC/MS, Fisher Scientific). Data acquisition was performed using the instrument supplied Xcaliber^{TM} (version 3.0) software. The mass spectrometer was operated in the positive ion mode and in the data-dependent acquisition mode. In one scan cycle, peptide ions were first scanned by full MS at resolution 60,000 (FWHM at m/z 200), and then the top 12 intensive ions (2 m/z isolation window) were sequentially subjected to HCD fragmentation and detected at resolution 15,000. Dynamic exclusion was set to 20 s. Spray voltage was set to 2.5 kV, S-lends RF level at 55, and heated capillary at 275ºC.

Protein Identification: MS/MS spectra data were extracted from raw data files and exported as mascot generic format files (mfg) using MassMatrix. The mgf files were then searched against the SwissProt database using an in-house Mascot^{TM} server (Version 2.2.06, Matrix Science). Mass tolerances were +/- 10 ppm for MS peaks and +/- 0.1 Da for MS/MS fragment ions. Trypsin specificity was used, allowing for one missed cleavage. Methionine oxidation, proline hydroxylation, protein N-terminal acetylation, and peptide N-terminal pyroglutamic acid formation were allowed for variable modifications while carbamidomethyl of Cys was set as a fixed modification.

Scaffold (version 4.4, Proteome Software) was used to filter tandem MS based peptide and protein identifications. Peptide and protein identifications were accepted if they could be established at greater than 95% and 99% probability, respectively, as specified by the Peptide

10

Prophet algorithm. Protein identifications also required at least two identified unique peptides.

Proliferation assay: Human MDA-MB231 and MCF10DCIS.com breast cancer cells were plated at 4,000 cells per well +/- $5x10^8$ EVs in a 96 well plate and phase contrast images were taken every 4 hours using an IncuCyte instrument (Essen BioScience, Ann Arbor, MI). After 72 h, images were analyzed using Incucyte Zoom software and the percentage of surface area covered by tumor cells was determined.

Motility assays: For the migration assays, MCF10DCIS.com human breast cancer cells were plated at 40,000 cells per well in a 96 well plate coated with 0.2 mg/ml matrigel (Corning) and incubated overnight at 37^oC. Uniform wounds were created in the center of each well using the IncuCyte Wound Maker (Essen BioScience). Cells were washed, incubated in low-serum media +/- $5x10^8$ EVs, and bright-field images were taken every 2 h using an Incucyte instrument (Essen BioScience). After 24 h, images were analyzed using IncuCyte Zoom software and the density of cells in each wound was calculated relative to the initial wound density. The invasion assay was performed as described for the migration assay except a 2 mg/ml matrigel pad was layered over the cells after wounding.

Statistical Analysis: Two groups were compared using an unpaired two-tailed Student's *t* test, three or more groups were compared using one-way ANOVA, and three or more groups with multiple measures were compared using two-way ANOVA using GraphPad Prism software version 6.0. Where appropriate, p values are adjusted for multiple comparisons and multiple measurements.

11

Results

Extracellular vesicles are found in both human and rodent plasma

Translational studies investigating the role of extracellular vesicles (EVs) in breast cancer as potential diagnostic or therapeutic targets will be facilitated by isolation methods that seamlessly purify EVs with similar physical properties from both rodent breast cancer models and human breast cancer patients. We first sought to confirm the presence of EVs in plasma samples using nanoparticle tracking analysis (NTA) and western blot for typical EV markers. Relative to rat and mouse plasma, human plasma contained the highest level of total protein as measured by Bradford assay (mouse 23 +/- 0.6 mg/ml; rat 38 +/- 8.5 mg/ml; human 44 +/- 6.4 mg/ml). As expected, NTA measurements in the baseline plasma samples of all species were consistent with reported average particle sizes of EVs, allowing for the caveat that NTA measurements in unpurified samples potentially include signals from protein aggregates that overlap with the expected light scatter and Brownian motion of EVs [Figure 1a, (45)]. Rat plasma contained the highest concentration of particles as measured by NTA (mouse 1.6×10^{11} +/- 6×10^{9} particle/ml; rat 5.4×10^{11} +/- 2×10^{10} particles/ml; human 3.3×10^{11} +/- 5.4×10^{10} particles/ml, Figure 1a), while the average size of particles in human plasma was slightly larger (mouse 93 +/- 1.3 nm; rat 91 +/- 0.8 nm; human 106 +/- 2.0 nm). We determined that plasma from mouse, rat, and human subjects mixed with lysis buffer contained detectable levels of the putative EV proteins Hsp70, CD63, and CD81 by western blot (Figure 1b and Supplemental Figure 1), indicating EVs may be present in samples from all three species. Consistent with previous studies, these proteins are detected at multiple molecular weights, likely due to their known isoforms, differential glycosylation patterns, and mixed origin (46-49). CD9 was not reliably detected by western blot of plasma samples (data not shown). These results confirm previously

12

reported interspecies variability in plasma protein levels (37) and demonstrate potential differences in particle concentration and size between rodent and human plasma EVs.

Size-exclusion chromatography effectively separates EVs from plasma across species

Our interest in analyzing the protein content of EVs in rodent models of breast cancer and in breast cancer patient samples by mass spectrometry prompted us to test size exclusion chromatography (SEC) as a potential method for the purification of plasma EVs, which has been shown to reduce the level of abundant plasma proteins (32). We first sought to determine if the physical properties of EVs isolated by SEC were similar across species and whether the variability observed in plasma samples (Figure 1) would also be present in isolated EVs. We loaded concentrated plasma on a Sepharose CL-2B column bed and analyzed 30 gravity filtration fractions for nanoparticle concentration and protein content. We consistently found detectable concentrations of nanoparticles in early fractions (Figure 2a, fractions 5 through 10), while detectable protein concentrations were found in later fractions (Figure 2a, fractions 12 through 25), suggesting that SEC effectively separates the majority of soluble plasma proteins and aggregates from EVs across species. As a further validation of this technique, we found that average particle sizes in the first EV fractions were larger than average particle sizes in the later EV fractions, demonstrating that larger nanoparticles elute before smaller particles (Figure 2b). Furthermore, there was a negative linear trend between mean particle size and fraction number in all species (mouse $p = 0.0089$, rat $p = 0.0005$, human $p < 0.0001$). These data suggest that the Sepharose CL-2B column successfully fractionates nanoparticles by size and separates fractions containing the highest concentration of eluted particles from the fractions containing the highest concentration of soluble proteins, indicating that SEC is a promising method for the separation of

13

EVs in plasma samples when high purity is desirable.

To compare the physical characteristics of EVs purified by SEC from rodent and human plasma samples, we combined and concentrated column fractions 5 through 10 (early EV fractions). The average size and particle yield was analyzed by NTA, protein content by western blot, and morphology by electron microscopy. Despite the interspecies differences seen in measurement of EVs in unpurified plasma (Figure 1) and differences in the anticoagulants used for mouse (heparin) and rat and human (sodium citrate) sample collection, the average particle sizes and yields were similar across species and in the reported range for exosomes (Figure 2c and d). Furthermore, <u>SEC-purified EVs contained putative EV proteins CD63 and Hsp70 with some variability in molecular weight detected across species (Figure 2e)</u>. SEC-purified EVs also had a spherical cup-shaped appearance by electron microscopy (Figure 2f and Supplemental Figure 2). These results indicate that SEC consistently purifies nanoparticles from mouse, rat, and human plasma that are morphologically intact and biochemically similar to reported EVs.

Size-exclusion chromatography effectively separates EVs from abundant proteins in rat plasma

Analyses of EV proteins by mass spectrometry requires a highly pure sample with low levels of contaminating plasma proteins. SEC is reported to separate EVs from plasma proteins, resulting in identification of EV-specific proteins by mass spectrometry (34), while ultracentrifugation often pellets abundant plasma proteins along with EVs (30-32). Thus, we compared the protein content of EVs purified from plasma using ultracentrifugation or SEC to determine whether SEC more effectively reduces abundant plasma proteins and allows for the successful identification of EV-associated proteins.

14

Ultracentrifugation of rat and human plasma resulted in nanoparticles with a typical size distribution as measured by NTA (Supplemental Figure 3; rat 120 nm, human 130 nm). The particle yield per ml of plasma was higher for ultracentrifugation compared to SEC isolation, potentially due to the aforementioned caveats of NTA analysis, in which measurements of protein aggregates overlap with those of EVs. Consistent with this hypothesis, electron microscopy revealed that these preparations were highly contaminated with visible protein aggregates (Supplemental Figure 2a). However, the EV protein markers Hsp70, CD63, and CD81 were still identifiably increased in ultracentrifugation pellets of rat and human plasma compared to ultracentrifugation supernatants by western blot (Supplemental Figure 3c), suggesting that most EVs were successfully pelleted using this method.

We next used a proteomics approach to directly compare the protein content of EVs purified by ultracentrifugation and SEC. As expected, supernatants from ultracentrifugation high levels of the most abundant proteins in the plasma proteome reference set (Figure 3a, (50)). However, there was evidence of persistent contamination of the ultracentrifugation pellets by non-EV proteins, as they also contained high levels of the most abundant plasma proteins. Though there was a differential separation of protein between the ultracentrifugation pellet and supernatant (Figure 3c), the most abundant proteins identified in ultracentrifugation pellets were not bone fide EV-associated proteins, but rather apolipoproteins, immunoglobulins, fibronectin, fibrinogen, and complement components. Since these proteins are known to form large aggregates, they may account for the protein aggregates observed by EM imaging of EVs isolated by ultracentrifugation.

In contrast, using the SEC column separation method, abundant plasma proteins were decreased in the earlier EV-containing fractions and increased in the late column fractions

15

(Figure 3b). Furthermore, SEC EV fractions contained a large number of EV-associated proteins that have been identified in previous proteomics studies and are reported in the online databases Exocarta and Vesiclepedia (51, 52). We found that SEC isolation enriched for EV proteins known to be vital in the biosynthesis and release of EVs from the cell of origin (Figure 3b, e.g. Rab proteins, HSP7C, CD9, myosin, clathrin, tubulin, serglycin, and vinculin), adhesion to and internalization of EVs in target cells and tissues (collagen, integrins, galectin-3, C4 binding protein, basigin, SVEP1, DMBT1, and CECAM-1), potential markers of the cell of origin (platelet glycoproteins and erythrocyte Band 3), and the potential function of EVs once in target cells (Rap1b, reelin, 14-3-3 protein, CD151, GNAI2, TGFβ1, and ADAM10) (1, 53-57). Some identified proteins may be both markers of the originating cell type and play a potential role in the adhesion or function of EVs in target cells (CD44, CD47, CD59, CD48, MYADM, and Thy1) (54, 57, 58). These results indicate that SEC enriched for EV proteins, allowing for their identification in rat plasma by mass spectrometry, while ultracentrifugation resulted in a high abundance of large serum protein complexes that impair the identification of the more rare EV proteins.

Size-exclusion chromatography effectively separates EVs from abundant proteins in human plasma

To determine if SEC also successfully separates soluble proteins from EVs in human plasma samples, we analyzed the total protein content of EVs from two healthy human donors using a coomassie-stained SDS-PAGE gel (Supplemental Figure 4). We found that the protein bands consistent with human albumin (66.5 kDa) and IgG heavy chain (53 kDa) were greatly reduced in the EV samples prepared by SEC compared to those prepared by ultracentrifugation,

16

suggesting that abundant plasma proteins were more effectively reduced in human EV samples prepared by SEC. We next compared the protein content of early EV-containing fractions from three healthy human donors prepared by SEC to the late fractions from the same donors. Similar to rat samples, abundant plasma proteins were consistently identified in the late fractions, while EV proteins were consistently identified in the early EV-containing fractions (Figure 4a). The most abundant EV-specific proteins identified in human samples were similar to those identified in the rat samples (Figure 4b). Some notable differences included soluble scavenger receptor cysteine-rich domain containing protein (SRCRL), a pattern recognition receptor that facilitates binding to pathogens and extracellular matrix proteins (59, 60), and Ig-binding receptors (IgGFc binding protein and polymeric Ig receptor) [Figure 4b, (61, 62)].

In addition to the most abundant proteins, we also analyzed less abundant EV-associated proteins that were consistently identified in human plasma EVs purified by SEC (Figure 4c). Largely overlapping with those identified in rat plasma EVs, human EV proteins included putative EV markers (CD81, CD63, HSP7C, and several tetraspanins) and proteins involved in EV biosynthesis, adhesion, and function (57). We identified additional adhesion molecules including CD31, desmoplakin, CD226, CD47, CD91, desmoglein, and junction plakglobulin (63). Furthermore, we identified several proteins that may have activity in target cells including CD92, annexin A11, serum deprivation-response protein, CD36, thrombospondin-1, HLA Class I, CD82, S100A9, and aminopeptidase N (1, 54). These results indicate that SEC successfully separates EVs from soluble plasma proteins and is a viable purification method for studying the protein content of EVs in translational studies of both human and rodent plasma.

Breast cancer EVs purified by size-exclusion chromatography increase proliferation and

17

motility of less aggressive breast cancer cells

Since the choice of EV isolation method can impact their function in downstream analyses (3, 36, 39), and few studies have shown whether SEC-purified EVs can impact cellular processes *in vitro*, we next determined if EVs purified from breast cancer cell culture supernatants by SEC effect migration, invasion, and proliferation of the non-invasive breast cancer line MCF10DCIS.com. EVs from the parental MCF10a non-tumorigenic cell line have been previously characterized (14, 64), however the protein content and function of EVs produced by MCF10DCIS.com cells, which form DCIS-like tumors in non-immunogenic mice and can become invasive (43, 65), have not been described. We chose to use EVs produced by the MDA-MB231 breast cancer line, aggressive triple negative breast cancer cells that form invasive carcinomas in xenograft models (41), as a positive control for inducing invasive properties. To purify EVs produced by breast cancer cells, we layered concentrated cell culture supernatants over a Sepharose CL-2B and collected 30 fractions, similar to the purification method used for plasma described above. We found that EVs from both invasive MDA-MB231 media and non-invasive MCF10DCIS.com breast cancer media eluted in fractions 5 through 11 (Figure 5a). Since these cells were incubated in serum-free media, proteins in the late fractions were below the limit of detection for the Bradford assay (data not shown). After combining and concentrating the EV-containing fractions, we determined that SEC purification resulted in a similar particle size and protein yield to previously reported results for UC purification of MDA-MB231 EVs [Figure 5b, (25)]. These EVs also expressed the putative EV proteins Hsp70, CD63, and CD9 (Figure 5c and Supplemental Figure 5).

Previous studies have shown that EVs produced by invasive MDA-MB231 breast cancer cells and purified by ultracentrifugation increase the proliferation and motility of less invasive

18

breast cancer lines (25). To determine if purification of EVs by SEC maintains their functional

capacity, we performed *in vitro* proliferation, migration, and invasion assays. We found that the

addition of $5x10^8$ EVs from invasive MDA-MB231 cells (approximately 50 µg) increased the

confluence of both MDA-MB231 and MCF10DCIS.com cells at 72 h and 48 h, respectively

(Figure 5d). Furthermore, MDA-MB231 EVs increased the migration of MCF10DCIS.com cells

across a scratch wound (Figure 5e) and the invasion of MCF10DCIS.com cells into a matrigel

pad (Figure 5f). In contrast, EVs from less aggressive MCF10DCIS.com cells did not increase

invasion, but only increased the migration of MCF10DCIS.com cells in the scratch wound assay.

There was no significant effect of EVs on the motility of MDA-MB231 cells in these assays

(data not shown), suggesting that these cells are already maximally invasive and added EVs offer

no additional aggression to their behavior. These results also indicate that overall EVs purified

by SEC are functionally active and alter the rate of proliferation, migration, and invasiveness of

cancer cells *in vitro*.

The protein content of EVs from breast cancer cell conditioned media are consistent with

their function and cell of origin

The differential effect of EVs from invasive and non-invasive breast cancer cells

suggested there may be proteomic differences between EVs isolated from these cell lines. We

compared the total protein content of EVs isolated from two independent preparations of

conditioned media from MDA-MB231 and MCF10DCIS.com cells by mass spectrometry. Of

the 1,109 proteins identified in MCF10DCIS.com EVs and the 1,032 proteins identified in

MDA-MB231 EVs, 632 proteins were shared between the two cell lines. Overall functional

annotation of proteins with 6 or more spectral matches using the DAVID Bioinformatics

19

Resource (66, 67) revealed that EVs produced by the invasive MDA-MB231 cells were significantly enriched for proteins involved in vesicle formation (6.16 enrichment score with the entire dataset as background), protein synthesis (4.9), proteolysis (3.56), and glycolysis (1.54). In contrast, MCF10DCIS.com EVs were significantly enriched for membrane proteins (12.65 enrichment score), adhesion molecules (10.33), proteins involved in cellular migration (4.21), and components of the extracellular matrix (3.65). Shared proteins identified in EVs from both cell lines were enriched for vesicle proteins (7.4 enrichment score), membrane components (2.97), regulators of cell death (2.86), contractile fibers (2.56), adhesion molecules (1.89), and proteins that promote cell motility (1.84). Reflecting these differences, the most abundant proteins uniquely identified in MDA-MB231 EVs were those involved in transcriptional regulation (splicesome, transcription factors, ribosomal proteins, tRNA ligases), proteolysis (proteasome units, pyrophosphatase), EV formation (annexin and vesicle markers LAMP-1 and EEA1), cell cycle (NUMA1), and cell motility and adherence to extracellular matrices (vitronectin, collagen, filamin proteins, and EDIL3) (Table 1). In contrast, the most abundant proteins uniquely identified in EVs from the MCF10DCIS.com cells were cellular adhesion proteins (cadherin family members, laminin proteins, proteoglycans, Syndecan-1, EPCAM, b-catenin, and collagen), regulators of cellular proliferation (CD109, RARRES1, PTGFRN, FAT1, S100A14, and Amphiregulin), and metabolic proteins (calcium-binding proteins, serine proteases, and cholesterol- and lipoprotein-binding proteins) (27, 56). The protein content of EVs from MDA-MB231 and MCF10DCIS.com cells may reflect the biologic differences between these invasive and non-invasive breast cancer cells and contribute to their altered functional activity.

20

Discussion

Circulating EVs hold the promise to provide a source of relevant biomarkers for breast cancer onset and recurrence, which would represent an important advancement for early detection and post-treatment surveillance of breast cancer patients. In addition to serving as a biomarker for the disease state of breast cancer patients, EVs secreted by breast cancer cells have functional consequences on their surrounding environment and at distant sites of metastasis and therefore represent potential novel targets for therapeutic development (22, 68). However, nearly all cells in the body are reported to produce EVs (1) and EVs from normal cells likely outnumber those secreted by the cancer cells in tumor-bearing hosts. A critical step to move EV research from cell lines to human cancer clinical samples has been the need to identify techniques that effectively separate EVs from contaminating plasma proteins and permit detailed study of their protein content. Additionally, these needed techniques must permit the isolation of EVs from clinically relevant human samples that can be used in downstream functional assays to identify the EVs role(s) in cancer progression, immune suppression and metastasis. Lastly, protein markers that distinguish cancer-specific EVs from those secreted by healthy cells need to be identified for the development of potential novel therapeutics.

Herein, we demonstrate that SEC successfully purifies EVs from mouse, rat, and human plasma samples with a consistent composition, size, and morphology, despite differences in the composition of baseline plasma across species. In comparison to ultracentrifugation, SEC allowed for the identification of many putative EV proteins using a standard proteomics workflow. Ultracentrifugation did not provide adequate separation of EVs and plasma proteins, resulting in a high level of contaminating blood proteins that confounded proteomic studies. However, ultracentrifugation remains a very useful technique for studies using cancer cell lines

21

grown in serum-free conditions, where the presence of plasma protein is not a confounding

factor (69). At present, we suggest that the optimal purification technique for a study must be

determined by the source of the sample, the efficiency of the technique for large numbers of

samples, and the downstream assays that will be performed that may be affected by the choice of

isolation method (36). We show for the first time that EVs purified by SEC from breast cancer

cell culture supernatants function *in vitro* and alter breast cancer cell behavior, similar to

previously reported EVs purified by ultracentrifugation. Therefore, SEC is an effective method

for the purification of EVs from plasma samples across species that uniquely permits

simultaneous functional and protein content analysis from one isolation step and therefore will

be a highly useful technique for future proteomic studies of breast cancer patient-derived EVs.

Determining the protein content of circulating EVs from healthy donors gives insight into

their normal biologic function and provides a point of comparison for studies of EVs in various

disease states. We consistently identified many EV-associated proteins in samples from all three

healthy donors, including those used to characterize EVs by western blot (CD9, CD81, CD63,

and HSP70). Not surprisingly, EVs from healthy donors contained proteins that are vital for EV

formation, such as Rab proteins, tetraspanins, clatherin components, and myosin proteins (1).

However, these EVs also contained proteins that may play a role in their downstream location

and function. Specific integrin combinations have been shown to direct EVs to certain organ

tissues (70), suggesting that the integrins and other adhesion molecules identified in this dataset

may be responsible for EV localization in a non-disease state. These EVs also contained

components of the MAPK/ERK signaling pathway, molecules involved in antigen presentation,

and proteins that regulate immune responses, all of which support a role for EVs in normal

physiologic processes (1, 71, 72). Breast cancer cells have been shown to take advantage of

22

these normal functions by producing EVs that activate MAP kinases (56, 73), downregulate an important tumor-recognizing molecule on NK cells and T cells (22), and modulate macrophage function (74). Our dataset and others will be an important comparison for future studies of breast cancer EVs in patients, with the goal of identifying additional, potentially targetable, mechanisms by which EVs promote tumor cell metastases and immune cell evasion.

EVs produced by the invasive triple negative MDA-MB231 breast cancer cell line increased the proliferation rate of both MDA-MB231 and non-invasive MCF10DCIS.com cells *in vitro*. Furthermore, EVs from MDA-MB231 cells increased both the migration and invasion of MCF10DCIS.com cells in scratch wound assays. These results support previous studies showing that EVs produced by highly invasive breast cancer cells influence their surrounding microenvironment, potentially increasing the growth and metastatic potential of neighboring breast cancer cells (68, 75). EV proteins that regulate gene expression within target cells have the potential to indirectly alter motility and proliferation (57). EVs from MDA-MB231 cells may induce more functional changes in target cells relative to EVs from the non-invasive MCF10DCIS.com cells due to an increase in proteins that regulate transcriptional activity and proteolysis. EVs from MDA-MB231 cells also contained proteins that may directly contribute to their increased functional activity, including Filamin A and EDIL-3. Overexpression of Filamin A, a protein with a complex role in regulating cell motility and invasion through cytoskeletal reorganization, is associated with known risk factors for breast cancer, and reduced expression of this molecule decreases migration and invasion of breast cancer cells *in vitro* and breast cancer metastasis *in vivo* (76, 77). EDIL-3 has been shown to regulate epithelial-mesenchymal transition in hepatocellular carcinoma (78), directly contributes to the induction of angiogenesis and migration by EVs from bladder cancer cells (79), and was recently shown to

23

mediate increased invasion and metastasis by breast cancer EVs (75). These results highlight some promising candidate proteins that may be involved in the downstream effects of EVs produced by invasive breast cancer cells and whose presence in EVs purified from breast cancer patient plasma will be investigated in our future studies.

In contrast to the invasive MDA-MB231 EVs, those produced by the tumorigenic but non-invasive MCF10DCIS.com cells were enriched for cellular adhesion proteins, likely reflecting this cell line's increased tendency to maintain cell-to-cell contact *in vitro*. Interestingly, although MCF10DCIS.com EVs did not significantly increase proliferation, they were enriched for proteins that drive cell cycle, including CD109 and S100A14. For example, CD109 inhibits TGF-β signaling, enhances EGF signaling, and promotes cell cycle progression in breast cancer cells (80). In addition, S100A14 modulates expression of p53 and stimulates proliferation of esophageal squamous cell carcinoma at low doses (81). These molecules may not have significant activity in target cells after co-incubation with EVs or their activity may be balanced by negative regulators of cell cycle that are also present in MCF10DCIS.com EVs such as FAT1 and RARRES1 (82, 83). However, increased expression of CD109 and S100A14 in cancer stem cells and whole tumor sections, respectively, correlates with prognostic indicators and disease-free survival in triple negative breast cancer patients (80, 84). Therefore, despite their apparent lack of activity in the proliferation assays presented here, EVs expressing CD109 and S100A14 molecules may serve as biomarkers for clinical outcomes in breast cancer patients.

A reliable and consistent EV isolation method is important for the discovery of new EV-associated biomarkers, for mechanistic studies into the downstream effects of EVs, and for comparisons of EV biomarkers and function across species. This study demonstrates that SEC successfully separates functional EVs from the large majority of plasma proteins in multiple

24

species and lays the groundwork for future studies of EVs in rodent models of breast cancer and

in breast cancer patients. Together, these data indicate that SEC is a very effective purification

method for studying the protein content and functional nature of EVs in multiple animal models

and patient samples to advance our understanding of the role of EVs in cancer.

Bibliography

1.   Yanez-Mo M, Siljander PR, Andreu Z, Zavec AB, Borras FE, Buzas EI, et al. Biological properties of extracellular vesicles and their physiological functions. J Extracell Vesicles. 2015;4:27066.
2.   Tkach M, Thery C. Communication by Extracellular Vesicles: Where We Are and Where We Need to Go. Cell. 2016;164(6):1226-32.
3.   Taylor DD, Shah S. Methods of isolating extracellular vesicles impact down-stream analyses of their cargoes. Methods. 2015;87:3-10.
4.   Colombo M, Raposo G, Thery C. Biogenesis, secretion, and intercellular interactions of exosomes and other extracellular vesicles. Annu Rev Cell Dev Biol. 2014;30:255-89.
5.   Peinado H, Lavotshkin S, Lyden D. The secreted factors responsible for pre-metastatic niche formation: old sayings and new thoughts. Semin Cancer Biol. 2011;21(2):139-46.
6.   Costa-Silva B, Aiello NM, Ocean AJ, Singh S, Zhang H, Thakur BK, et al. Pancreatic cancer exosomes initiate pre-metastatic niche formation in the liver. Nat Cell Biol. 2015;17(6):816-26.
7.   Fujita Y, Yoshioka Y, Ochiya T. Extracellular vesicle transfer of cancer pathogenic components. Cancer Sci. 2016.
8.   He M, Qin H, Poon TC, Sze SC, Ding X, Co NN, et al. Hepatocellular carcinoma-derived exosomes promote motility of immortalized hepatocyte through transfer of oncogenic proteins and RNAs. Carcinogenesis. 2015;36(9):1008-18.
9.   Chan YK, Zhang H, Liu P, Tsao SW, Lung ML, Mak NK, et al. Proteomic analysis of exosomes from nasopharyngeal carcinoma cell identifies intercellular transfer of angiogenic proteins. Int J Cancer. 2015;137(8):1830-41.
10.   Marimpietri D, Petretto A, Raffaghello L, Pezzolo A, Gagliani C, Tacchetti C, et al. Proteome profiling of neuroblastoma-derived exosomes reveal the expression of proteins potentially involved in tumor progression. PLoS One. 2013;8(9):e75054.
11.   Overbye A, Skotland T, Koehler CJ, Thiede B, Seierstad T, Berge V, et al. Identification of prostate cancer biomarkers in urinary exosomes. Oncotarget. 2015;6(30):30357-76.
12.   Szajnik M, Derbis M, Lach M, Patalas P, Michalak M, Drzewiecka H, et al. Exosomes in Plasma of Patients with Ovarian Carcinoma: Potential Biomarkers of Tumor Progression and Response to Therapy. Gynecol Obstet (Sunnyvale). 2013;Suppl 4:3.
13.   Redzic JS, Ung TH, Graner MW. Glioblastoma extracellular vesicles: reservoirs of potential biomarkers. Pharmgenomics Pers Med. 2014;7:65-77.

25

14.   Melo SA, Luecke LB, Kahlert C, Fernandez AF, Gammon ST, Kaye J, et al. Glypican-1 identifies cancer exosomes and detects early pancreatic cancer. Nature. 2015;523(7559):177-82.

15.   Matsumura T, Sugimachi K, Iinuma H, Takahashi Y, Kurashige J, Sawada G, et al. Exosomal microRNA in serum is a novel biomarker of recurrence in human colorectal cancer. Br J Cancer. 2015;113(2):275-81.

16.   Haney MJ, Klyachko NL, Zhao Y, Gupta R, Plotnikova EG, He Z, et al. Exosomes as drug delivery vehicles for Parkinson's disease therapy. J Control Release. 2015;207:18-30.

17.   Batrakova EV, Kim MS. Using exosomes, naturally-equipped nanocarriers, for drug delivery. J Control Release. 2015.

18.   Tran TH, Mattheolabakis G, Aldawsari H, Amiji M. Exosomes as nanocarriers for immunotherapy of cancer and inflammatory diseases. Clin Immunol. 2015;160(1):46-58.

19.   Pitt JM, Charrier M, Viaud S, Andre F, Besse B, Chaput N, et al. Dendritic cell-derived exosomes as immunotherapies in the fight against cancer. J Immunol. 2014;193(3):1006-11.

20.   Viaud S, Thery C, Ploix S, Tursz T, Lapierre V, Lantz O, et al. Dendritic cell-derived exosomes for cancer immunotherapy: what's next? Cancer Res. 2010;70(4):1281-5.

21.   Siegel R, Naishadham D, Jemal A. Cancer statistics, 2013. CA Cancer J Clin. 2013;63(1):11-30.

22.   Yu DD, Wu Y, Shen HY, Lv MM, Chen WX, Zhang XH, et al. Exosomes in development, metastasis and drug resistance of breast cancer. Cancer Sci. 2015;106(8):959-64.

23.   Lowry MC, Gallagher WM, O'Driscoll L. The Role of Exosomes in Breast Cancer. Clin Chem. 2015.

24.   Villagrasa A, Alvarez PJ, Osuna A, Garrido JM, Aranega A, Rodriguez-Serrano F. Exosomes Derived from Breast Cancer Cells, Small Trojan Horses? J Mammary Gland Biol Neoplasia. 2014;19(3-4):303-13.

25.   Harris DA, Patel SH, Gucek M, Hendrix A, Westbroek W, Taraska JW. Exosomes released from breast cancer carcinomas stimulate cell movement. PLoS One. 2015;10(3):e0117495.

26.   O'Brien K, Rani S, Corcoran C, Wallace R, Hughes L, Friel AM, et al. Exosomes from triple-negative breast cancer cells can transfer phenotypic traits representing their cells of origin to secondary cells. Eur J Cancer. 2013;49(8):1845-59.

27.   Higginbotham JN, Demory Beckler M, Gephart JD, Franklin JL, Bogatcheva G, Kremers GJ, et al. Amphiregulin exosomes increase cancer cell invasion. Curr Biol. 2011;21(9):779-86.

28.   Singh R, Pochampally R, Watabe K, Lu Z, Mo YY. Exosome-mediated transfer of miR-10b promotes cell invasion in breast cancer. Mol Cancer. 2014;13:256.

29.   Jeppesen DK, Hvam ML, Primdahl-Bengtson B, Boysen AT, Whitehead B, Dyrskjot L, et al. Comparative analysis of discrete exosome fractions obtained by differential centrifugation. J Extracell Vesicles. 2014;3:25011.

30.   Lobb RJ, Becker M, Wen SW, Wong CS, Wiegmans AP, Leimgruber A, et al. Optimized exosome isolation protocol for cell culture supernatant and human plasma. J Extracell Vesicles. 2015;4:27031.

31.   Caradec J, Kharmate G, Hosseini-Beheshti E, Adomat H, Gleave M, Guns E. Reproducibility and efficiency of serum-derived exosome extraction methods. Clin Biochem. 2014;47(13-14):1286-92.

26

32. Muller L, Hong CS, Stolz DB, Watkins SC, Whiteside TL. Isolation of biologically-active exosomes from human plasma. J Immunol Methods. 2014;411:55-65.

33. Welton JL, Webber JP, Botos LA, Jones M, Clayton A. Ready-made chromatography columns for extracellular vesicle isolation from plasma. J Extracell Vesicles. 2015;4:27269.

34. de Menezes-Neto A, Saez MJ, Lozano-Ramos I, Segui-Barber J, Martin-Jaular L, Ullate JM, et al. Size-exclusion chromatography as a stand-alone methodology identifies novel markers in mass spectrometry analyses of plasma-derived vesicles from healthy individuals. J Extracell Vesicles. 2015;4:27378.

35. Boing AN, van der Pol E, Grootemaat AE, Coumans FA, Sturk A, Nieuwland R. Single-step isolation of extracellular vesicles by size-exclusion chromatography. J Extracell Vesicles. 2014;3.

36. Nordin JZ, Lee Y, Vader P, Mager I, Johansson HJ, Heusermann W, et al. Ultrafiltration with size-exclusion liquid chromatography for high yield isolation of extracellular vesicles preserving intact biophysical and functional properties. Nanomedicine. 2015;11(4):879-83.

37. Windberger U, Bartholovitsch A, Plasenzotti R, Korak KJ, Heinze G. Whole blood viscosity, plasma viscosity and erythrocyte aggregation in nine mammalian species: reference values and comparison of data. Exp Physiol. 2003;88(3):431-40.

38. Mestas J, Hughes CC. Of mice and not men: differences between mouse and human immunology. J Immunol. 2004;172(5):2731-8.

39. Van Deun J, Mestdagh P, Sormunen R, Cocquyt V, Vermaelen K, Vandesompele J, et al. The impact of disparate isolation methods for extracellular vesicles on downstream RNA profiling. J Extracell Vesicles. 2014;3.

40. Harris PA, Taylor R, Thielke R, Payne J, Gonzalez N, Conde JG. Research electronic data capture (REDCap)--a metadata-driven methodology and workflow process for providing translational research informatics support. J Biomed Inform. 2009;42(2):377-81.

41. Cailleau R, Olive M, Cruciger QV. Long-term human breast carcinoma cell lines of metastatic origin: preliminary characterization. In Vitro. 1978;14(11):911-5.

42. Hu M, Yao J, Carroll DK, Weremowicz S, Chen H, Carrasco D, et al. Regulation of in situ to invasive breast carcinoma transition. Cancer Cell. 2008;13(5):394-406.

43. Lyons TR, O'Brien J, Borges VF, Conklin MW, Keely PJ, Eliceiri KW, et al. Postpartum mammary gland involution drives progression of ductal carcinoma in situ through collagen and COX-2. Nat Med. 2011;17(9):1109-15.

44. Wisniewski JR, Zougman A, Nagaraj N, Mann M. Universal sample preparation method for proteome analysis. Nat Methods. 2009;6(5):359-62.

45. Filipe V, Hawe A, Jiskoot W. Critical evaluation of Nanoparticle Tracking Analysis (NTA) by NanoSight for the measurement of nanoparticles and protein aggregates. Pharm Res. 2010;27(5):796-810.

46. Zlotogorski-Hurvitz A, Dayan D, Chaushu G, Salo T, Vered M. Morphological and molecular features of oral fluid-derived exosomes: oral cancer patients versus healthy individuals. J Cancer Res Clin Oncol. 2016;142(1):101-10.

47. Wang J, Zhou Y, Lu J, Sun Y, Xiao H, Liu M, et al. Combined detection of serum exosomal miR-21 and HOTAIR as diagnostic and prognostic biomarkers for laryngeal squamous cell carcinoma. Med Oncol. 2014;31(9):148.

48. Burns G, Brooks K, Wildung M, Navakanitworakul R, Christenson LK, Spencer TE. Extracellular vesicles in luminal fluid of the ovine uterus. PLoS One. 2014;9(3):e90913.

49.   Epple LM, Griffiths SG, Dechkovskaia AM, Dusto NL, White J, Ouellette RJ, et al. Medulloblastoma exosome proteomics yield functional roles for extracellular vesicles. PLoS One. 2012;7(7):e42064.

50.   Farrah T, Deutsch EW, Omenn GS, Campbell DS, Sun Z, Bletz JA, et al. A high-confidence human plasma proteome reference set with estimated concentrations in PeptideAtlas. Mol Cell Proteomics. 2011;10(9):M110 006353.

51.   Kalra H, Simpson RJ, Ji H, Aikawa E, Altevogt P, Askenase P, et al. Vesiclepedia: a compendium for extracellular vesicles with continuous community annotation. PLoS Biol. 2012;10(12):e1001450.

52.   Keerthikumar S, Chisanga D, Ariyaratne D, Al Saffar H, Anand S, Zhao K, et al. ExoCarta: A Web-Based Compendium of Exosomal Cargo. J Mol Biol. 2016;428(4):688-92.

53.   Yue S, Mu W, Erb U, Zoller M. The tetraspanins CD151 and Tspan8 are essential exosome components for the crosstalk between cancer initiating cells and their surrounding. Oncotarget. 2015;6(4):2366-84.

54.   Raposo G, Stoorvogel W. Extracellular vesicles: exosomes, microvesicles, and friends. J Cell Biol. 2013;200(4):373-83.

55.   Webber J, Steadman R, Mason MD, Tabi Z, Clayton A. Cancer exosomes trigger fibroblast to myofibroblast differentiation. Cancer Res. 2010;70(23):9621-30.

56.   Gangoda L, Boukouris S, Liem M, Kalra H, Mathivanan S. Extracellular vesicles including exosomes are mediators of signal transduction: are they protective or pathogenic? Proteomics. 2015;15(2-3):260-71.

57.   Ung TH, Madsen HJ, Hellwinkel JE, Lencioni AM, Graner MW. Exosome proteomics reveals transcriptional regulator proteins with potential to mediate downstream pathways. Cancer Sci. 2014;105(11):1384-92.

58.   Jung T, Castellana D, Klingbeil P, Cuesta Hernandez I, Vitacolonna M, Orlicky DJ, et al. CD44v6 dependence of premetastatic niche preparation by exosomes. Neoplasia. 2009;11(10):1093-105.

59.   Miro-Julia C, Rosello S, Martinez VG, Fink DR, Escoda-Ferran C, Padilla O, et al. Molecular and functional characterization of mouse S5D-SRCRB: a new group B member of the scavenger receptor cysteine-rich superfamily. J Immunol. 2011;186(4):2344-54.

60.   Goncalves CM, Castro MA, Henriques T, Oliveira MI, Pinheiro HC, Oliveira C, et al. Molecular cloning and analysis of SSc5D, a new member of the scavenger receptor cysteine-rich superfamily. Mol Immunol. 2009;46(13):2585-96.

61.   Kobayashi K, Ogata H, Morikawa M, Iijima S, Harada N, Yoshida T, et al. Distribution and partial characterisation of IgG Fc binding protein in various mucin producing cells and body fluids. Gut. 2002;51(2):169-76.

62.   Ogawa Y, Miura Y, Harazono A, Kanai-Azuma M, Akimoto Y, Kawakami H, et al. Proteomic analysis of two types of exosomes in human whole saliva. Biol Pharm Bull. 2011;34(1):13-23.

63.   Rebhan M, Chalifa-Caspi V, Prilusky J, Lancet D. GeneCards: integrating information about genes, proteins and diseases. Trends Genet. 1997;13(4):163.

64.   Johnson KP, Stoute DC, Yearby L, Beverly G, Skripnikova E, Ochieng J. Exosomal media enhances proliferation, migration, and invasion in triple negative breast cancer. Faseb J. 2013;27.

65.   Miller FR, Santner SJ, Tait L, Dawson PJ. MCF10DCIS.com xenograft model of human comedo ductal carcinoma in situ. J Natl Cancer I. 2000;92(14):1185-6.

66.   Huang da W, Sherman BT, Lempicki RA. Bioinformatics enrichment tools: paths toward the comprehensive functional analysis of large gene lists. Nucleic Acids Res. 2009;37(1):1-13.

67.   Huang da W, Sherman BT, Lempicki RA. Systematic and integrative analysis of large gene lists using DAVID bioinformatics resources. Nat Protoc. 2009;4(1):44-57.

68.   Gorczynski RM, Erin N, Zhu F. Serum-derived exosomes from mice with highly metastatic breast cancer transfer increased metastatic capacity to a poorly metastatic tumor. Cancer Med. 2016;5(2):325-36.

69.   Thery C, Amigorena S, Raposo G, Clayton A. Isolation and characterization of exosomes from cell culture supernatants and biological fluids. Curr Protoc Cell Biol. 2006;Chapter 3:Unit 3 22.

70.   Hoshino A, Costa-Silva B, Shen TL, Rodrigues G, Hashimoto A, Tesic Mark M, et al. Tumour exosome integrins determine organotropic metastasis. Nature. 2015;527(7578):329-35.

71.   Harding CV, Heuser JE, Stahl PD. Exosomes: looking back three decades and into the future. J Cell Biol. 2013;200(4):367-71.

72.   Calzolari A, Raggi C, Deaglio S, Sposi NM, Stafsnes M, Fecchi K, et al. TfR2 localizes in lipid raft domains and is released in exosomes to activate signal transduction along the MAPK pathway. J Cell Sci. 2006;119(Pt 21):4486-98.

73.   Ochieng J, Pratap S, Khatua AK, Sakwe AM. Anchorage-independent growth of breast carcinoma cells is mediated by serum exosomes. Exp Cell Res. 2009;315(11):1875-88.

74.   Chow A, Zhou W, Liu L, Fong MY, Champer J, Van Haute D, et al. Macrophage immunomodulation by breast cancer-derived exosomes requires Toll-like receptor 2-mediated activation of NF-kappaB. Sci Rep. 2014;4:5750.

75.   Lee JE, Moon PG, Cho YE, Kim YB, Kim IS, Park H, et al. Identification of EDIL3 on extracellular vesicles involved in breast cancer cell invasion. J Proteomics. 2016;131:17-28.

76.   Tian HM, Liu XH, Han W, Zhao LL, Yuan B, Yuan CJ. Differential expression of filamin A and its clinical significance in breast cancer. Oncol Lett. 2013;6(3):681-6.

77.   Jiang X, Yue J, Lu H, Campbell N, Yang Q, Lan S, et al. Inhibition of filamin-A reduces cancer metastatic potential. Int J Biol Sci. 2013;9(1):67-77.

78.   Xia H, Chen J, Shi M, Gao H, Sekar K, Seshachalam VP, et al. EDIL3 is a novel regulator of epithelial-mesenchymal transition controlling early recurrence of hepatocellular carcinoma. J Hepatol. 2015;63(4):863-73.

79.   Beckham CJ, Olsen J, Yin PN, Wu CH, Ting HJ, Hagen FK, et al. Bladder cancer exosomes contain EDIL-3/Del1 and facilitate cancer progression. J Urol. 2014;192(2):583-92.

80.   Tao J, Li H, Li Q, Yang Y. CD109 is a potential target for triple-negative breast cancer. Tumour Biol. 2014;35(12):12083-90.

81.   Jin Q, Chen H, Luo A, Ding F, Liu Z. S100A14 stimulates cell proliferation and induces cell apoptosis at different concentrations via receptor for advanced glycation end products (RAGE). PLoS One. 2011;6(4):e19375.

82.   Morris LG, Kaufman AM, Gong Y, Ramaswami D, Walsh LA, Turcan S, et al. Recurrent somatic mutation of FAT1 in multiple human cancers leads to aberrant Wnt activation. Nat Genet. 2013;45(3):253-61.

29

83.   Peng Z, Shen R, Li YW, Teng KY, Shapiro CL, Lin HJ. Epigenetic repression of RARRES1 is mediated by methylation of a proximal promoter and a loss of CTCF binding. PLoS One. 2012;7(5):e36891.

84.   Ehmsen S, Hansen LT, Bak M, Brasch-Andersen C, Ditzel HJ, Leth-Larsen R. S100A14 is a novel independent prognostic biomarker in the triple-negative breast cancer subtype. Int J Cancer. 2015;137(9):2093-103.

30
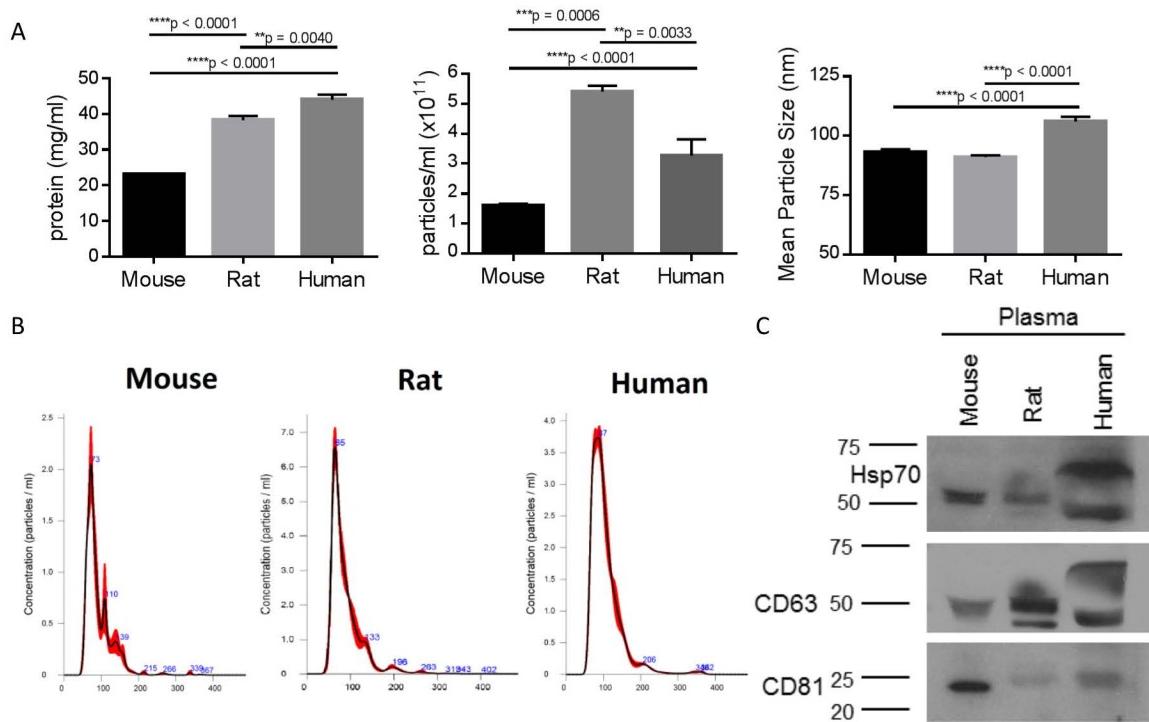
Figure 1. Extracellular vesicles (EVs) are present in plasma samples across species. A. Mouse, Rat, and Human plasma samples were characterized for protein content by Bradford Assay and for nanoparticle concentration and size by Nanoparticle Tracking Analysis (NTA). Groups were compared using one-way ANOVA, p values are adjusted for multiple comparisons, and error bars represent standard error of the mean. Particles consistent with EVs are identified in human and rodent plasma samples, with variability in protein concentration, particle concentration, and particle size across species. B. NTA traces of EVs in plasma samples. C. Plasma samples were lysed in RIPA buffer and 20 μg of total protein was analyzed by western blot for the putative EV markers. Plasma of all species contained detectable levels of Hsp70, CD63, and CD81 but not CD9 (not shown).
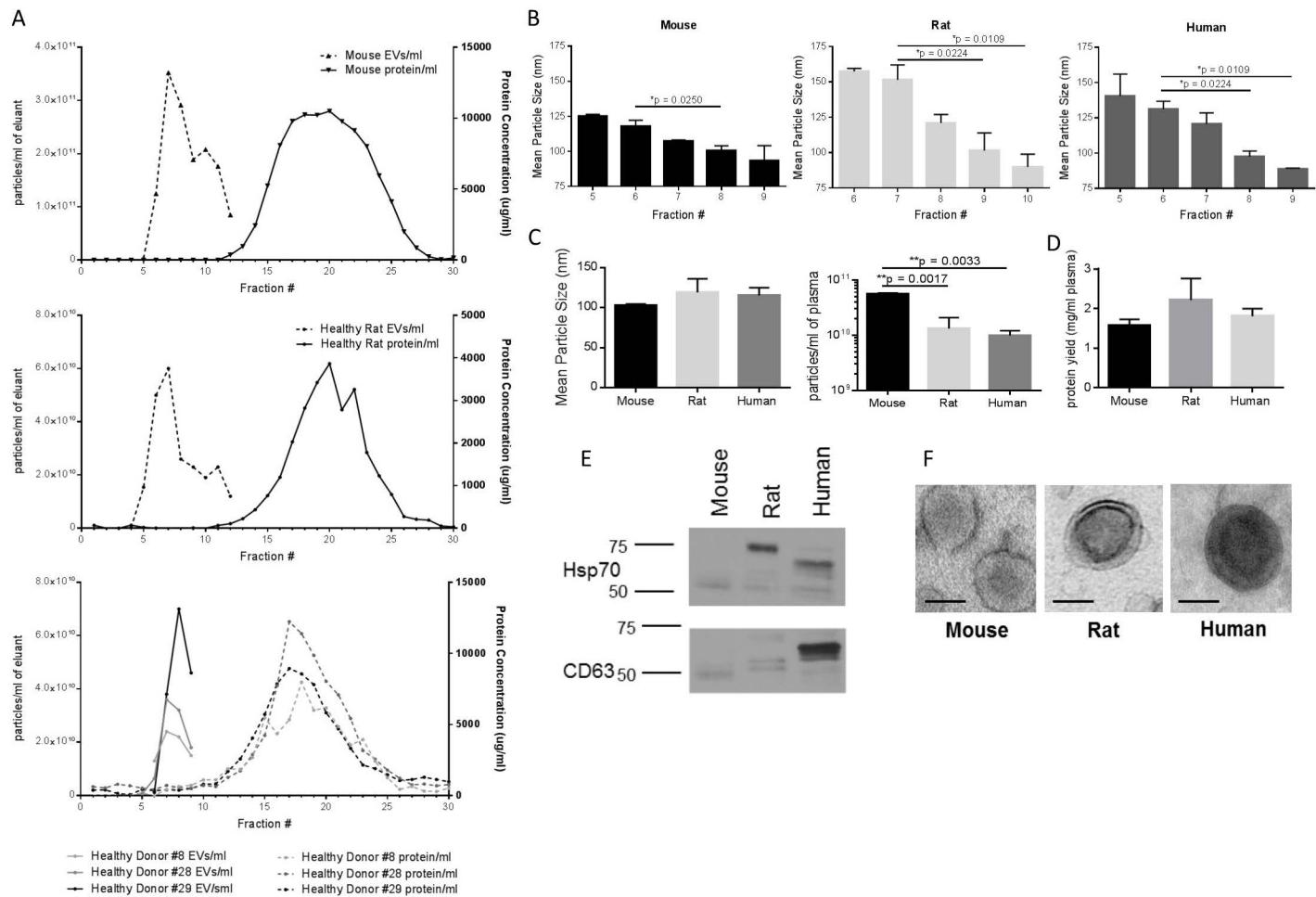
Figure 2. Size-exclusion chromatography separates EVs from other plasma proteins. A. Mouse, Rat, and Human plasma samples were concentrated in ultrafiltration tubes (100 kd molecular weight cut-off), layered over a Sepharose CL -2B size-exclusion column (GE Healthcare), and 30 fractions were collected by gravity filtration. The EV content of each fraction was determined by NTA and the protein content was characterized by Bradford Assay. B. The size of EVs in each fraction was determined and compared using a one-way ANOVA, p values are adjusted for multiple repeated measures, and error bars represent the standard error of the mean. EV-containing fractions 5 through 10 from were combined, concentrated, and analyzed by NTA (C), BCA Assay (D), western blot (E), and electron microscopy (F). The sizing bar represents 50 nm. SEC isolates nanoparticles from plasma with a size, shape, and protein content consistent with EVs.
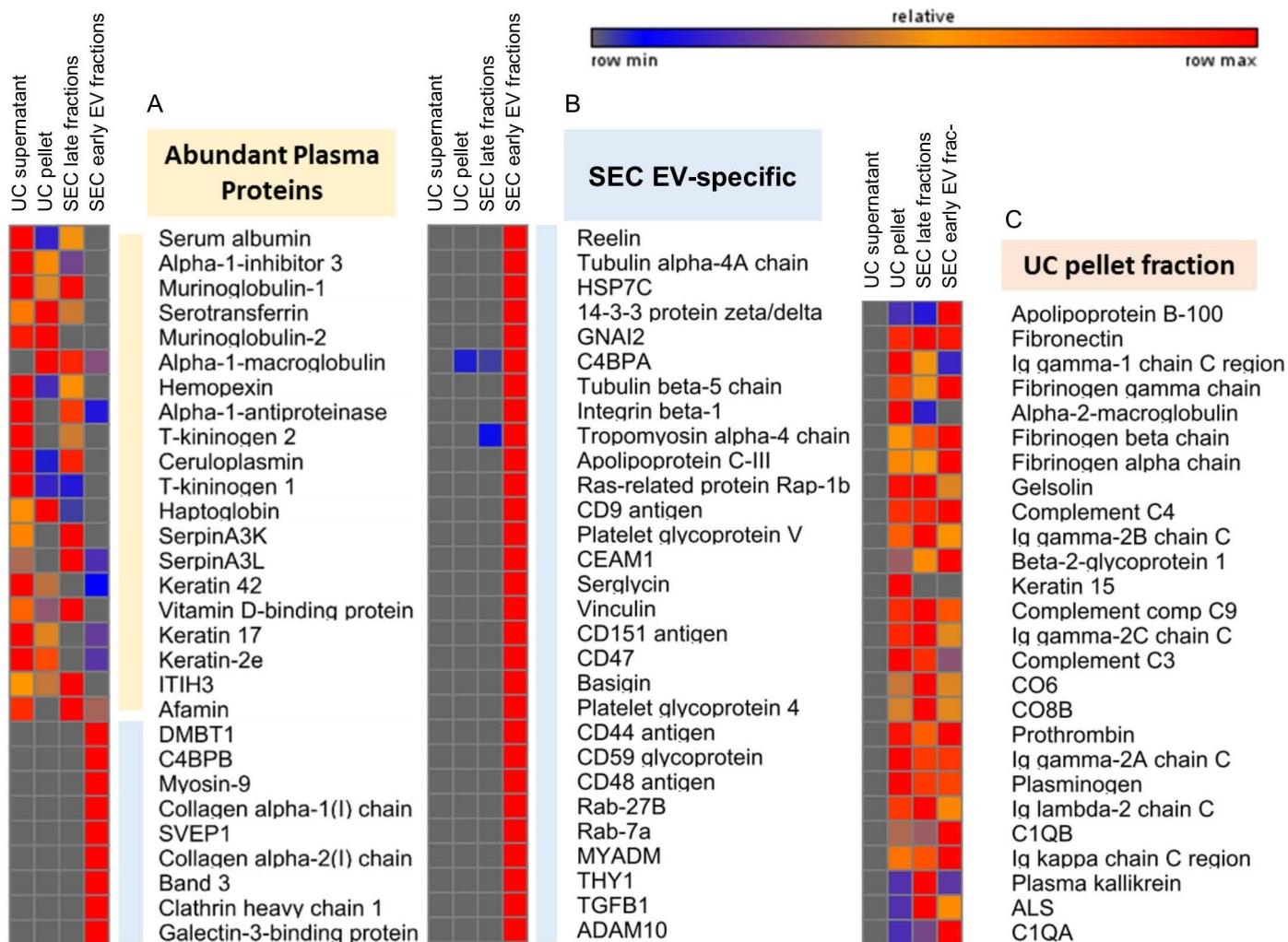
Figure 3. Comparison of the protein content of rat plasma EVs purified by ultracentrifugation and SEC by mass spectrometry. Heat map and analysis of peptide spectral matches from EVs isolated from pooled rat plasma samples. A. Abundant plasma proteins (in beige) are the top 20 proteins in the Plasma Proteome Reference Set (50). SEC reduced the amount of contaminating plasma proteins in EV fractions. B. Abundant EV proteins are those that resulted in the highest ratio of spectral matches compared to plasma. Many EV-specific proteins were identified in the SEC EV sample, but not in the ultracentrifugation EV sample. C. Abundant ultracentrifugation pellet proteins are those with the highest ratio of spectral matches compared to ultracentrifugation supernatants. Although ultracentrifugation differentially separated some proteins from the supernatant, these were not EV-specific.
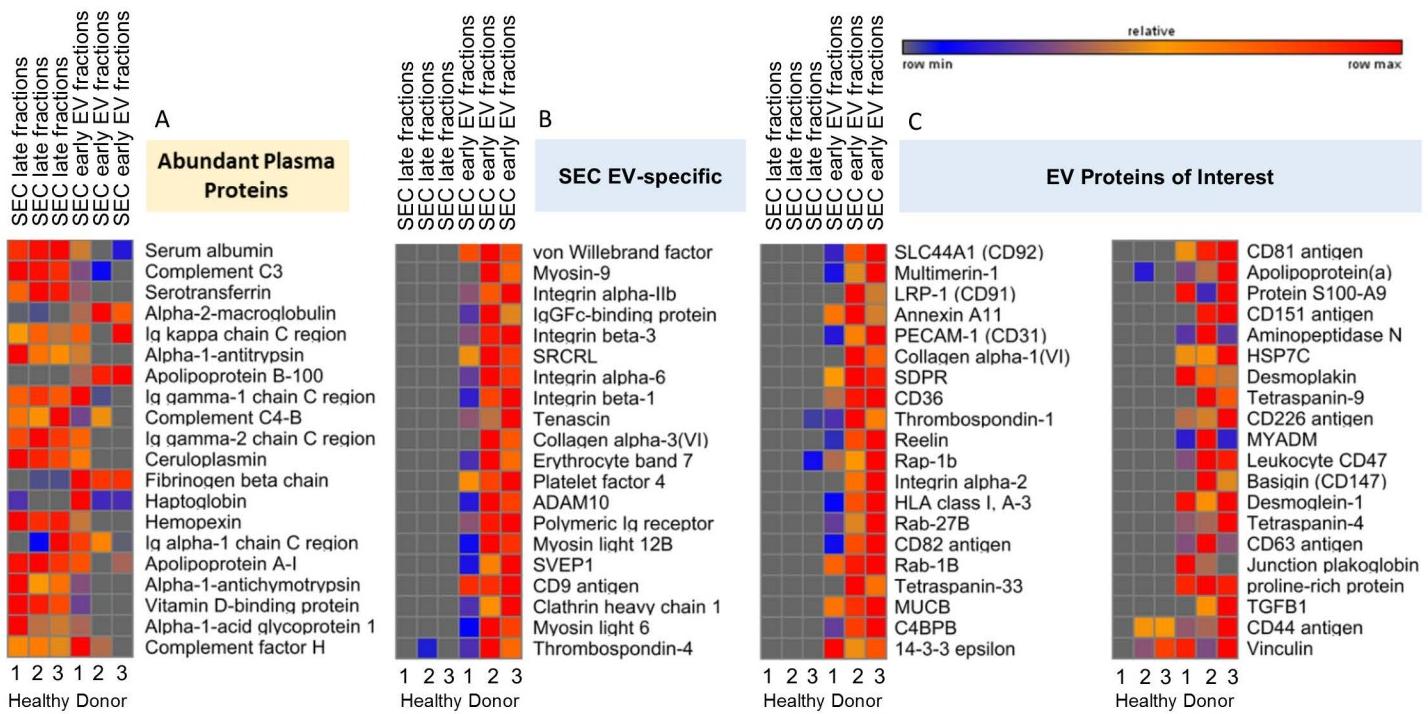
Figure 4. Comparison of the protein content of human plasma SEC late fractions and early EV fractions by mass spectrometry. Heat map and analysis of peptide spectral matches from EVs isolated from three healthy donor plasma samples. A. Abundant plasma proteins are the top 20 proteins in the Plasma Proteome Reference Set (50). SEC reduced the amount of contaminating plasma proteins in all three human EV fractions. B. Abundant EV proteins are those that resulted in the highest ratio of spectral matches compared to late fractions. Many EV-specific proteins were enriched in the EV fractions of all three donors. C. Lower abundance EV proteins of interest were selected based on the ratio of spectral matches compared to late fractions and their known role in EV formation and function.
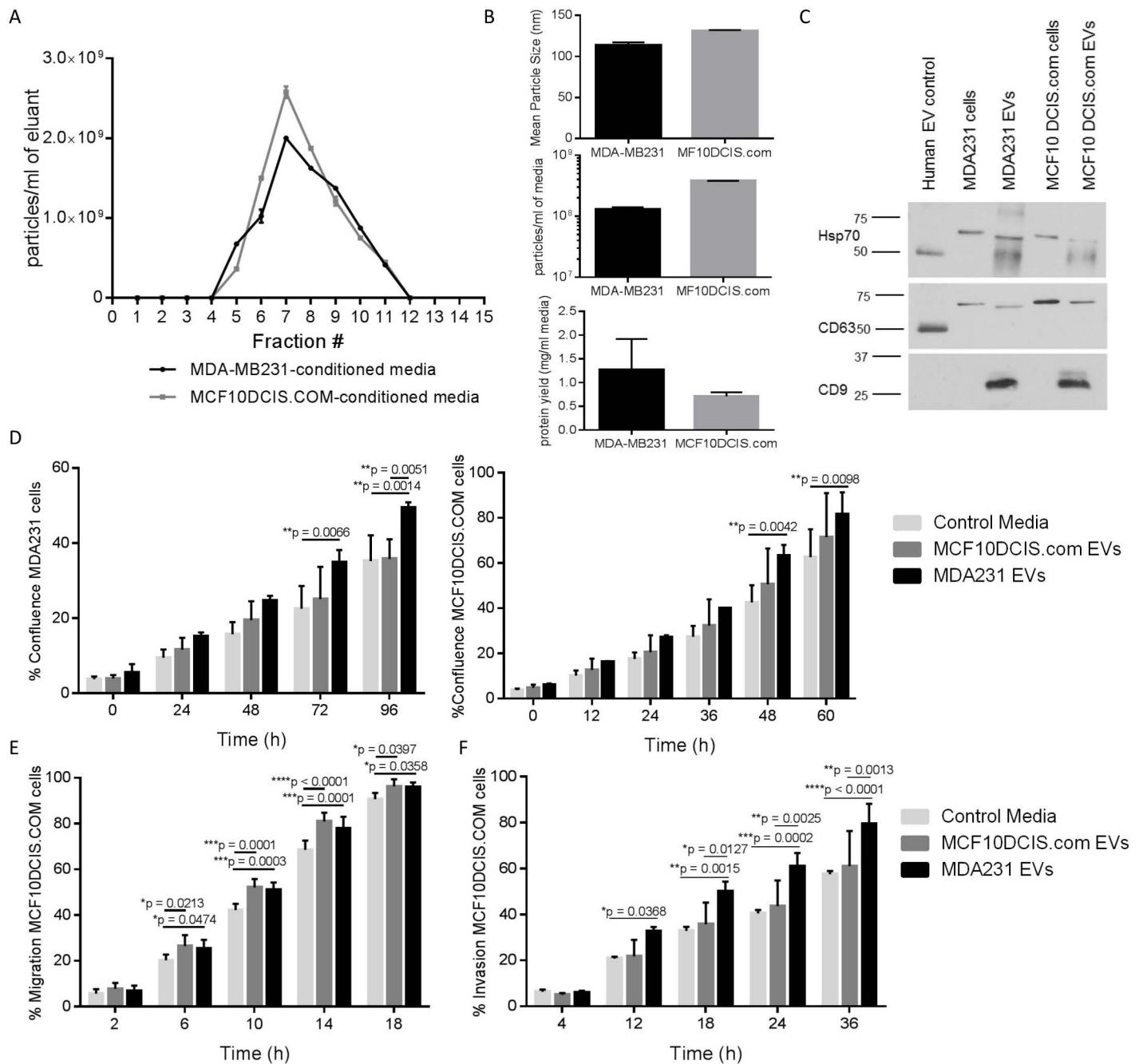
Figure 5. EVs isolated by size-exclusion chromatography increase proliferation and motility of breast cancer cell lines. A. To isolate EVs from human breast cancer lines, MDA-MB231 and MCF10-DCIS.com cells were grown to confluence and transferred into serum-free media. After 48 h, conditioned media was harvested, concentrated in ultrafiltration tubes, and EVs were isolated by size-exclusion chromatography. Fractions 5-10 were combined and characterized by NTA and BCA assay (B), and western blot (C). D. MDA-MB231 (left) or MCF10-DCIS.com cells (right) were seeded at 4,000 cells per well in a 96-well plate +/- 5×10^8 EVs and phase contrast images were taken over 96 or 60 h using an Incucyte instrument. EVs from MDA-MB231 media increased the proliferation of both breast cancer cell lines, while EVs from the less aggressive MCF10-DCIS.com cells did not. E. For the migration assay, MCF10-DCIS.com cells were plated and grown to confluence in a 96-well plate coated with 0.5 mg/ml matrigel. A scratch wound assay was performed +/- 5×10^8 EVs and imaged over 18 h using an Incucyte instrument. EVs from both MDA-MB231 and MCF10-DCIS.com media increased the migration of MCF10-DCIS.com cells. F. For the invasion assays, cells were plated on matrigel-coated wells as in (E) and covered with a 2 mg/ml matrigel pad after wounding. Cell invasion was determined +/- 5×10^8 EVs over 36 h using an Incucyte instrument. EVs from MDA-MB231 media increased the invasion of MCF10-DCIS.com cells, while EVs from the MCF10-DCIS.com cells did not. Averages of at least 4 independent experiments, each with 4 to 5 replicate wells, are shown. Groups were compared using two-way ANOVA and p values were adjusted for multiple repeated measures. Error bars represent the standard deviation of the mean.

Table 1. The most abundant proteins uniquely identified MDA-MB231 or MCF10DCIS.com EVs purified from cell culture supernatants.

| MDA-MB231 EVs			MCF10DCIS.com EVs		
Protein Name	Gene Name	# of Spectral Matches	Protein Name	Gene Name	# of Spectral Matches
Complement C4-B	C4B	140.2	Protocadherin Fat 2	FAT2	264.6
EGF-like repeat and discoidin I-like protein 3	EDIL3	101.7	Laminin subunit beta-3	LAMB3	238.6
Vitronectin	VTN	101.2	Chondroitin sulfate proteoglycan 2	CSPG2	200.7
Annexin A6	ANXA6	88.5	CD109 antigen	CD109	196.8
NUMA1 variant protein	NUMA1	88.3	Retinoic acid receptor responder protein 1	RARRES1	189.0
Filamin-C	FLNC	50.3	Prostaglandin F2 receptor negative regulator	PTGFRN	160.1
Thioredoxin reductase 1	TXNRD1	47.5	Laminin, alpha 4	LAMA4	147.3
Collagen, type V, alpha 1	COL5A1	44.4	Syndecan-1	SDC1	139.9
Proteasome subunit beta type-4	PSMB4	39.4	Protocadherin Fat 1	FAT1	110.0
Filamin-A	FLNA	38.2	Stromal cell derived factor 4	SDF4	108.3
U5 small nuclear ribonucleoprotein	SNRNP200	37.9	Epithelial cell adhesion molecule	EPCAM	105.3
Early endosome antigen 1	EEA1	37.6	Protein S100-A14	S100A14	97.3
Ectonucleotide pyrophosphatase	ENPP1	36.2	SPARC related modular calcium binding 1	SMOC1	83.9
Proteasome subunit alpha type-1	PSMA1	32.4	Fibulin-1	FBLN1	68.9
Interleukin enhancer-binding factor 2	ILF2	30.8	Suppressor of tumorigenicity 14 protein	ST14	65.6
60S ribosomal protein L12	RPL12	28.7	Catenin, beta 1	CTNNB1	59.4
Ubiquitin-like protein ISG15	ISG15	27.8	Serpin peptidase inhibitor, clade E	SERPINE2	56.1
Aspartate--tRNA ligase	DARS	25.6	Follistatin	FST	48.0
Proteasome subunit beta type 7	PSMB7	24.5	Collagen alpha-1	COL17A1	45.2
Serum paraoxonase/arylesterase 1	PON1	23.1	Claudin	CLDN1	45.1
26S proteasome non-ATPase subunit 6	PSMD6	22.1	Amphiregulin	AREG	44.0
Lysosomal-associated membrane protein 1	LAMP1	21.5	Lipolysis-stimulated lipoprotein receptor	LSR	43.8
Ferritin light chain	FTL	20.8	Fascin	FSCN1	42.5
26S protease subunit 8	PSMC5	20.6	Plakophilin-3	PKP3	41.5
60S ribosomal protein L27	RPL27	19.8	Isoform 4 of Scavenger receptor class B1	SCARB1	40.5
SARS protein	SARS	19.3	Solute carrier 16, member 1	SLC16A1	37.1
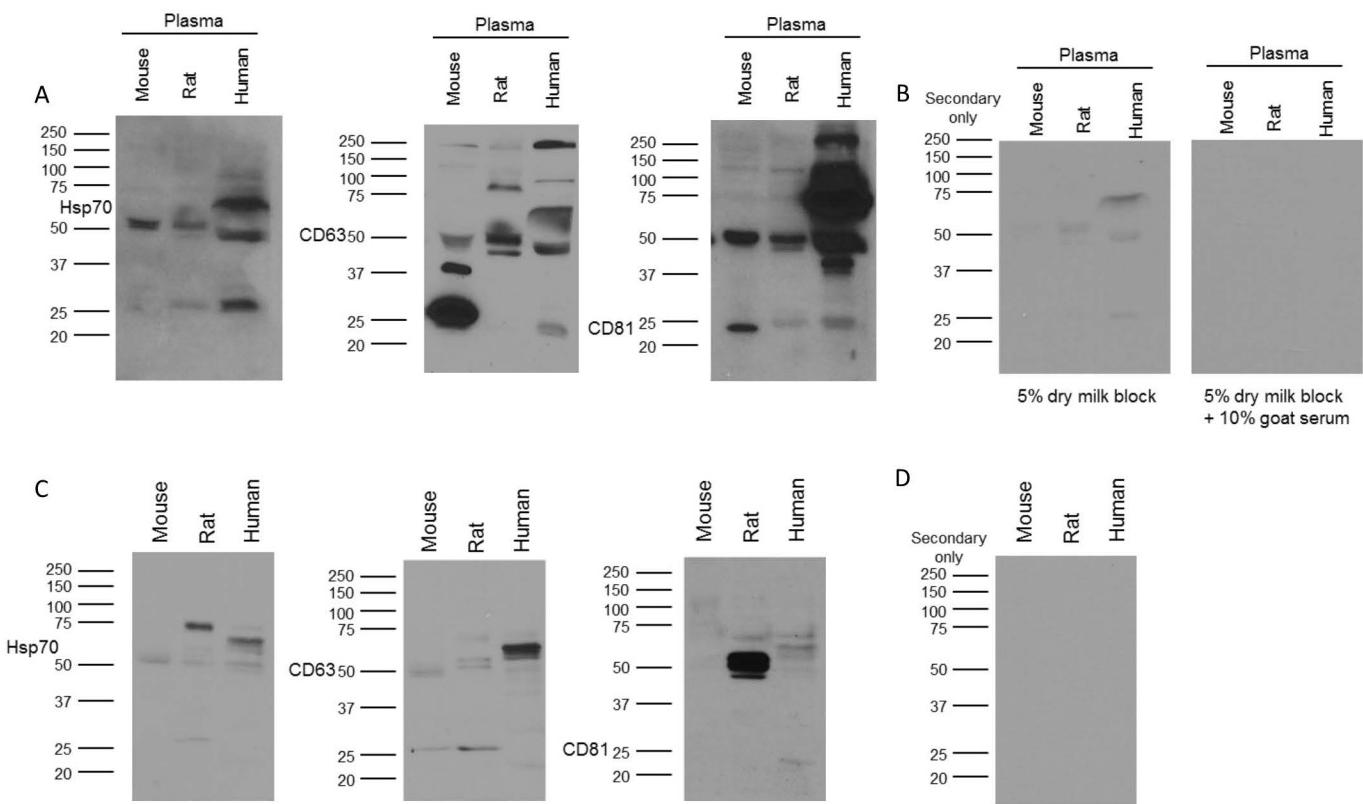
Supplemental Figure 1. Western blot analysis of EV-associated proteins in serum and SEC-purified EVs. A. Sera from a healthy mouse, rat, and human were combined with 2x RIPA lysis buffer for a final concentration of 1x RIPA buffer and separated by 10% SDS-PAGE. Membranes were blocked in 5% non-fat dry milk plus 10% goat serum for 1 h at room temperature, followed by a 1:1,000 dilution of primary antibody, per the manufacturer's recommendations, and a 1:20,000 dilution of goat anti-rabbit HRP secondary. Hsp70 was developed with a 1 min film exposure using ECL Plus substrate, CD63 was developed with a 5 min exposure using SuperSignal West Pico substrate, and CD81 was developed with a 5 min exposure using ECL Plus substrate. B. Blots prepared and blocked as in (A) were blocked in either 5% non-fat dry milk (left) or 5% dry milk plus 10% goat serum (right), incubated with a 1:20,000 dilution of goat anti-rabbit HRP secondary, and developed with a 10 min exposure using SuperSignal West Pico substrate. C. EVs purified by size-exclusion chromatography were combined with 2x RIPA lysis buffer and evaluated by western blot as described above. All three antibodies were developed with a 20 min film exposure using ECL Plus substrate. The low molecular weight CD81 band was only detected in human SEC EVs. D. Blots prepared and blocked as in (C) were incubated with secondary antibody only and developed with a 20 min exposure using ECL Plus substrate.
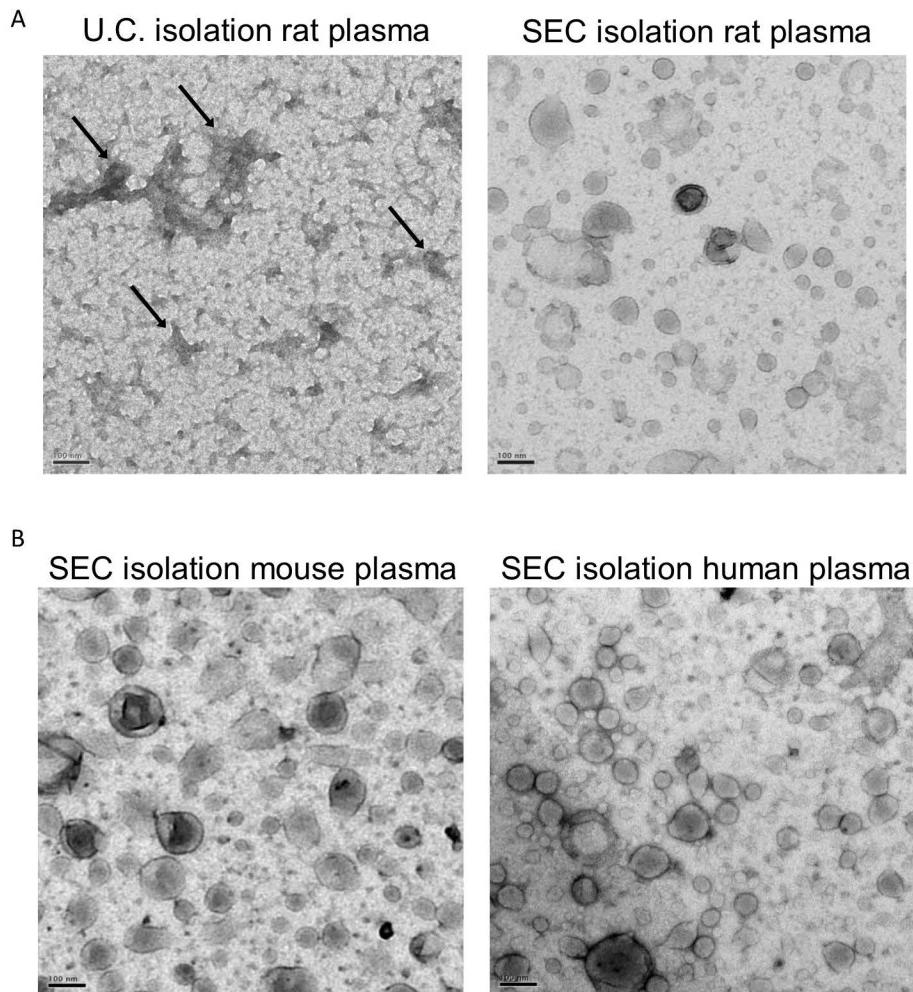
Supplemental Figure 2. SEC isolation reduces protein aggregates in electron microscope imaging. A. EVs were purified from rat plasma samples using ultracentrifugation or size-exclusion chromatography and electron microscopy images were taken after staining with 5% uranyl acetate. The bar represents 100 nm. Arrows indicate examples of possible protein aggregate. B. Representative large-scale EM image of EVs isolated using SEC from mouse and human plasma. Small scale high resolution images are shown in Figure 3f.
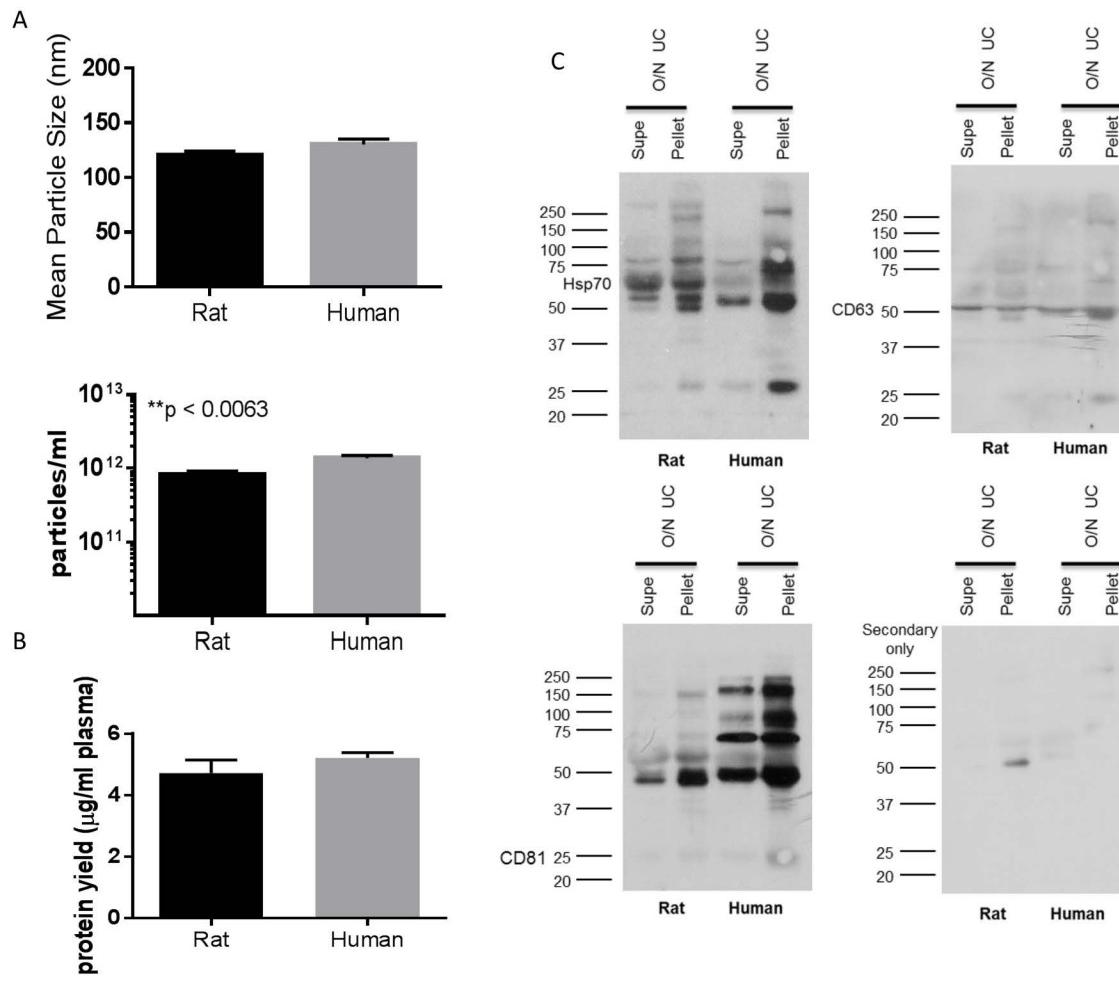
Supplemental Figure 3. Comparison of EV enrichment by 2 hour and overnight ultracentrifugation. Rat and Human plasma samples were ultracentrifuged at 100,000 x g for 2 h or overnight. EV pellets were resuspended in PBS for characterization by NTA (A) or in RIPA buffer for protein characterization by Bradford Assay (B) and western blot (C). Groups were compared using a Student's *t* test. Overnight ultracentrifugation yields more nanoparticles and protein compared to 2 hour ultracentrifugation and enriches for EV markers. Overnight ultracentrifugation pellets contained increased EV markers Hsp70 and CD63 compared to supernatants. The low molecular weight CD81 band was faint, but detectable in UC EV pellets.
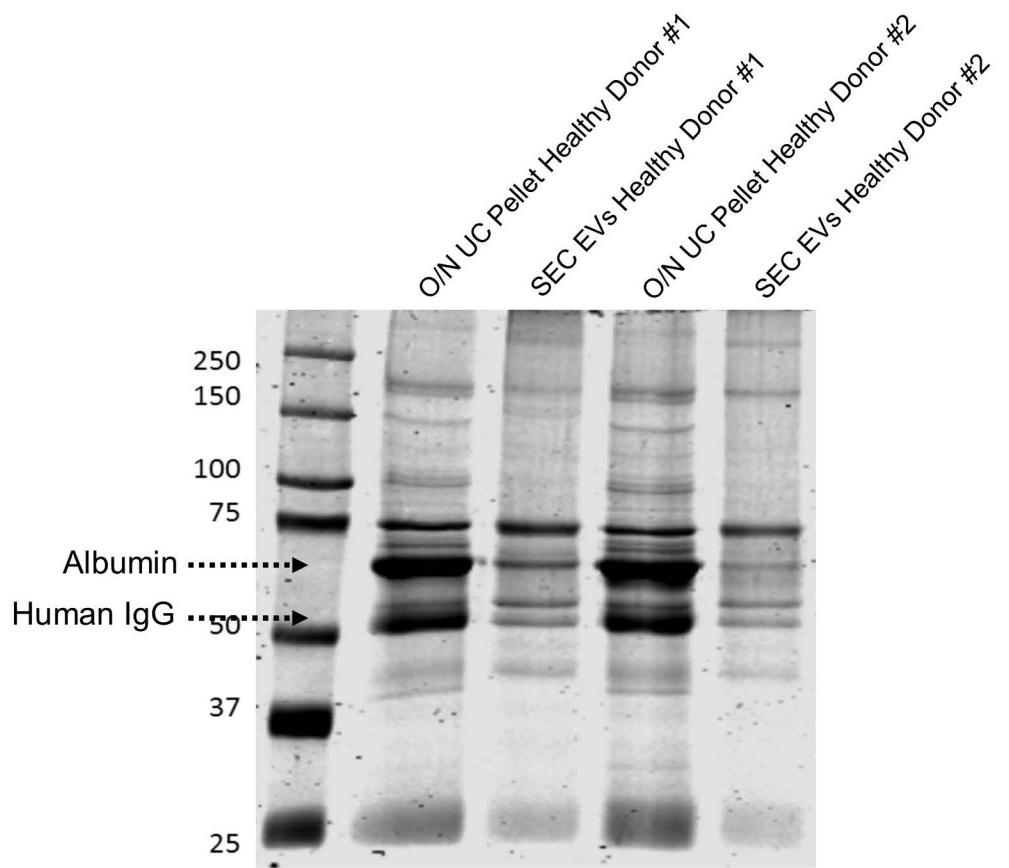
Supplemental Figure 4. SEC isolation reduces the level of contaminating plasma proteins in EV preparations from human plasma compared to ultracentrifugation. EVs were purified from two human plasma samples by overnight ultracentrifugation or size-exclusion chromatography, lysed in RIPA buffer, and 20ug of total protein was separated by SDS-PAGE on a 10% Tris-HCl gel. The gel was stained with Coomassie Blue and imaged using a Licor instrument.
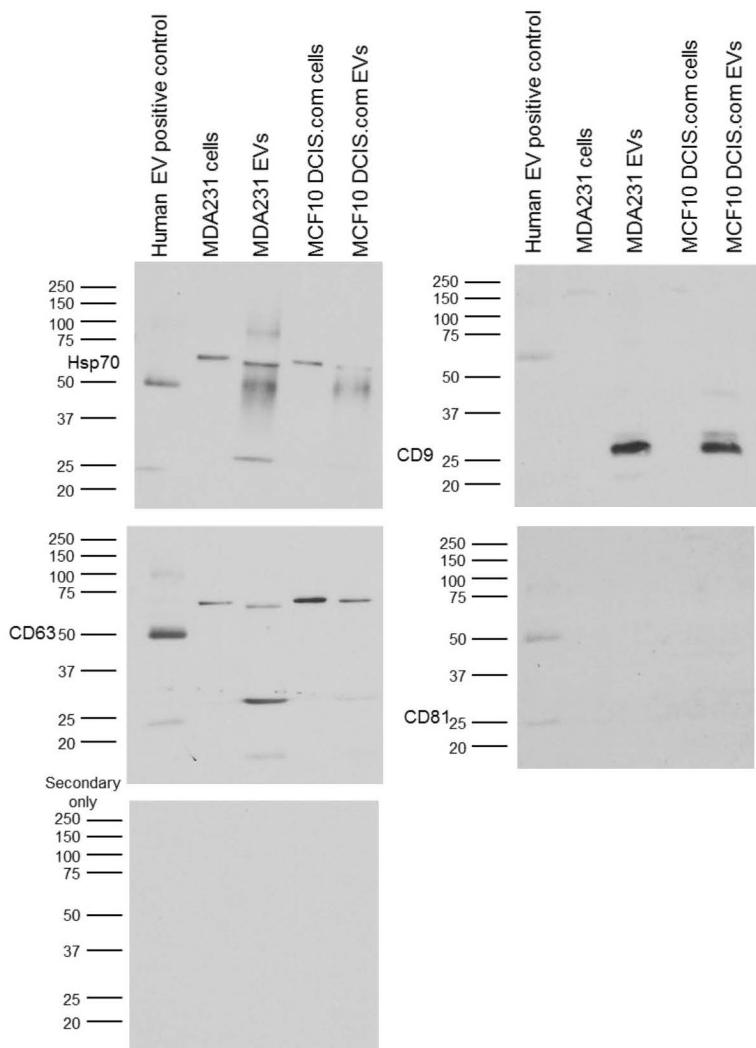
Supplemental Figure 5. Western blot analysis of EV-associated proteins in breast cancer cell conditioned media. Cell lysates, EVs purified from supernatants of MDA-MB231 or MCF10DCIS.com cells, or human positive control EVs (System Biosciences, EXOAB-POS-1) were separated by 10% SDS-PAGE. Membranes were blocked in 5% non-fat dry milk plus 10% goat serum for 1 h at room temperature, followed by a 1:1,000 dilution of primary antibody, per the manufacturer's recommendations, and a 1:20,000 dilution of goat anti-rabbit HRP secondary. All three antibodies and secondary only blots were developed with a 20 min film exposure using ECL Plus substrate. The low molecular weight CD81 band was only detected in human positive control EVs . CD9 was only detected in SEC-purified EVs from the breast cancer lines.